博士論文

Study on Signal Molecules Regulating Strigolactones and Brassinosteroids Function

（ストリゴラクトン・ブラシノステロイドの機能を制御する
シグナル分子に関する研究）

ジュティポーン　タッサグンパニト

Study on Signal Molecules Regulating Strigolactones and Brassinosteroids Function

（ストリゴラクトン・ブラシノステロイドの機能を制御するシグナル分子に関する研究）

Jutiporn Thussagunpanit

Supervisor: Prof. Dr. Tadao Asami

A thesis for the degree of Doctor of Philosophy in The Applied Biological Chemistry

東京大学
THE UNIVERSITY OF TOKYO

Tokyo, 2017

Contents

Contents (continued)

Contents (continued)

List of Figures

List of Figures (continued)

List of Figures (continued)

List of Tables

Abbreviations

Abbreviation	Full name
2-epiCS	2-Epicastasterone
2,3-diepiCS	2,3-Diepicastasterone
5DS	5-Deoxystrigol
α-DHECD	7,8-Dihydro-5α,8α-20-hydroxyecdysone
ABA	Abscisic acid
AM	Arbuscular mycorrhizal fungi
At	*Arabidopsis thaliana*
BAK1	BRI1-ASSOCIATED KINASE 1
BBXs	B-box zinc-finger transcription factors
BES1	BR-INSENSITIVE-EMS-SUPPRESSOR 1
bes1-D	The gain-of-function *bes1-D*, *BR-Insensitive-EMS-Suppressor 1-Dominance*
bHLHs	Basic helix-loop-helix transcription factors
BIL1	BRZ-INSENSITIVE-LONG HYPOCOTYL 1
bil1-1D	The gain-of-function *bil1-1D*, *Brz Insensitive-Long hypocotyl 1-Dominance*
BIM1	BES1-INTERACTING MYC-LIKE 1
BIN2	BRASSINOSTEROID INSENSITIVE 2
BL	Brassinolide
bp	Base pair
BR	Brassinosteroid
BRI1	BRASSINOSTEROID INSENSITIVE 1
BRRE	Brassinosteroid responsive element
BRs	Brassinosteroids
Brz	Brassinazole
BSU1	BRASSINOSTEROID INSENSITIVE 1 SUPPRESSOR 1
bZIPs	Basic leucine zipper transcription factors
BZR1	BRASSINAZOLE-RESISTANT 1

BZS1	BRASSINAZOLE-RESISTANT 1-SUPPRESSOR 1
CaMV	Cauliflower mosaic virus
CCD	CAROTENOID CLEAVAGE DIOXYGENASE
CCT	CO-COL-TOC1, CONSTANS-CONSTANS LIKE-TIMING OF CAB1
CDD	COP10-DDB1-DET1 complex
cDNA	Complementary DNA
Chl	Chlorophyll
CHS	Chalcone synthase
CK	Cytokinin
CLA	Carlactonic acid
Col	Columbia
COL3	CONSTANS LIKE 3
COP	CONSTITUTIVE PHOTOMORPHOGENIC
CPD	Cytochrome 90A1
Cry	Crytpochrome
CSN	COP9 signalosome
CUL1	Cullin 1
CycD3	Cyclin-D3
CYP	Cytochrome P450
D14	DWARF14
D27	DWARF27
Da	Dalton
de P-BIL1	Dephosphorylated BIL1/BZR1
DET	DE-ETIOLATED
DHECD	7,8-Dihydro-8α-20-hydroxyecdysone
DMF	Dimethylformamide
DMSO	Dimethyl sulfoxide
DTT	Dithiothreitol
DWF4	DWARF4
E. coli	*Escherichia coli*

ECD	20-Hydroxyecdysone
EDTA	Ethylenediaminetetraacetic acid
ELIPs	Early Light-Induced Proteins
EMSA	Electrophoretic mobility shift assay
ent-5DS	*ent*-5-Deoxystrigol
ET	Ethylene
EXP1	EXPANSIN
FAM	6-Carboxyfluorescein
FUS	FUSCA
FW	Fresh weight
GA	Gibberellin
gDNA	Genomic DNA
GFP	Green fluorescent protein
GSK3	GLYCOGEN SYNTHASE KINASE 3
GUS	β-Glucuronidase
HCl	Hydrochloric acid
His	Histidine
HY5	ELONGATED HYPOCOTYL 5
HYH	ELONGATED HYPOCOTYL 5 HOMOLOG
IC_{50}	The half inhibitory concentration
JA	Jasmonic acid
KAR	Karrikin
LBO	LATERAL BRANCHING OXIDOREDUCTASE
Ler	Landsberg erecta
LHCB1	Light-harvesting chlorophyll a/b binding protein
LLR	Leucine-rich repeat
LLR-RLK	Leucine-rich repeat receptor-link kinase
LZF1	LIGHT-REGULATED ZINC FINGER PROTEIN 1
MAX	MORE AXILLARY GROWTH
MBP	Maltose binding protein
Me	Methyl group

MeCLA	Methyl carlactonoate
MS	Murashige and Skoog
Na_2CO_3	Sodium carbonate
$NaNO_2$	Sodium nitrite
Native-PAGE	Native-Polyacrylamide gel electrophoresis
NMR	Nuclear magnetic resonance spectroscopy
NOE	Nuclear overhauser effect
NPH1	NON-PHOTOTROPIC HYPOCOTYL 1
P-BIL1	Phosphorylated BIL1/BZR1
PAGE	Polyacrylamide gel electrophoresis
PBS	Phosphate-buffered saline
Phy	Phytochrome
pifq	Quadruple *phytochrome interacting factor* (*pif1pif3pif4pif5*)
PIFs	PHYTOCHROME INTERACTING FACTORS
PIN1	AUXIN EFFLUX CARRIER COMPONENT 1
PSII	Photosystem II
qRT–PCR	Quantitative real-time PCR
rac-GR24	The GR24 racemic mixture
rbcS	The *small subunit* of RuBisCO
SA	Salicylic acid
SAUR-AC1	Early auxin-inducible gene
SCF	SKP1-CUL1-F-box-protein
SDS	Sodium dodecyl sulfate
SDS-PAGE	Sodium dodecyl sulfate-Polyacrylamide gel electrophoresis
SERK	The somatic embryogenesis receptor kinase
SKP1	S-phase kinase-associated protein 1
SL	Stigolactone
SLs	Stigolactones
SMXL	SUPPRESSOR OF MAX2 1-LIKE
SPA	Suppressor of phytochrome A
ssDNA	Sonicated salmon sperm DNA

STH	SALT TOLERANCE HOMOLOG
STH7	SALT TOLERANCE HOMOLOG 7
STH7ox	*STH7*-overexpressing
STH7-SRDX	Functionally defective *STH7*
STO	SALT TOLERANCE
TBE	Tris-Borate-EDTA
TBS	Tris-buffered saline
TCH4	Xyloglucan-endotransglycosylase
Trx	Thioredoxin
Ub	Ubiquitin
WT	Wild-type *Arabidopsis*
X-Gluc	5-Bromo-4-chloro-3-indolyl-β-glucronide
XTHs	Xyloglucan endotransglucosylase/hydrolase

CHAPTER 1: Introduction

Plant hormones are small molecules produced through several metabolic pathways. Research of plant hormone started around 1800s since the discovery of some small molecules that are present in a small amount in plants. They can move throughout the plants and regulate plant growth [1]. Later, these small molecules were called as plant hormones. Plant hormones play critical roles in plant growth, differentiation and development from embryogenesis stage to plant senescence. Nowadays, at least nine groups of plant hormones including auxins, gibberellins, cytokinins, ethylene, abscisic acid (ABA), brassinosteroids (BRs), jasmonic acid (JA), salicylic acid (SA) and stigolactones (SLs) have been reported [2] (Fig. 1-1). The study of functions of plant hormones and the interaction among hormones are essential for understanding plant life cycles. In this thesis, two kinds of plant hormone, strigolactones (SLs) and brassinosteroids (BRs) have been focused.

1.1 Strigolactones

Strigolactones (SLs) are a small group of compound that first isolated from root exudates from the host of parasitic *Striga* and *Orobanche*. The root exudates stimulate the seed germination of these parasites [3–5]. Later, SLs were confirmed to be produced also from non-host plants of root parasites [5]. SLs are derived from carotenoid and typically consist of four rings (A-D) [3–5]. Base on their structures, SLs divided into 1) the canonical SLs containing ABC ring such as strigol-like and orobanchol-like compounds (Fig. 1-2A) and 2) the non-canonical SLs which lack the tricyclic lactone ring such as carlactone, carlactonoic acid (CLA), and methyl carlactonoate (MeCLA) (Fig. 1-2B) [3]. Although ABC ring is substituted with various functional groups to give a lot of derivatives the butenolide D ring is highly conserved and important for the biological activity of SL [3]. This butenolide moiety is also found in karrikins which are byproducts of smoke and have signal transduction and biological activities similar to SLs [6].

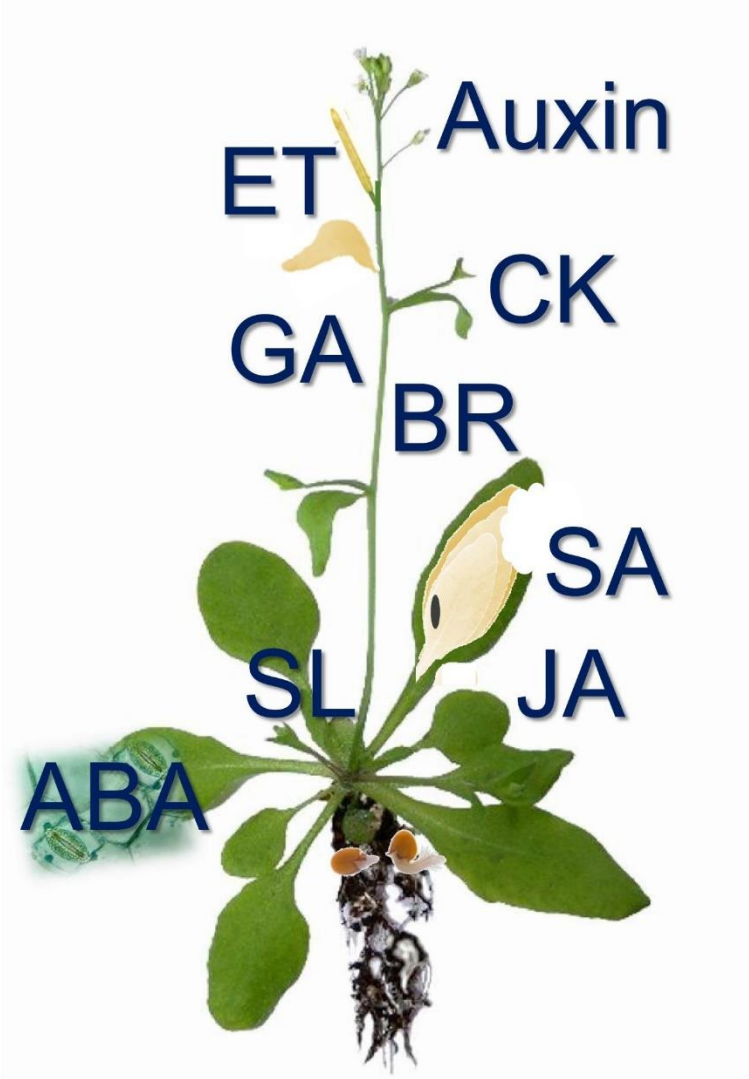

Fig. 1-1 Plant hormones regulate plant growth in whole part of plant

Auxin stimulate cell elongation and apical dominance. Cytokinin (CK) regulates cell division and attenuate apical dominance. Gibberellin (GA) promotes stem elongation by increase cell division and cell elongation. Brassinosteroind (BR) controls growth and development and stimulates photomorphogenesis. Salicylic acid (SA) and Jasmonic acid (JA) are essential for plant defensive system to pathogen or wounding. Strigolactone (SL) induces seed germination, regulates root growth and inhibits branching. Abscisic acid (ABA) involves plant responses to biotic and abiotic stress and control stomatal opening. Ethylene (ET) regulates fruit ripening and senescence.

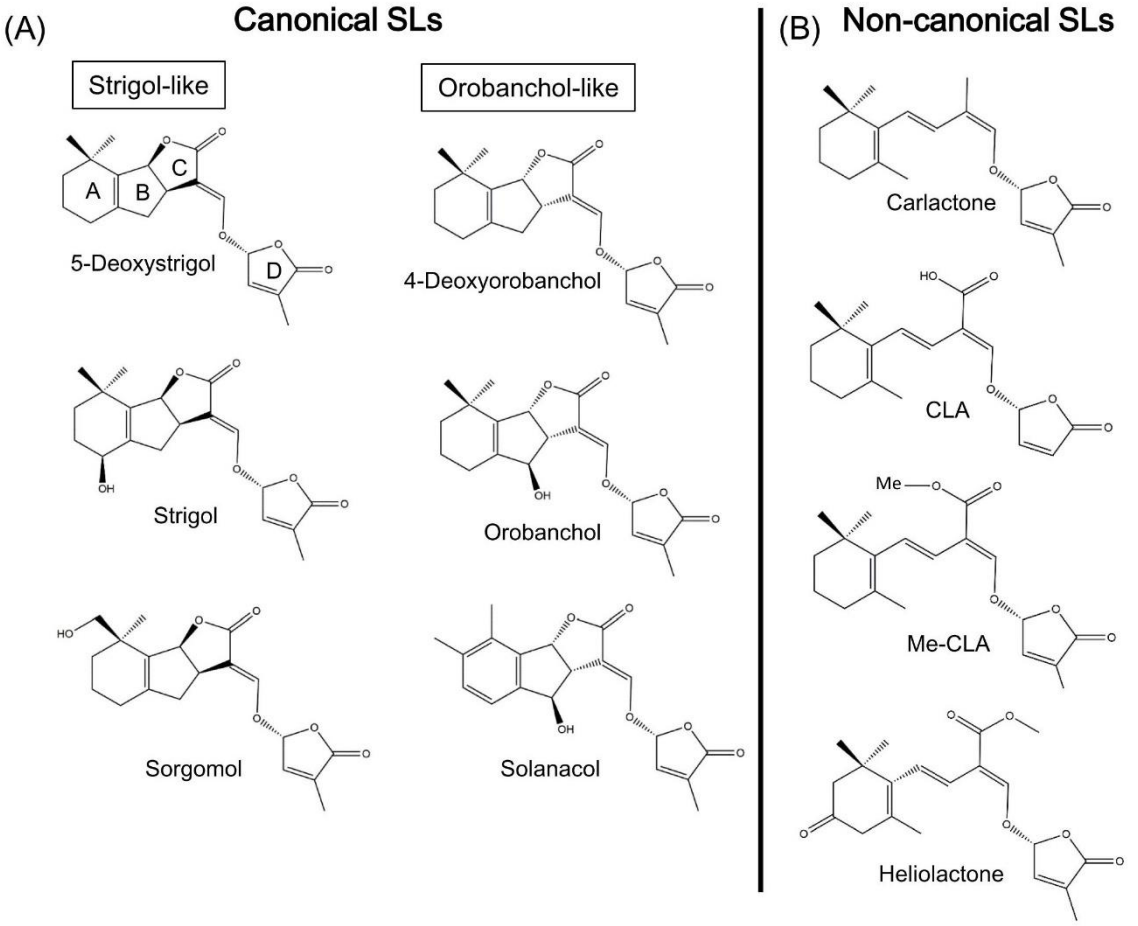

Fig. 1-2 Strigolactones structures

SLs consist of four rings (A-D). SLs divided into (A) the canonical SLs containing ABC ring e.g. strigol-like and orobanchol-like, and (B) the non-canonical SLs which lack of tricyclic lactone e.g. carlactone, carlactonoic acid (CLA), methyl carlactonoate (MeCLA), and heliolactone.

1.1.1 Strigolactone biosynthesis

SLs are derived from carotenoids and pathway from β-carotene to SL consists of enzymes catalyzing isomerization, cleavages and oxidation [3, 4]. Considering the different structures between carotenoids and SLs, four key catalytic enzymes are required for SL production [3]. SL biosynthesis pathway is shown in Fig. 1-3. First step is a reversible step and isomerizes all-*trans*-β-carotene to 9-*cis*-β-carotene by DWARF27 (D27). Next, CAROTENOID CLEAVAGE DIOXYGENASE 7 and 8 (CCD7 and CCD8) convert 9-*cis*-β-carotene and its product, respectively, to carlactone. CCD7 and CCD8 are, respectively, encoded by *MAX3* and *MAX4* in *Arabidopsis* and encoded by *D17* and *D10* in rice [3, 4]. In *Arabidopsis*, carlactone is translocated to cytosol and oxidized by the cytochrome P450, CYP711A1, encoded by *MAX1* to give CLA. Later, CLA is changed to MeCLA. Lastly, MeCLA is catalyzed by LATERAL BRANCHING OXIDOREDUCTASE encoded by *LBO* to give unknown compound (MeCLA + 16 Da) which is the essential substance for branching development [4]. In rice, carlactone is catalyzed by CYP711A2 to give 4-deoxyorobanchol, a common precursor of various SLs [4, 5].

1.1.2 Signal transduction of strigolactones

Plants require two proteins to response to SL molecules. First protein is the leucine-rich-repeat F-box protein encoding by MAX2 or D3 in *Arabidopsis* and rice, respectively. Another is the α/β-hydrolase encoding by D14 recognized as SL receptor. When the hydrolytic product produced from D-ring of SLs binds to the active site of D14, the SL-bound D14 stimulate the association of F-box proteins–MAX2 and SKP1-CUL1-F-box-protein (SCF)-ubiquitin ligase complexes [3, 6, 7]. Targets of SCF^{MAX2} are SMXL6,7,8 or D53 in *Arabidopsis* or rice, respectively, for proteasomal degradation leading to present the SL responses [6]. The summary of SL perception and transduction are shown in Fig. 1-4.

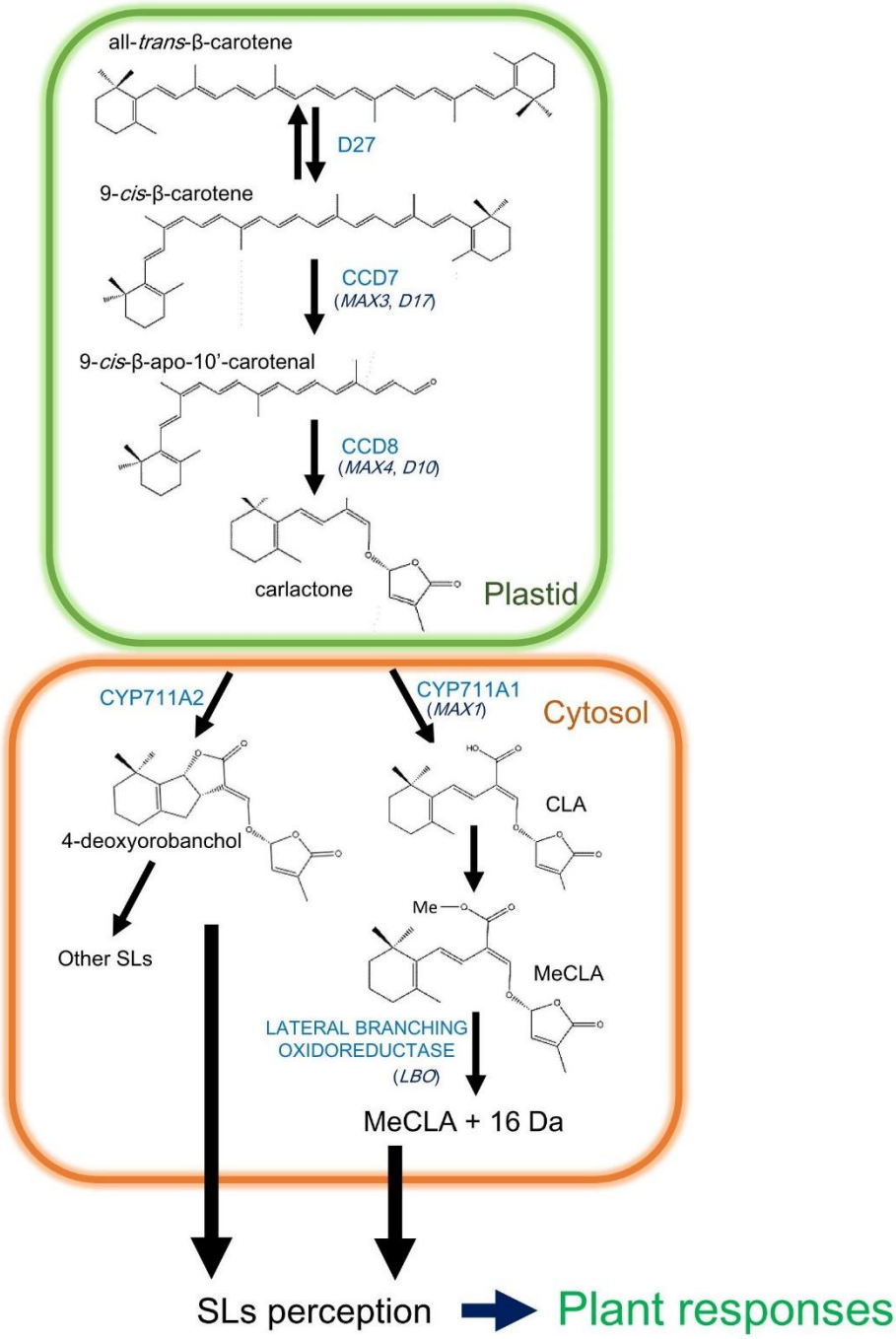

Fig. 1-3 Strigolactone biosynthesis

SL biosynthesis is derived from carotenoid biosynthesis pathway. D27, CCD7, CCD8 and CYP711 (A1 or A2) shown in light blue letters are the four key enzymes that are important for each step of SL biosynthesis. The genes that encode SL biosynthesis enzyme were shown in dark blue under its enzyme.

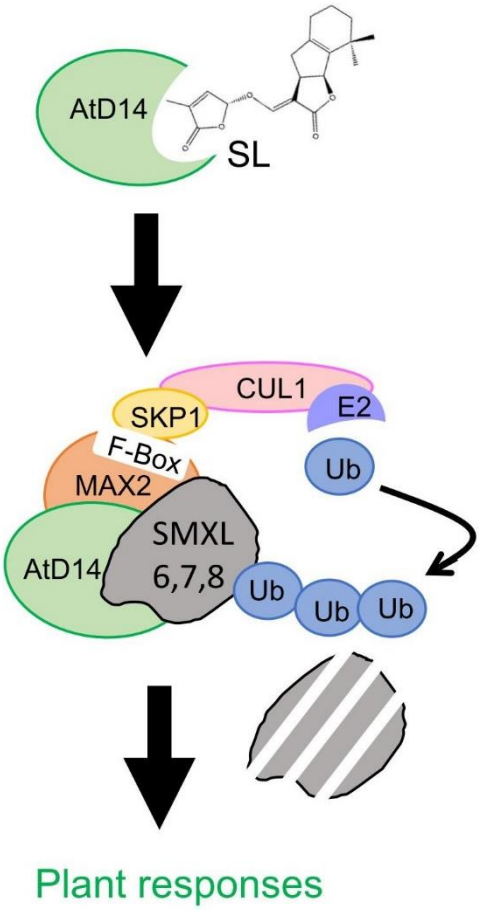

Fig. 1-4 Signal transduction of strigolactone in *Arabidopsis*

A model for the perception and signal transduction of the SL signal by the α/β hydrolase AtD14 is shown. AtD14 bound with SL changes its conformation. After that AtD14 interacts with the F-box protein MAX2, the other partners of the SCF^{MAX2} complex and SL-repressor proteins–SMXL6/7/8. Repressor proteins are recognized by the AtD14-SCF^{MAX2} complex and they are ubiquitinated by 26s proteasome leading to induce plant responses to SL.

1.1.3 Biological activities of strigolactones

Seed germination stimulant

SLs have been identified as a seed germination stimulant of parasitic plants *Striga ssp.* and *Orobanche spp.* [5, 7]. These parasitic plants play a major impacts on the destruction of crop such as maize, sorghum, millet, rice, and some legumes [7]. Generally, the parasitic seeds are dormant until they receive host-derived stimulants, including SLs. After germination, parasitic seedlings attach host plants with a haustorium which is a special structure for penetration into host root. Parasite plants remain in soil for several weeks or months and then emerge the flower shoots under the ground. The parasite can produce a large number of small seeds which can survive in soil for many years and they will cause the problem for future crop [5, 7] (Fig. 1-5). However, *Striga* and *Orobanche* cannot survive without their host plants and cannot germinate without SLs exuded from host roots. The control of SLs in soil is the essential key to protect crop from parasitic plants. Not only parasitic plant but SLs also contribute a seed germination in non-parasitic plant such as *Arabidosis thaliana* [7, 8]. SLs have been reported on the alleviation of seed germination under high temperature [8]. Base on the thermoinhibition, SLs play a role with other phytohormones such as, gibberellin, cytokinin, ethylene and ABA to control seed germination [8].

Branching inhibition

The role of SLs in shoot-branching was elucidated by SL-signaling and SL-deficient mutants. For example, the *more axillary growth 2* (*max2*), *max3* and *max4* mutants in *Arabidopsis* exhibit a large number of rosette branching [9, 10]. However, the more bud outgrowth in SL-biosynthesis mutants can be recovered by the application of both natural SLs e.g. 5-deoxystrigol, strigol and synthetic SL analogues e.g. GR24 [5, 9]. Crosstalk between SLs and auxins in controlling bud outgrowth has been investigated. In SL biosynthesis mutants including *max1*, *max3* and *max4* auxin transport and the accumulation of auxin exporter protein PIN1 clearly increased [11]. Treatment of SL

accelerates the depletion of PIN1 locating in the plasma membrane of xylem [12, 13]. Therefore, it is thought that SL inhibits bud outgrowth by impairing auxin transport.

Regulation of root growth

Root is the main organ for absorption water and nutrient into whole plant. Several reports demonstrated that SLs affect root development in many aspects. In the initial stage of root development, SLs have positive effects on root hair formation [14, 15]. SLs are involved in root hair elongation by regulating auxin efflux in root [14]. Moreover, SLs and other plant hormones such as cytokinins and auxins have been suggested to regulate cell division, cell elongation and differentiation in the root apical meristem [16]. SL mutants display shorter primary root length than wild-type plant. The shortened primary root in SL-deficient mutant (*max1*, *max3* and *max4*) but not in SL signaling mutant, *max2*, can be rescued by exogenous SL application [17]. In the secondary development of root, SLs repress lateral root [14, 17] and adventitious root formation [18]. Treatment of GR24 in *Arabidopsis* seedling reduces lateral root density [17]. Auxins promote adventitious root development, while SLs and cytokinins suppress adventitious root formation. However, role of these three hormones on adventitious roots are independent each other. The SL-deficient mutants in *Arabidopsis* and pea display more formation of adventitious root [18]. Overall, SLs should play important roles in root from primary growth to secondary development.

Promotion of branching in Arbuscular mycorrhizal fungi

Arbuscular mycorrhizal (AM) fungi are microorganisms in soil that have the symbiotic associations with about 80% of all plant species [19–21]. AM fungi cannot be alive without a host root [19]. At the initiation stage of AM fungi symbiosis with their plant host, a plant signal molecule, so called branching factor, exuded from the host root regulates hyphal development of AM fungi [21]. The branching factor exudated from host roots was isolated and identified as SL such as 5-deoxystrigol [19]. To confirm SL function as a branching factor in AM fungi, natural SL, 5-deoxystrigol,

sorgolactone and strigol, and a synthetic analogue, GR24, were applied to AM fungi. The result showed that these SLs could induce the hyphal branching in germinating spores of the AM fungus at very low concentrations [19]. SLs are essential for the symbiotic growth in AM fungi [19, 20] and may enhance the mycorrhizal signaling factors leading to increase the symbiotic signals [20].

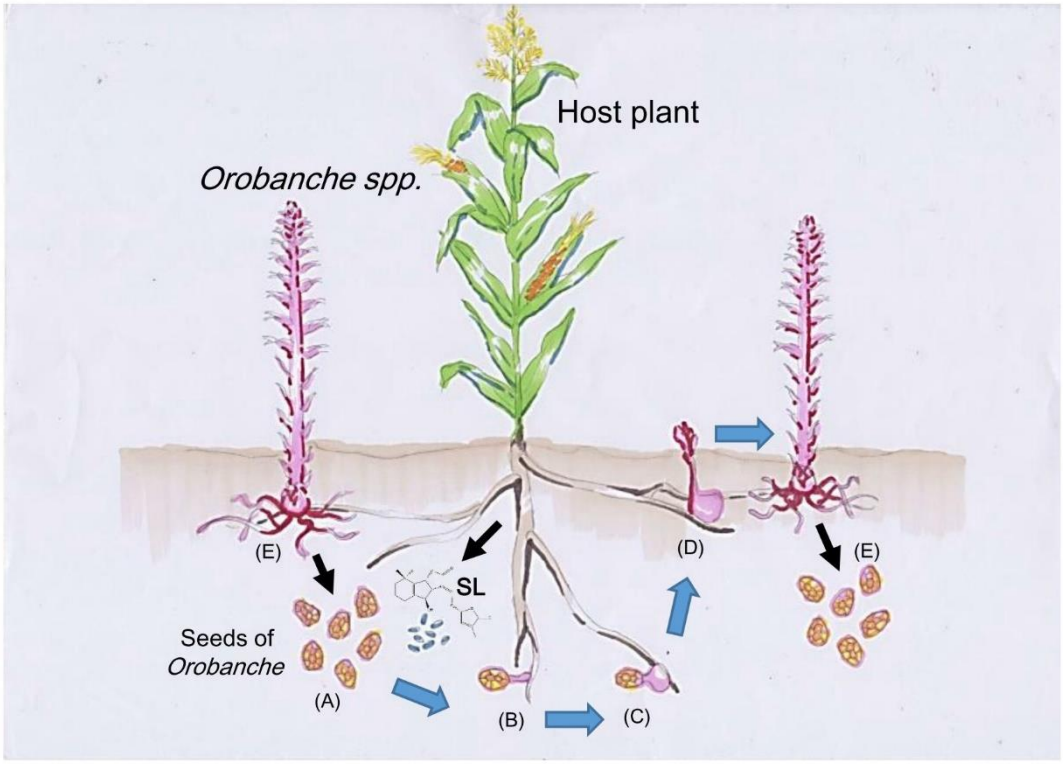

Fig. 1-5 Life cycle of parasitic plant *Orobanche spp.*

(A) *Orobanche spp* seeds germinate by the stimulation of strigolactone (SL). (B-D) Parasitic seedlings attach into the host plant with a haustorium and develop themselves to mature plants. (E) Parasite plants produce seeds which can remain in soil for many years. (Modified from Xie and Yoneyama [5])

1.2 Brassinosteroids

BRs are a group of endogenous plant hormones that regulate multiple physiological processes required for normal plant growth and development. BRs were first discovered as brassinolide (BL) in pollen of *Brassica napus* in 1979 [22]. The structures of BRs are similar to those of animal steroid hormones e.g. estrogen, progesterone and testosterone, which have well-known functions in regulating embryonic development and adult homeostasis [23]. Moreover, ecdysteroids which are an arthropod molting hormone also display the structure similar to BRs [24, 25]. In this group, 20-hydroxyecdysone is a common representative phytoecdysteroid which is produced in many plants [24]. BRs regulate gene expressions controlling metabolic pathways, contribute to the regulation of cell division, cell elongation and differentiation, and regulate the developmental programs in plants [23, 26, 27]. The development of chemicals that are BR agonists might be the good way to study BR functions. The study of BR mimicked compounds will be described in Chapter 2.

1.2.1 Brassinosteroids biosynthesis

The biosynthesis pathway of BL which is the most active BRs was initially found in *Catharanthus roseus* cells culture. The studies demonstrated that there are two parallel pathways to produce BL called early and late C-6 oxidation pathways, and campesterol is the precursor of BRs biosynthesis [23, 28]. Campesterol is catalyzed to produce campestanol. The conversion of campestanol to 6-deoxocathasterone in late C-6 oxidation pathway and of 6-oxocampestanol to cathasterone in early C-6 oxidation pathway are C-22 hydroxylation steps both catalyzed by DWF4, a cytochrome P450 [23]. Moreover, there are several enzymes necessary for BL biosynthesis such as DET2, CPD and BR6ox as shown in Fig.1-6.

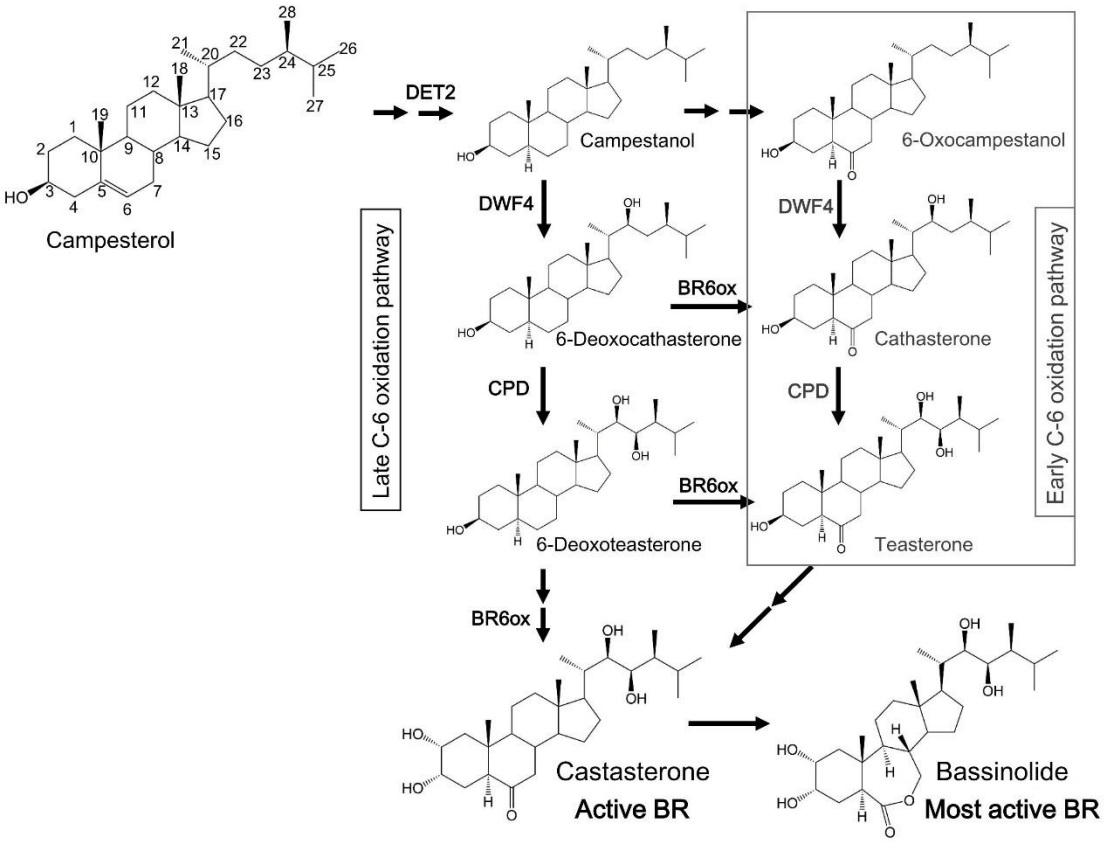

Fig. 1-6 Brassinosteroids biosynthesis

The most active BRs, brassinolide, is produced from the early C-6 oxidation and late C-6 oxidation (in grey square) pathways. Enzymes that are necessary for each step of BR biosynthesis are shown by bold letter above arrow.

1.2.2 Signal transduction of brassinosteroids

BRs are directly perceived by the transmembrane polypeptide receptor–BRASSINOSTEROID INSENSITIVE1 (BRI1). BRI1 is a protein belonging to the Leucine-Rich Repeat Receptor-like Kinase (LLR-RLK) family [29]. BRs signaling start from the binding of BR to the complex of its receptor BRI1 and co-receptor, BRI1-ASSOCIATED KINASE 1 (BAK1) [30]. The key master regulator of BRs signaling pathway is descripted in Fig. 1-7.

The phosphorylation and dephosphorylation cascade including GSK3-like kinase BRASSINOSTEROID INSENSITIVE 2 (BIN2) control the transduction of BR signals to the downstream BR specific transcription factors. BRZ-INSENSITIVE-LONG HYPOCOTYL 1/BRASSINAZOLE-RESISTANT1 (BIL1/BZR1) and BR-INSENSITIVE-EMS-SUPPRESSOR1 (BES1/BZR2) are the positive regulators of BR responses. The accumulation of dephosphorylated BIL1 and/or BES1 in nucleus activate BR signals by binding to the promoter of more than 2,000 genes and drive plant responses [30] (Fig. 1-7).

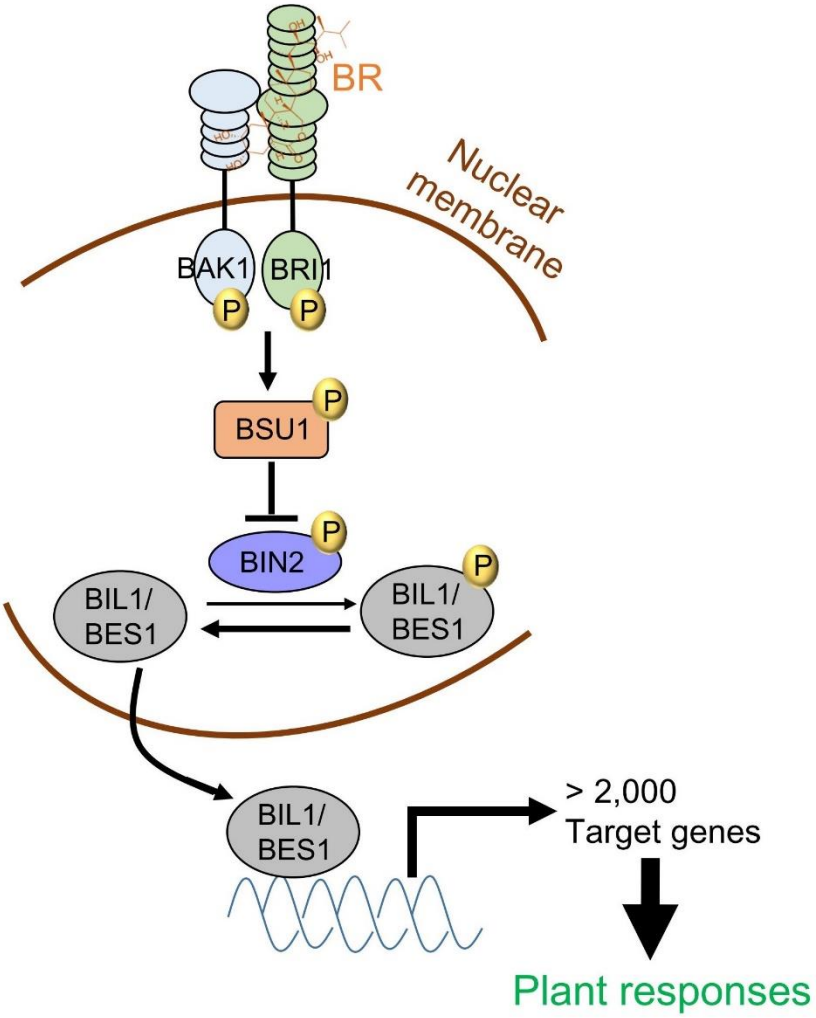

Fig. 1-7 Signal transduction of brassinosteroids

In the presence of BR, BR binds to its receptor BRI1/BAK1 complex. BRI1/BAK1 is autophosphorylation and cascades BR response by phosphorylation. Phosphorylated BSU1 inhibits BIN2 function. The activated form of BIN2 (phosphorylated BIN2) can phosphorylate the master transcription factors of BR, BIL1 and BES1. The accumulation of dephosphorylated BIL1 and BES1 activate BR signals and stimulate plant responses.

1.2.3 Biological activities of brassinosteroids

Enhancement of cell division and cell elongation

BRs promote cell proliferation in a similar manner to cytokinin. That is, cytokinin regulates cell division by increasing D type cyclin, *CycD3*, expression level. CycD3 is a protein involved in the regulation of G1/S transition in the cell cycle. The application of 24-epibrassinolide, which is the synthetic BRs, to *det2* (BR biosynthesis mutant) cell suspension cultures induced the increase of *CycD3* transcript level. Moreover, 24-epibrassinolide could be substituted with zeatin which is a natural cytokinin and induces cell division in *Arabidopsis* callus and cell suspension cultures [31]. Next step of cell growth is cell elongation. The process of cell elongation partly consists of cell wall relaxation occurred by maintaining turgor pressure and cell wall synthesis to remain cell wall thickness. BRs modulate water uptake into cell through aquaporins and vascular H^+-ATPase activity [27]. Furthermore, BRs also induce cell wall loosen and enhance cell wall modification enzymes such as, xyloglucan endotransglucosylase/hydrolase (XTHs), expanxin, sucrose synthase and cellulose synthase [23, 27].

Promotion of xylem differentiation

BRs play important roles during vascular development. BR-deficient *Arabidopsis*, *det2* mutant, exhibited the impaired vascular system which has lower xylem to phloem ratio comparing to wild-type *Arabidopsis* [23]. In *Zinnia* cell culture, BRs enhance xylem differentiation by controlling the initial differentiation of procambial cells to tracheary elements formation. BRs induce xylem cell differentiation through the expression of genes related to the secondary cell wall formation and programmed cell death [32].

Enhancement of pollen tube growth

BRs play a critical role in plant reproductive growth especially in the regulation of male fertility. Pollen is known as a rich source of endogenous BRs [22]. The BR-

deficient mutants e.g. *dwf4* and *cpd*, and BR-signaling mutant e.g. *bri1*, are male sterile or exhibited the significant decrease of male fertility [33]. In *cpd* mutant, the pollen failed to elongate after germination resulting male sterility [33]. However, the exogenously treatment of BR can promote the pollen tube elongation [23, 34].

Regulation of senescence

BRs have been reported to regulate the senescence in plants. The gain-of-function *bes1-D* mutant which exhibits the constitutive BR response phenotype showed the acceleration of leaf senescence in *Arabidopsis* [33]. On the other hand, the BR-deficient and BR-insensitive mutants delay the senescence [31]. The mechanism of BR regulating senescence could be ascribed to the BR regulation of scavenging of reactive oxygen species by control peroxidase, superoxide dismutase, and catalase activities.

Promotion of photosynthesis

The exogenously application of BR enhances the photosynthetic rate. The changes of photosynthesis by BRs cause the increase of stomatal conductance and quantum efficiency of PSII as well as the decrease of chlorophyll fluorescence [36, 37]. Moreover, BR treatment could maintain the high photosynthetic rate under unsuitable environments such as under salt stress [36] and heat stress [38].

1.3 Photomorphogenesis

Light is one of environmental stimuli that regulates the numerous growth and development of plant starting from seed germination through early seedling growth. Moreover, light also stimulates a shade avoidance, a circadian rhythm, a flowering, and so on [39]. During seeds germination in darkness such as in the soil, young seedlings will develop skotomorphogenesis or etiolation that exhibit unopened hooks, closed cotyledons and elongated hypocotyls. When those seedlings protrude from soil, they will undergo photomorphogenesis or de-etiolation. The photomorphogenesis is a light-adapted development of plants that cause shortened hypocotyls, opened cotyledons, true leaves development and the synthesis of photosynthetic pigments such as chlorophyll and anthocyanin [39, 40]. Many research reported that multiple plant hormones including BR and SL modulate light-adapted growth in plant. The regulation of plant hormones in photomorphogenesis will be described in Chapter 2–4.

1.3.1 Light perception

Light is perceived in plants by the photoreceptors depending on the difference of light wavelengths. Red and far-red light are perceived by phytochrome family including five members, phytochrome A (PhyA) to phytochrome E (PhyE). Among these family, PhyA is primarily responsible for seedling de-etiolation under continuous far-red light whereas, phyB mainly control light responses under continuous red light [41–43]. Under light condition, phyB, phyD, and phyE are co-regulated to activate the shade avoidance [42]. Photoreceptors for blue light compose of three members, crytpochrome 1 (Cry1), Cry2 and phototropin. Cry1 is the major photoreceptor for blue light and UV perception. Cry1 is necessary for modulating growth under medium or high-light intensities, while Cry2 has a main function under low intensity of blue light. The last blue light photoreceptor is phototropin encoded by NON-PHOTOTROPIC HYPOCOTYL 1 (*NPH1*). Photophorin plays main role in phototropism response [41].

1.3.2 Light signal transduction

The mutants related to downstream signals from the photoreceptors exhibited photomorphogenic changes in the dark. This phenotype was observed in *constitutive photomorphogenic/de-etiolated/fusca* (*cop/det/fus*) group mutants [40]. Moreover, COP9 signalosome or CSN which is a multisubunit regulatory complex consisting of at least eight subunits has been reported to play as the master repressor of photomorphogenesis under darkness [41, 44]. CSN recognize the CONSTITUTIVE PHOTOMORPHOGENIC 1 (COP1) which is a key negative regulatory factor of photomorphogenesis [40]. COP1 protein contains three regions, a RING finger domain at N-terminal, WD-40 repeats at C-terminal and coiled-coil region (Fig. 1-8). The coiled-coil region of COP1 allows the formation of a member protein in SPA family [45]. Under darkness, CSN, COP1 and CDD (COP10, DDB1, DET1) complex works together to enhance the ubiquitination of photomorphogenesis transcription factors such as ELONGATED HYPOCOTYL 5 (HY5). HY5 is a positive regulatory factor for promoting photomorphogenesis [40, 41, 44]. The CSN directly bind to CDD complex that interacts with RING finger domain of COP1. The CDD complex enhances E2 activity whereas HY5 that interacts with the WD40 repeat domain of COP1 is ubiquitinated by the ubiquitin E3 ligase activity of COP1. Lastly, the polyubiquitination of HY5 is recognized and then degraded by the 26s proteasome leading to inhibit photomorphogenesis [44–46] (Fig. 1-8). When plants perceive light signal, visible light promotes the nuclear export of COP1 causing the suppression of COP1 function in nucleus and allowing light-adapted responses [45] (Fig. 1-8).

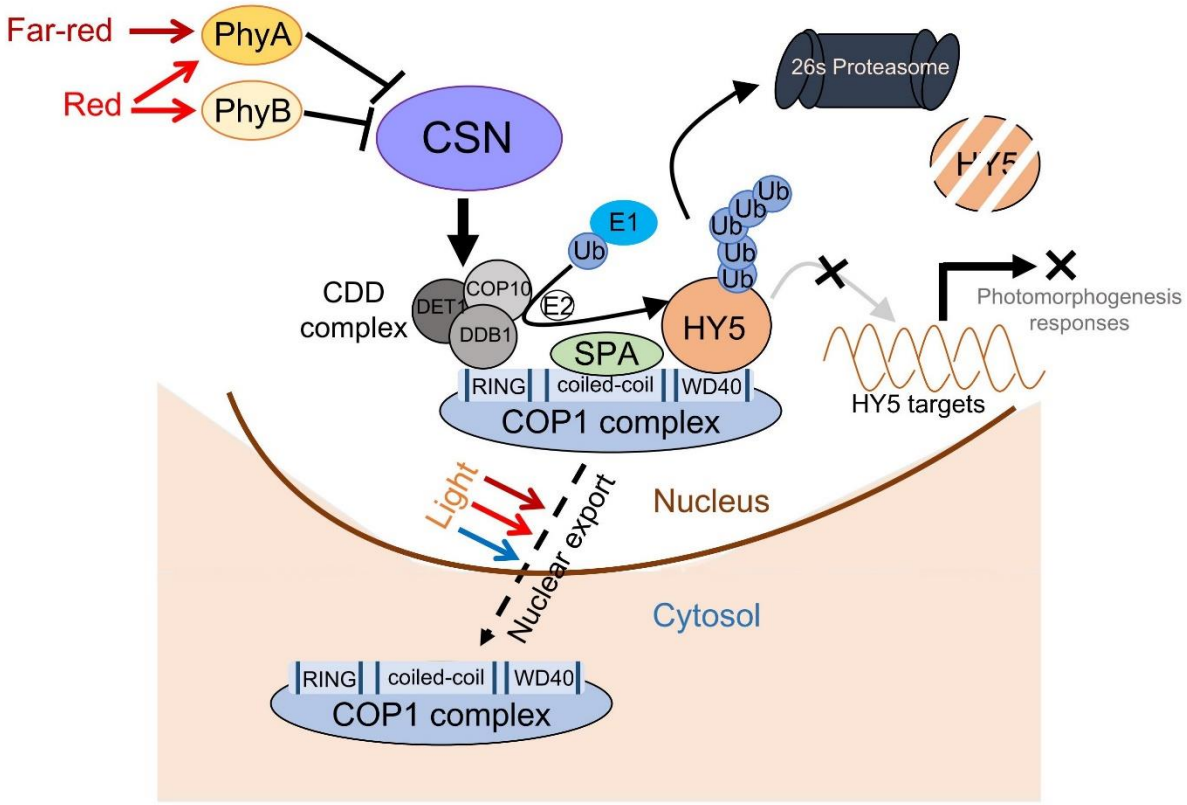

Fig. 1-8 Model of light signal transduction regulating photomorphogenesis

Different light qualities are sensed by their photoreceptors; for example, far-red light is perceived by PhyA and red light is mainly perceived by PhyB. Light signals initially start a signal transduction cascade that abolish the repressory action of the COP9 signalosome (CSN). Under darkness, the complex of CSN, CDD, and SPA-bound COP1 work together to promote the ubiquitination of photomorphogenesis-promoting transcription factors, such as HY5 by 26s proteasome. Under light, COP1 is exported to outside of nucleus. HY5 can downstream its target genes to promote photomorphogenesis.

1.3.3 Transcriptional regulators in photomorphogenesis

Many aberrant responses in photomorphogenesis of *Arabidopsis* mutants were used to identify positive and negative transcriptional regulators in photomorphogenesis. The basic transcriptional regulators are basic leucine zipper transcription factors (bZIPs), basic helix-loop-helix transcription factors (bHLHs), and B-box zinc-finger transcription factors (BBXs) families. The brief detail of each family is following;

Basic leucine zipper transcription factors

In the bZIP family, HY5 and its homolog, HYH, are the members that show the positive roles in photomorphogenesis [40, 41, 44]. HY5 functions contribute to the regulation by various light wavelengths and integrate light signaling and plant hormone signaling pathways [45]. Moreover, HY5 have been reported as the direct target of promoters in light response genes such as *LHCB1*, *rbcS* and *CHS* [47].

Basic helix-loop-helix transcription factors

PHYTOCHROME INTERACTING FACTORS (PIFs) are the first group of bHLH transcription factor found as the negative regulator of photomorphogenesis. The quadruple *pif1pif3pif4pif5* (*pifq*) *Arabidopsis* mutant exhibit the constitutively photomorphogenic-like phenotype with shortened hypocotyls and green-opened cotyledons under darkness in contrast with the long hypocotyl phenotype of *phyA* and *phyB* mutants in the light. Therefore, PIFs and phytochromes play an antagonistic roles in light-adapted development [48].

B-box zinc-finger transcription factors

The BBX protein family consist of five subfamilies [49] (Fig. 1-9). Subfamily I (BBX1–BBX6) and subfamily II (BBX7–BBX13) contain two B-box motifs whereas subfamily III (BBX14–BBX17) contain only one B-box motif at the N-terminal. All

subfamily I – III have a CCT (CO-COL-TOC1) domain at the C-terminal [49]. Subfamily IV (BBX18–BBX25) and subfamily V (BBX26–BBX32) contain two B-box motifs and one B-box motif, respectively [49, 50]. Many transcription factors in the BBXs family especially in subfamily IV play an important role as positive or negative regulators in photomorphogenesis [50]. For example BBX4/COL3, BBX20/BZS1/STH7, BBX21/STH2, and BBX22/LZF1 are positive regulators in photomorphogenesis. On the other hand, BBX24/STO and BBX25/STH play as the negative regulator in photomorphogenesis [49]. Some of BBXs such as BBX21 have the interaction with COP1 and HY5 to control the light-adapted responses [51]. In this thesis I have focused on the BBX20/STH7 as the regulating factor of light-adapted development. The details will be explained in Chapter 3 and 4.

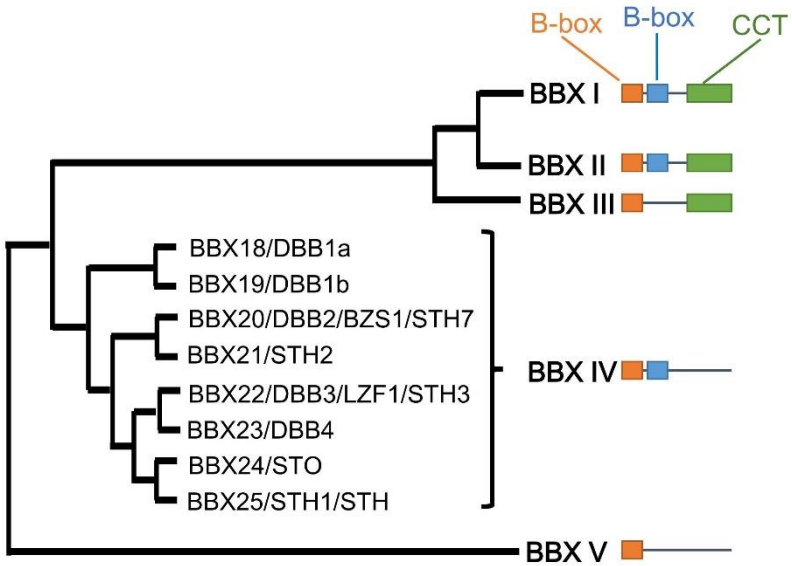

Fig. 1-9 Phylogenetic tree of B-box zinc-finger transcription factor (BBX)

The BBX protein family consists of five subfamilies BBX I – BBX V. The orange and blue boxes represent B-box type 1 and type 2 at the N-terminal, respectively. The green box represents the CCT (CO COL TOC) domain at the C-terminal. (Modified from Sarmiento [50])

1.4 Objectives

The main object of this research is the study on the factors mediating BRs and SLs functions in photomorphogenesis or light-adapted development. In Chapter 2, I aim to develop chemicals that can be applied as BR mimics by focusing on the negative response in photomorphogenesis. In the Chapter 3 and 4, I attempt to investigate the regulation of signal molecules that modulate roles of SLs and crosstalk between SLs and BRs in light-adapted development in *Arabidopsis*.

1.5 References

[1] Enders TA, Strader LC. Auxin activity: Past, present, and future. Am J Bot. 2015;102:180–196.

[2] Santner A, Calderon-Villalobos LI, Estelle M. Plant hormones are versatile chemical regulators of plant growth. Nat Chem Biol. 2009;5:301–307.

[3] Al-Babili S, Bouwmeester HJ. Strigolactones, a novel carotenoid-derived plant hormone. Annu Rev Plant Biol. 2015;66:161–186.

[4] Brewer PB, Yoneyama K, Filardo F, Meyers E, Scaffidi A, Frickey T, et al. *LATERAL BRANCHING OXIDOREDUCTASE* acts in the final stages of strigolactone biosynthesis in *Arabidopsis*. Proc Natl Acad Sci USA. 2016;113:6301–6306.

[5] Xie X, Yoneyama K. The strigolactone story. Annu Rev Phytopathol. 2010;48:93–117.

[6] Morffy N, Faure L, Nelson DC. Smoke and hormone mirrors: action and evolution of karrikin and strigolactone signaling. Trends Genet. 2016;32:176–188.

[7] Yamaguchi S, Williams M. Strigolactones. Teaching Tools in Plant Biology: Lacture Note. American Society of Plant Biologists. 2012.

[8] Toh S, Kamiya Y, Kawakami N, Nambara E, McCourt P, Tsuchiya Y. Thermoinhibition uncovers a role for strigolactones in Arabidopsis seed germination. Plant Cell Physiol. 2012;53:107–117.

[9] Nelson DC, Scaffidi A, Dun EA, Waters MT, Flematti GR, Dixon KW, et al. F-box protein MAX2 has dual roles in karrikin and strigolactone signaling in *Arabidopsis*

thaliana. Proc Natl Acad Sci USA. 2011;108:8897–8902.

[10] Stirnberg P, van De Sande K, Leyser HM, MAX1 and MAX2 control shoot lateral branching in *Arabidopsis*. Development. 2002;129:1131–1141.

[11] Bennett T, Sieberer T, Willett B, Booker J, Luschnig C, Leyser O. The *Arabidopsis* MAX pathway controls shoot branching by regulating auxin transport. Curr Biol. 2006;16:553–563.

[12] Crawford S, Shinohara N, Sieberer T, Williamson L, George G, Hepworth J, et al. Strigolactones enhance competition between shoot branches by dampening auxin transport. Development. 2010;137:2905–2913.

[13] Shinohara N, Taylor C, Leyser O. Strigolactone can promote or inhibit shoot branching by triggering rapid depletion of the auxin efflux protein PIN1 from the plasma membrane. PLoS Biol. 2013;11:1–14.

[14] Kapulnik Y, Delaux PM, Resnick N, Mayzlish-Gati E, Wininger S, Bhattacharya C, et al. Strigolactones affect lateral root formation and root-hair elongation in *Arabidopsis*. Planta. 2011;233:209–216.

[15] Koltai H., Strigolactones are regulators of root development. New Phytol. 2011;190:545–549.

[16] Pandey A, Sharma M, Pandey GK. Emerging roles of strigolactones in plant responses to stress and development. Front Plant Sci. 2016;7:1–17.

[17] Ruyter-Spira C, Kohlen W, Charnikhova T, van Zeijl A, van Bezouwen L, de Ruijter N, et al. Physiological effects of the synthetic strigolactone analog GR24 on root system architecture in *Arabidopsis*: another belowground role for strigolactones? Plant Physiol. 2011;155:721–734.

[18] Rasmussen A, Mason MG, de Cuyper C, Brewer PB, Herold S, Agusti J, et al. Strigolactones suppress adventitious rooting in *Arabidopsis* and pea. Plant Physiol. 2012;158:1976–1987.

[19] Akiyama K, Matsuzaki K, Hayashi H. Plant sesquiterpenes induce hyphal branching in arbuscular mycorrhizal fungi. Nature. 2005;435:824–827.

[20] Besserer A, Puech-Pagès V, Kiefer P, Gomez-Roldan V, Jauneau A, Roy S, et al. Strigolactones stimulate arbuscular mycorrhizal fungi by activating mitochondria. PLoS Biol. 2006;4:1239–1247..

[21] Buee M, Rossignol M, Jauneau A, Ranjeva R, Bécard G. The pre-symbiotic growth of arbuscular mycorrhizal fungi is induced by a branching factor partially purified from plant root exudates. Mol Plant Microbe Interact. 2000;13:693–698.

[22] Grove MD, Spencer GF, Rohwedder WK, Mandava N, Worley JF, Warthen JD, et al. Brassinolide, a plant growth-promoting steroid isolated from *Brassica napus* pollen. Nature. 1979;281:216–217.

[23] Clouse SD. Brassinosteroids. Arabidopsis Book. American Society of Plant Biologists. 2011.

[24] Dinan L. Phytoecdysteroids: biological aspects. Phytochemistry. 2001;57:325–339.

[25] Dinan L, Harmatha J, Volodin V, Lafont R. Phytoecdysteroids: Diversity, biosynthesis and distribution, in: Smagghe G (Ed), Ecdysone: Structures and Functions., Springer Science + Business Media, 2009, pp. 3–45.

[26] Fujioka S, Yokota T. Biosynthesis and metabolism of brassinosteroids. Annu Rev Plant Biol. 2003;54:137–164.

[27] Sasse JM. Physiological actions of brassinosteroids: an update. J Plant Growth Regul. 2003;22:276–288.

[28] Sakurai A, Fujioka S. Studies on biosynthesis of brassinosteroids. Biosci Biotechnol Biochem. 1997;61:757–762.

[29] Gruszka D. The brassinosteroid signaling pathway-new key players and interconnections with other signaling networks crucial for plant development and stress tolerance. Int J Mol Sci. 2013;14:8740–8774.

[30] Belkhadir Y, Jaillais Y. The molecular circuitry of brassinosteroid signaling. New Phytol. 2015;206:522–540.

[31] Hu Y, Bao F, Li J. Promotive effect of brassinosteroids on cell division involves a distinct CycD3-induction pathway in *Arabidopsis*. Plant J. 2000;24:693–701.

[32] Fukuda H. Signals that control plant vascular cell differentiation. Nat Rev Mol Cell Biol. 2004;5:379–391.

[33] Szekeres M, Németh K, Koncz-Kálmán Z, Mathur J, Kauschmann A, Altmann T, et al. Brassinosteroids rescue the deficiency of CYP90, a cytochrome P450, controlling cell elongation and de-etiolation in *Arabidopsis*. Cell. 1996;85:171–182.

[34] Hewitt FR, Hough T, O'Neill P, Sasse JM, Williams EG, Rowan KS. Effect of

brassinolide and other growth regulators on the germination and growth of pollen tubes of *Prunus avium* using a multiple hanging-drop assay. Aust J Plant Physiol. 1985;12:201–211.

[35] Yin Y, Wang ZY, Mora-Garcia S, Li J, Yoshida S, Asami T, et al. BES1 accumulates in the nucleus in response to brassinosteroids to regulate gene expression and promote stem elongation. Cell. 2002;109:181–191.

[36] Hayat S, Maheshwari P, Wani AS, Irfan M, Alyemeni MN, Ahmad A. Comparative effect of 28-homobrassinolide and salicylic acid in the amelioration of NaCl stress in *Brassica juncea* L. Plant Physiol Biochem. 2012;53:61–68.

[37] Yu JQ, Huang LF, Hu WH, Zhou YH, Mao WH, Ye SF, et al., A role for brassinosteroids in the regulation of photosynthesis in *Cucumis sativus*. J Exp Bot. 2004;55:1135–1143.

[38] Thussagunpanit J, Jutamanee K, Kaveeta L, Chai-arree W, Pankean P, Homvisasevongsa S, et al. Comparative effects of brassinosteroid and brassinosteroid mimic on improving photosynthesis, lipid peroxidation, and rice seed set under heat stress. J Plant Growth Regul. 2015;34:320–331.

[39] Wu SH. Gene expression regulation in photomorphogenesis from the perspective of the central dogma. Annu Rev Plant Biol. 2014;65:311–333.

[40] Eckardt NA. From darkness into light: factors controlling photomorphogenesis. The Plant Cell. 2001;13:219–221.

[41] Harari-Steinberg O, Ohad I, Chamovitz DA, Dissection of the light signal transduction pathways regulating the two early light-induced protein genes in *Arabidopsis*. Plant Physiol. 2001;127:986–997.

[42] Roig-Villanova I, Bou J, Sorin C, Devlin PF, Martínez-García JF. Identification of primary target genes of phytochrome signaling. Early transcriptional control during shade avoidance responses in *Arabidopsis*. Plant Physio. 2006;141:85–96.

[43] Stamm P, Kumar PP. The phytohormone signal network regulating elongation growth during shade avoidance. J Exp Bot. 2010;61:2889–2903.

[44] Wei N, Deng XW. Making sense of the COP9 signalosome. A regulatory protein complex conserved from *Arabidopsis* to human. Trends Genet. 1999;15:98–103.

[45] Lau OS, Deng XW. The photomorphogenic repressors COP1 and DET1: 20 years

later. Trends Plant Sci. 2012;17:584–593.
[46] Dolan L, Langdale JA. New insights into plant development in New England. Development. 2004;131:5215–5220.
[47] Zhang H, He H, Wang X, Yang X, Li L, Deng XW. Genome-wide mapping of the HY5-mediated gene networks in *Arabidopsis* that involve both transcriptional and post-transcriptional regulation. Plant J. 2011;65:346–358.
[48] Leivar P, Tepperman JM, Cohn MM, Monte E, Al-Sady B, Erickson E, et al. Dynamic antagonism between phytochromes and PIF family basic helix-loop-helix factors induces selective reciprocal responses to light and shade in a rapidly responsive transcriptional network in *Arabidopsis*. Plant Cell. 2012;24:1398–1419.
[49] Gangappa SN, Botto JF. The BBX family of plant transcription factors. Trends Plant Sci. 2014;19:460–470.
[50] Sarmiento F. The BBX subfamily IV: additional cogs and sprockets to fine-tune light-dependent development. Plant Signal Behav. 2013;8:e23831-1–e23831-7.
[51] Xu D, Jiang Y, Li J, Lin F, Holm M, Deng XW. BBX21, an *Arabidopsis* B-box protein, directly activates HY5 and is targeted by COP1 for 26S proteasome-mediated degradation. Proc Natl Acad Sci USA. 2016;113:7655–7660.

CHAPTER 2: Characterization of Synthetic Ecdysteroid Analogues as Functional Mimics of Brassinosteroids

2.1 Chapter introduction

BRs are a group of naturally occurring steroidal plant hormones that regulate many stages of the plant life cycle [1, 2]. BRs have various effects that influence a wide spectrum of cellular responses, including cell division, cell elongation, xylem differentiation, hypocotyl elongation [3], leaf expansion [4], pollen germination [5], and that are processes related to the regulation of gene expression [6]. BRs are also involved in the resistance of plants to biotic and abiotic factors e.g. cold stress, temperature stress, salt stress, and disease [6, 7]. BRs and related compounds have been used to enhance production in various crop species including tomato [5], mung bean [8], and rice [9]. Consequently, research has been directed towards the discovery of compounds that mimic BRs, and display improved activities and reasonable production costs.

The concentrations of BRs are very low in many plants, and consequently, the yield of naturally occurring BRs from plants is typically poor [10, 11]. For example, a trial extraction of BR from 40 kg of Rape (*Brassica napus*) pollen resulted in the isolation of only 4 mg of brassinolide [10], whereas the extraction of 40 kg of insect galls from Chestnut (*Castanea crenata*) yielded only 95 μg of castasterone [11]. Ecdysteroids are generally known as compounds that regulate molting and metamorphosis in insects and crustaceans [12, 13], but various plant species also produce these compounds (phytoecdysteroids), which are widely thought to inhibit the feeding of phytophagous insects [12]. In a study of *Vitex glabrata* which is a common plant in Thailand, 63 g of the phytoecdysteroid 20-hydroxyecdysone (ECD) was obtained from 4 kg of stem bark [14]. ECD was readily converted to 7,8-dihydro analogues, 7,8-dihydro-8α-20-hydroxyecdysone (DHECD) and 7,8-dihydro-5α,8α-20-hydroxyecdysone (α-DHECD), by catalytic hydrogenation and subsequent base-catalyzed epimerization [15]. The 2D and 3D chemical structure of BL which is the most potent BR, ECD, DHECD and α-DHECD are shown in Fig. 2-1 and Fig. 2-2, respectively.

In addition to their probable role in inhibiting insect feeding, phytoecdysteroids are thought to be involved in the regulation of developmental and physiological processes in plants [16, 17]. The hydroxysteroidal compounds, ECD, DHECD, and α-DHECD have chemical structures similar to those of BRs, so I hypothesized that they function as BR mimics. ECD acts synergistically with indole-3-acetic acid (a naturally occurring auxin) to elongate wheat coleoptiles [17], in a similar way to the synergistic interaction of BRs with auxin, which causes hypocotyl elongation in *Arabidopsis thaliana* [18]. Previous studies in rice have demonstrated that DHECD reduces heat stress with efficiency similar to that of 24-epibrassinolide, one of the BRs used commercially in agriculture [19, 20, 21]. DHECD promotes pollen viability, pollen germination [19], shoot biomass, leaf expansion [20], and photosynthetic activity under heat stress in rice [20, 21]. In this study the biological activities of ECD, DHECD, and α-DHECD were compared with those of BL by using plant physiological and molecular biological methods. The effects of these chemicals were evaluated through their effects on rice inclination, hypocotyl and root elongation in *Arabidopsis*, the expression BR-related genes, and the phosphorylation of BIL1/BZR1 which is a master transcription factor in BR signaling.

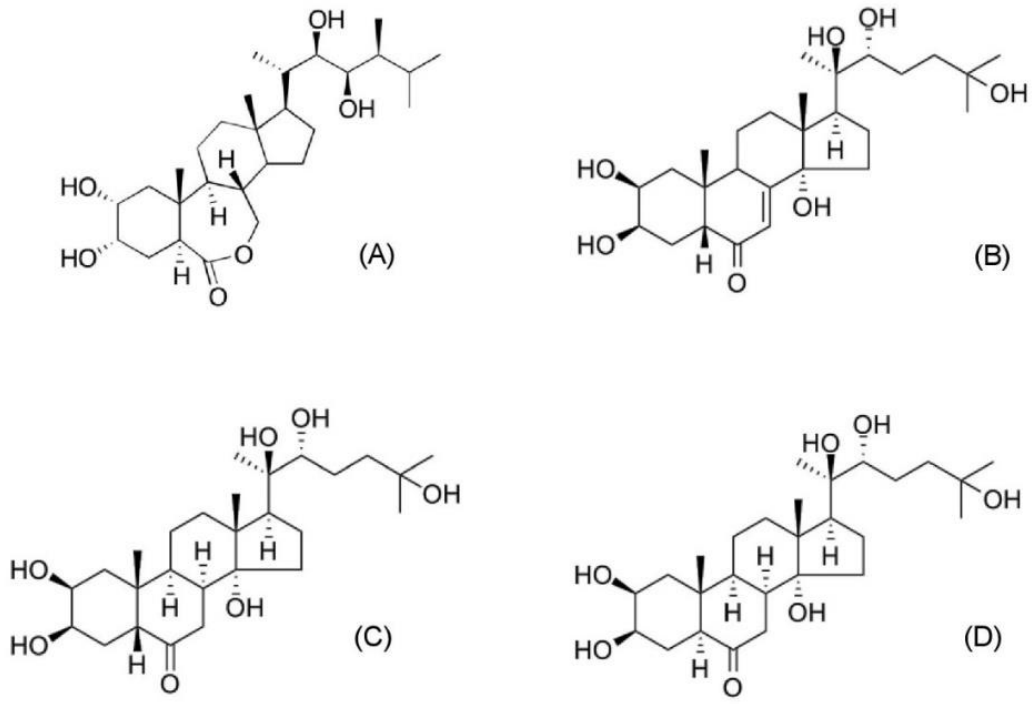

Fig. 2-1 2D chemical structures of the ecdysteroid analogues

Brassinolide (BL, A), 20-hydroxyecdysone (ECD, B), 7,8-dihydro-8α-20-hydroxyecdysone (DHECD, C), and 7,8-dihydro-5α,8α-20-hydroxyecdysone (α-DHECD, D).

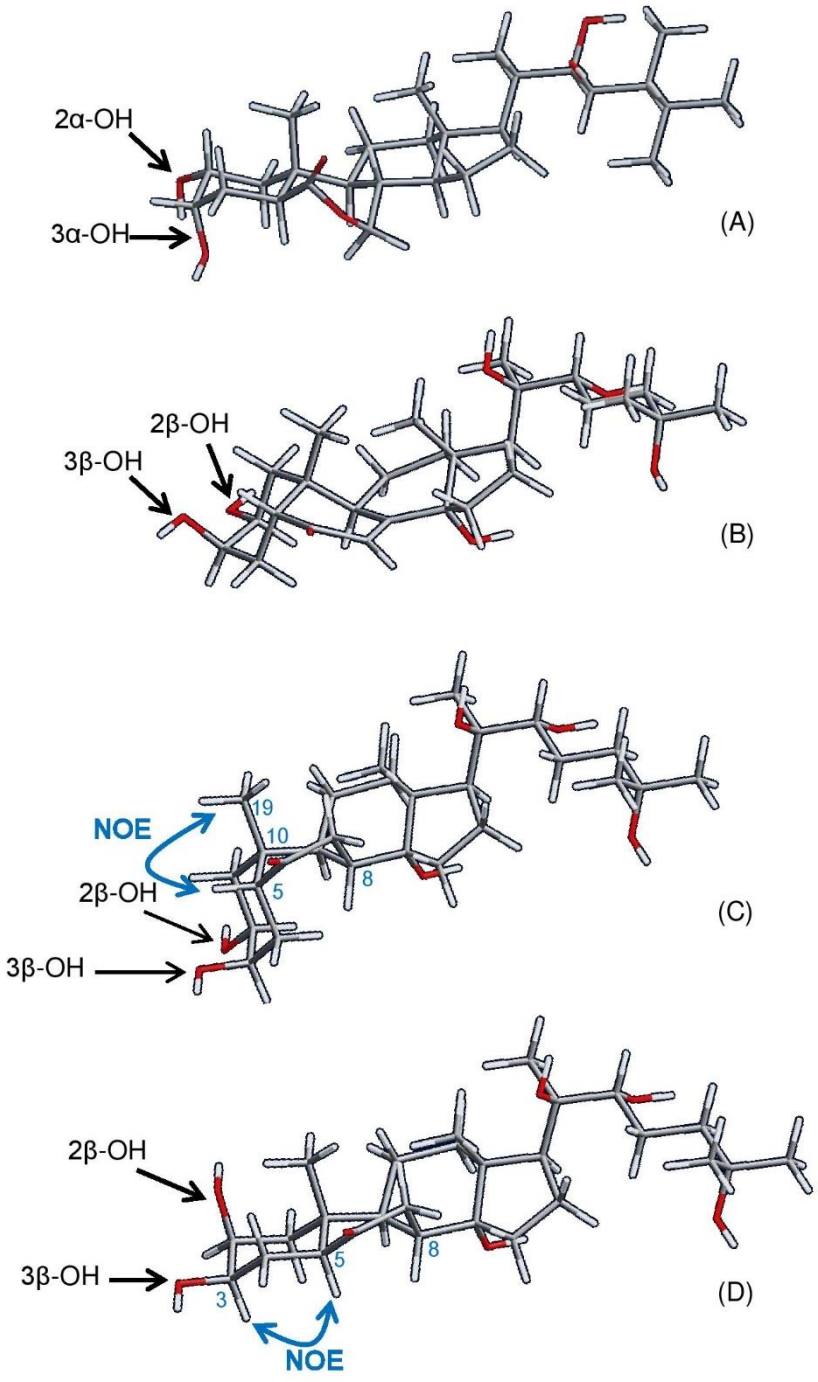

Fig. 2-2 3D chemical structures of the ecdysteroid analogues

Brassinolide (BL, A), 20-hydroxyecdysone (ECD, B), 7,8-dihydro-8α-20-hydroxyecdysone (DHECD, C), and 7,8-dihydro-5α,8α-20-hydroxyecdysone (α-DHECD, D). Two headed arrows indicate NOE correlation.

2.2 Results

2.2.1 Concentrations of brassinosteroids on rice lamina inclination and *Arabidopsis* growth

BL is known to strongly induce rice lamina inclination. The lamina joint of rice was treated with various concentrations of BL, ECD, DHECD, or α-DHECD, and the angle of inclination of the lamina was measured. DHECD and α-DHECD induced significant lamina bending, with the angle dependent on the concentration of the chemical (Fig. 2-3), but the effect of BL was greater. The lamina angle in rice treated with ECD was not significantly different from that of the control (Fig. 2-3). This result suggests that DHECD and α-DHECD should have BR-like activity in rice lamina inclination. In the further experiments, I used chemical concentration that caused the highest degree of lamina inclination. As 10^{-6} M of all compounds showed the most lamina bending activity (Fig. 2-3), those compounds at this concentration were tested. However, 10^{-6} M BL strongly reduced hypocotyl length of wild-type *Arabidopsis* (Fig. 2-4A) and BL significantly decreased root length associated with concentrations (Fig. 2-4B). Because BL clearly showed the inhibition of root elongation, I used this parameter to calculate the half inhibitory concentration (IC_{50}) of each compounds by IC_{50} Tool Kit from http://ic50.tk/index.html. The results showed that IC_{50} of BL, ECD, DHECD and α-DHECD were $\leq 10^{-10}$, $\geq 10^{-4}$, 1.16×10^{-5} and 1.04×10^{-5} M, respectively (Fig. 2-5). It was confirm that BL at 10^{-6} M is toxic on *Arabidopsis* root. Based on this reason, 10^{-8} M BL was used instead of 10^{-6} M BL in the following experiments.

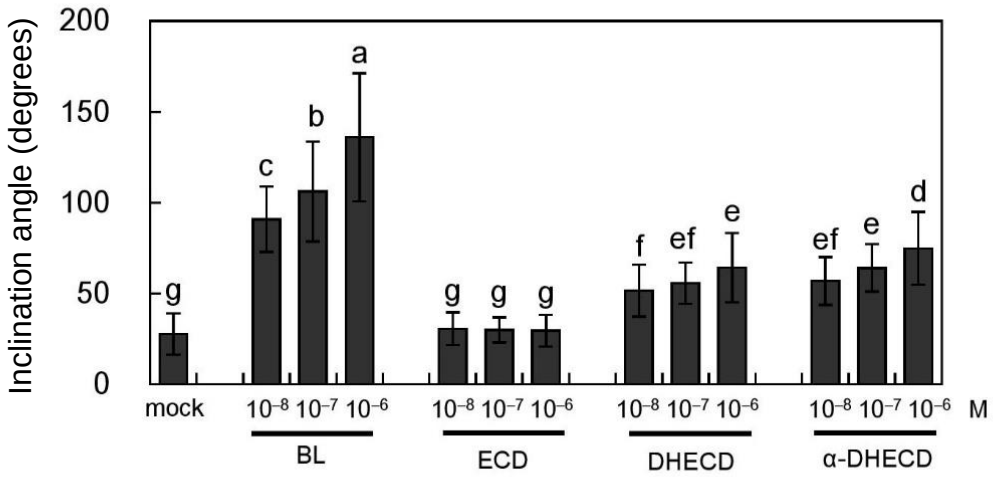

Fig. 2-3 Effect of brassinolide and ecdysteroid analogues on rice lamina inclination

DHECD and α-DHECD have the weak effect on the increase of rice lamina inclination. Data are the means of 30 replicates. Standard deviations are shown as vertical error bars. Means followed by the same letter are not significantly different at $p \leq 0.05$ according to Duncan's multiple range test.

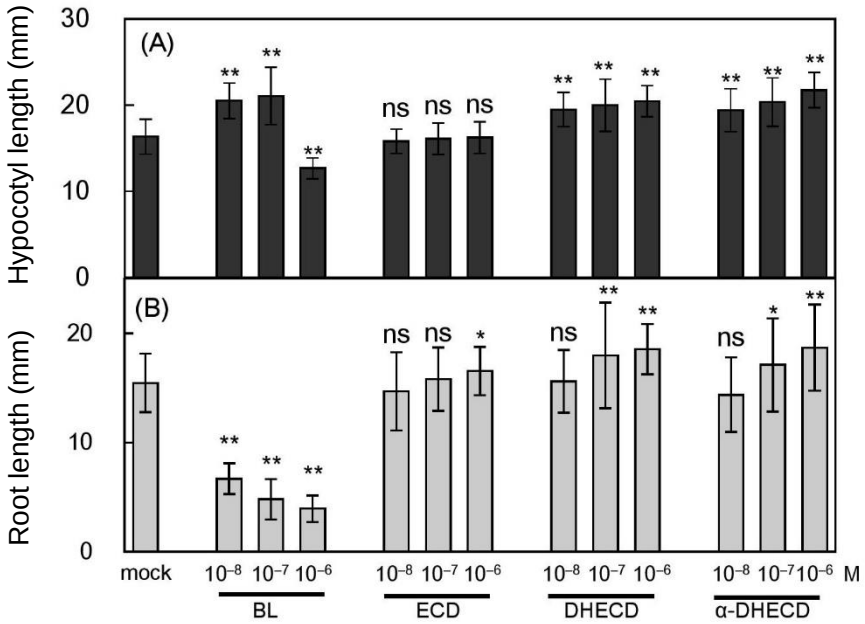

Fig. 2-4 Hypocotyl and root elongation of wild-type *Arabidopsis* treated with various concentrations of brassinolide and ecdysteroid analogues

Effects of various concentrations of BL, ECD, DHECD, and α-DHECD on hypocotyl length (A) and root length (B) in 10 days dark-grown wild-type *Arabidopsis*. Data are the means of 40 seedlings. Standard deviations are shown as vertical error bars. Statistically significant differences relative to the control are $^{**}p \leq 0.01$, $^{*}p \leq 0.05$, and ns: nonsignificant by Student's *t* test.

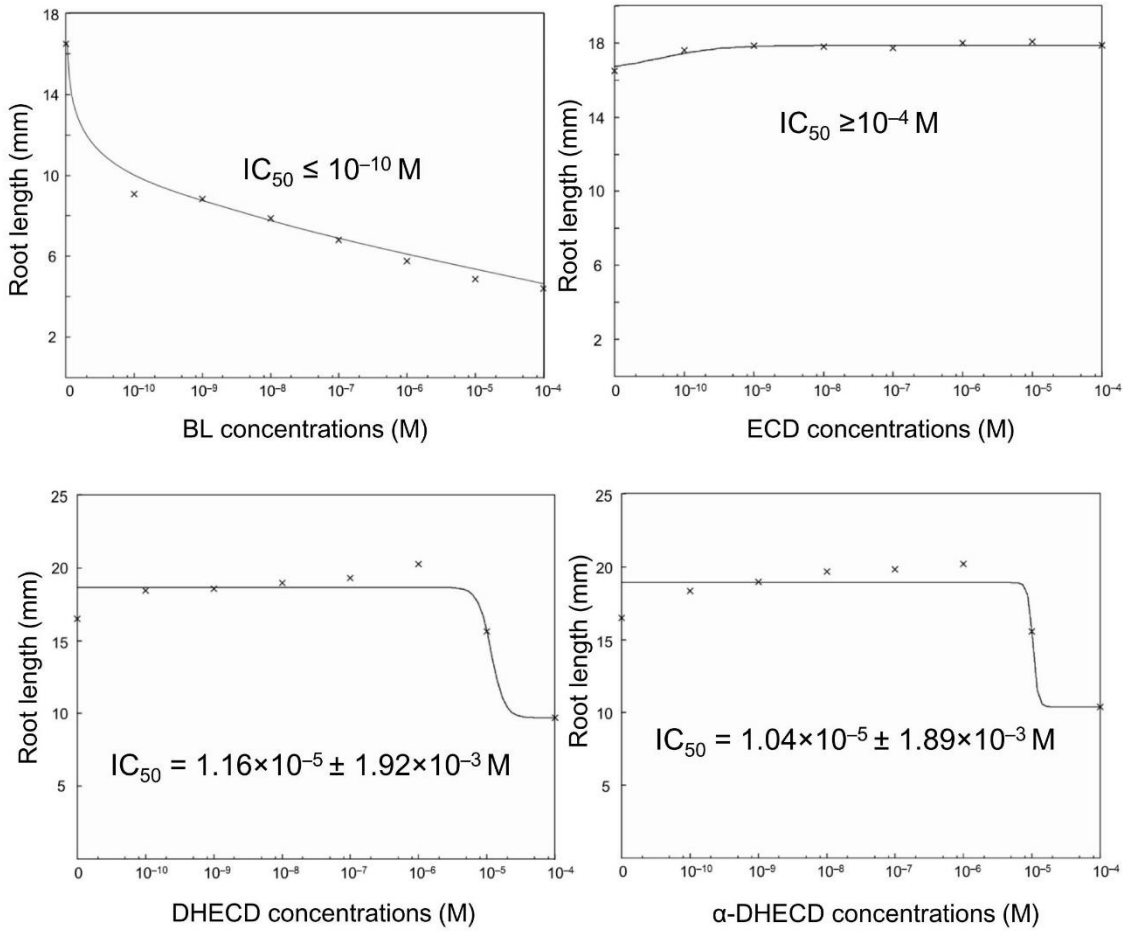

Fig. 2-5 The half inhibitory concentration (IC_{50}) of brassinolide and ecdysteroid analogues

BL (A), ECD (B), DHECD (C), and α-DHECD (D). The IC_{50} values were calculated from the inhibition of root elongation by each of compound. Wild-type *Arabidopsis* were grown 10 days under darkness. Data are the means of 20 seedlings. IC_{50} was calculated by IC_{50} Tool Kit (http://ic50.tk/index.html).

2.2.2 Effect of ecdysteroid analogues on *Arabidopsis* growth

In wild-type *Arabidopsis*, 10^{-8} M BL treatment significantly increased the hypocotyl length, but reduced the root length, whereas 10^{-6} M DHECD and 10^{-6} M α-DHECD increased both the hypocotyl and root lengths. However, ECD had no effect on hypocotyl or root elongation in *Arabidopsis* (Table 2-1A; Fig. 2-6A). The increase of hypocotyl elongation that observed in BL, DHECD and α-DHECD treatment showed that those compounds caused the negative response on photomorphogenesis.

Then, the specific BR biosynthesis inhibitor brassinazole (Brz) [22, 23] was used to clarify the functions of ECD, DHECD, and α-DHECD as BR mimics. The results showed that 0.3 and 3 μM Brz significantly reduced the hypocotyl length in wild-type *Arabidopsis*, but this effect was reversed by the application of BL. DHECD and α-DHECD also reversed this effect in wild-type *Arabidopsis* treated with 0.3 μM Brz, but not in the plants treated with 3 μM Brz. ECD had no effect on hypocotyl length at either Brz concentration (Tables 2-1B and C, Figs. 2-6B and C). Although the BL treatment recovered the dwarf phenotype of the wild-type *Arabidopsis* hypocotyls treated with Brz, it significantly reduced the root length. In contrast, DHECD or α-DHECD caused a significant increase root length of wild-type *Arabidopsis* treated with Brz (Tables 2-1B, C; Figs. 2-6B, C).

Moreover, BR-biosynthesis *det2* mutant was used to investigate the BR mimic activity of ECD, DHECD, and α-DHECD. The *det2* mutant showed the light-adapted response indicating with the shortened hypocotyls and opened cotyledons under darkness. The treatment of *det2* mutant hypocotyls with 10^{-6} M DHECD or 10^{-6} M α-DHECD reversed the *det2* dwarf phenotype by increasing the hypocotyl length, but to a lesser extent than did 10^{-8} M BL. ECD treatment had no effect on *det2* hypocotyl elongation. The effects of DHECD and α-DHECD on *det2* root length were similar to their effects in wild-type *Arabidopsis*, whereas BL application significantly reduced the root length in the *det2* mutant, both DHECD and α-DHECD increased the root length (Table 2-2; Fig. 2-6D).

Table 2-1 Effects of BL, ECD, DHECD, and α-DHECD on hypocotyl and root length in wild-type *Arabidopsis*

Wild-type *Arabidopsis* treated without Brz (A) and wild-type *Arabidopsis* treated with 0.3 μM Brz (B) or 3 μM Brz (C). Plants were grown in the dark for 10 days.

Treatment	Hypocotyl length (mm)[1]	Root length (mm)[1]
(A) Control	17.46 ± 2.38b	13.82 ± 2.20b
BL 10^{-8} M	21.32 ± 1.56a	6.21 ± 1.41c
ECD 10^{-6} M	17.87 ± 2.47b	13.42 ± 2.40b
DHECD 10^{-6} M	20.74 ± 2.23a	15.26 ± 2.12a
α-DHECD 10^{-6} M	21.06 ± 1.51a	15.75 ± 2.39a
(B) Control	17.46 ± 2.38a	13.82 ± 2.20b
Brz 0.3 μM	7.29 ± 1.21d	11.41 ± 2.26c
BL 10^{-8} M + Brz 0.3 μM	17.26 ± 1.90a	7.22 ± 2.22e
ECD 10^{-6} M + Brz 0.3 μM	7.29 ± 0.77d	10.16 ± 1.65d
DHECD 10^{-6} M + Brz 0.3 μM	10.31 ± 1.56c	14.90 ± 2.00a
(C) Control	17.46 ± 2.38a	13.82 ± 2.20a
Brz 3 μM	2.06 ± 0.41c	8.90 ± 1.98b
BL 10^{-8} M + Brz 3 μM	8.42 ± 2.50b	5.95 ± 1.69c
ECD 10^{-6} M + Brz 3 μM	2.17 ± 0.35c	9.02 ± 1.42b
DHECD 10^{-6} M + Brz 3 μM	2.25 ± 0.51c	14.52 ± 2.10a

[1]Data are the means of 40 seedlings ± SD. Means followed by the same letter are not significantly different at $p \leq 0.05$ according to Duncan's multiple range test.

Table 2-2 Effects of BL, ECD, DHECD, and α-DHECD on hypocotyl and root length in the *Arabidopsis det2* mutant

Arabidopsis det2 mutants were grown in the dark for 10 days.

Treatment	Hypocotyl length (mm)[1]	Root length (mm)[1]
Control	2.86 ± 0.40d	6.68 ± 1.84b
BL 10^{-8} M	11.66 ± 2.51a	4.79 ± 1.26c
ECD 10^{-6} M	2.99 ± 0.70d	5.14 ± 2.08c
DHECD 10^{-6} M	4.11 ± 0.52c	7.42 ± 2.05ab
α-DHECD^{-6} M	4.73 ± 0.73b	7.69 ± 1.98a

[1]Data are the means of 40 seedlings ± SD. Means followed with the same letter are not significantly different at $p \leq 0.05$ according to Duncan's multiple range test.

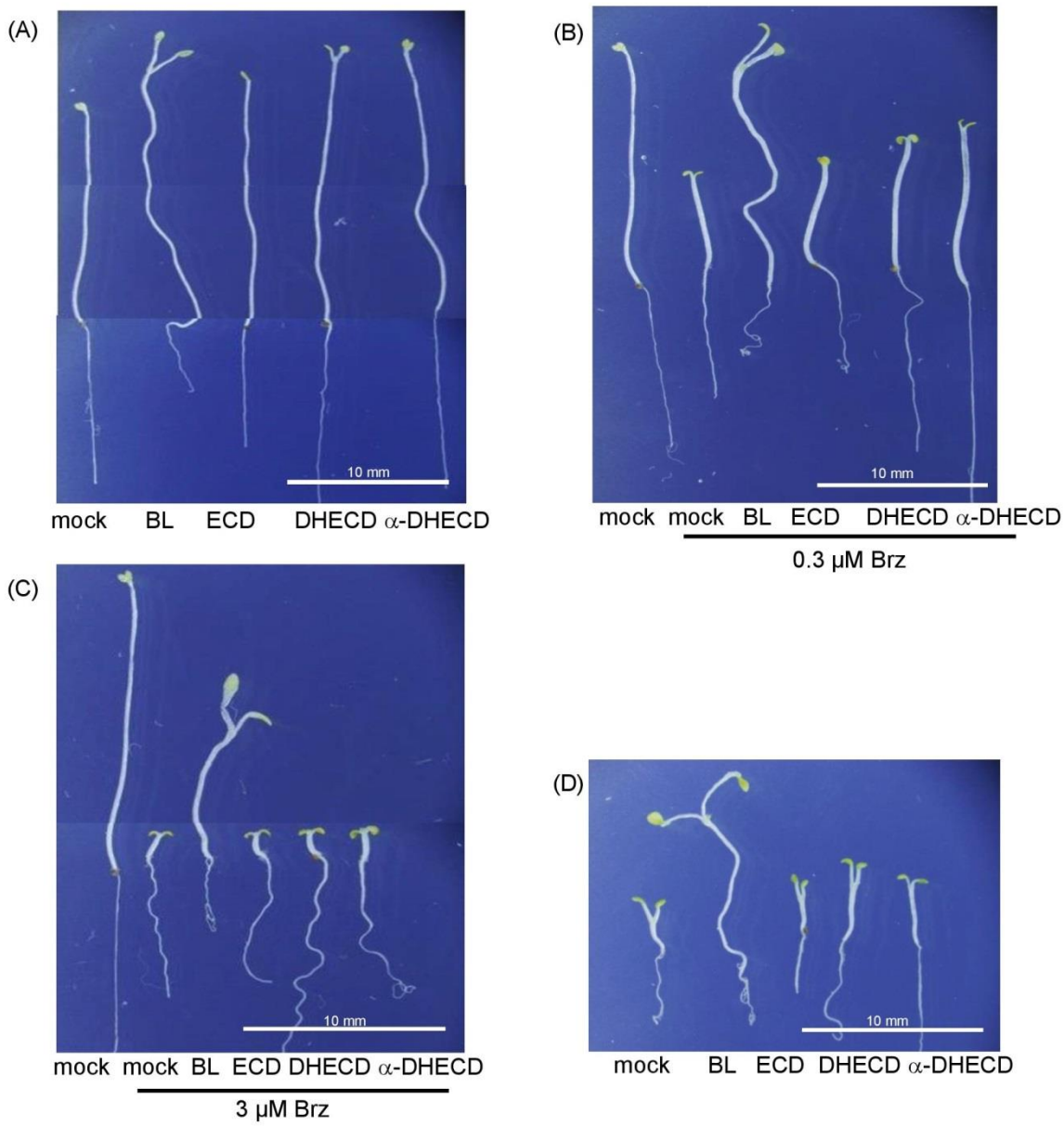

Fig. 2-6 Effect of brassinolide and ecdysteroid analogues on *Arabidopsis* growth

Arabidopsis hypocotyls and roots following treatment with 10^{-8} M BL, 10^{-6} M ECD, 10^{-6} M DHECD, and 10^{-6} M α-DHECD for 10 days. Wild-type *Arabidopsis* (A); wild-type *Arabidopsis* treated with 0.3 μM Brz (B); wild-type *Arabidopsis* treated with 3 μM Brz (C); and *Arabidopsis det2* mutant (D). Scale bars represent 10 mm.

2.2.3 Expression of BR-related genes under treatment of ecdysteroid analogues

To assess the regulatory effects of ECD, DHECD, and α-DHECD, I investigated the relative expression of BR-responsive genes in *Arabidopsis* treated with these compounds. The quantitative real-time PCR (qRT–PCR) showed that the expression of BR biosynthesis genes (*DWF4* and *CPD*) in BL-treated wild-type *Arabidopsis* was significantly down-regulated by negative feedback [24, 25]. Moreover, in BL-treated wild-type *Arabidopsis*, the expression of *TCH4* (a xyloglucan-endotransglycosylase-encoding gene that is usually induced by BR treatment) and *SAUR-AC1* (an early auxin-inducible gene that is regulated independently by BR) was up-regulated [24, 25]. Conversely, the expression of *DWF4* and *CPD* was up-regulated in BR-deficient plants, including Brz-treated wild-type *Arabidopsis* and the BR-biosynthesis *det2* mutant. Similarly, the expression of *TCH4* and *SAUR-AC1* was down-regulated in the BR-deficient plants (Fig. 2-7).

As shown in the physiological analysis based on hypocotyl elongation, the BR-related gene expression patterns in the DHECD- and α-DHECD-treated plants were similar. In these experiments BR-deficient *det2* mutant was more sensitive to BR-treatment stimulating gene expression of *TCH4* and *SAUR-AC1* than wild-type *Arabidopsis*. DHECD and α-DHECD also induced significant expression of the *TCH4* and *SAUR-AC1* genes in the *det2* mutant (Figs. 2-7C, D). The expression of *DWF4* in *det2* was down-regulated by both DHECD and α-DHECD, in a similar way to the down-regulation caused by BL treatment (Fig. 2-7A). Furthermore, the expression of the biosynthesis gene *CPD* in wild-type *Arabidopsis* was also down-regulated by DHECD and α-DHECD (Fig. 2-7B), whereas ECD rarely have no significant effect on BR-related gene expression (Fig. 2-7). This result parallels those in the experiments based on rice lamina inclination and *Arabidopsis* hypocotyl elongation.

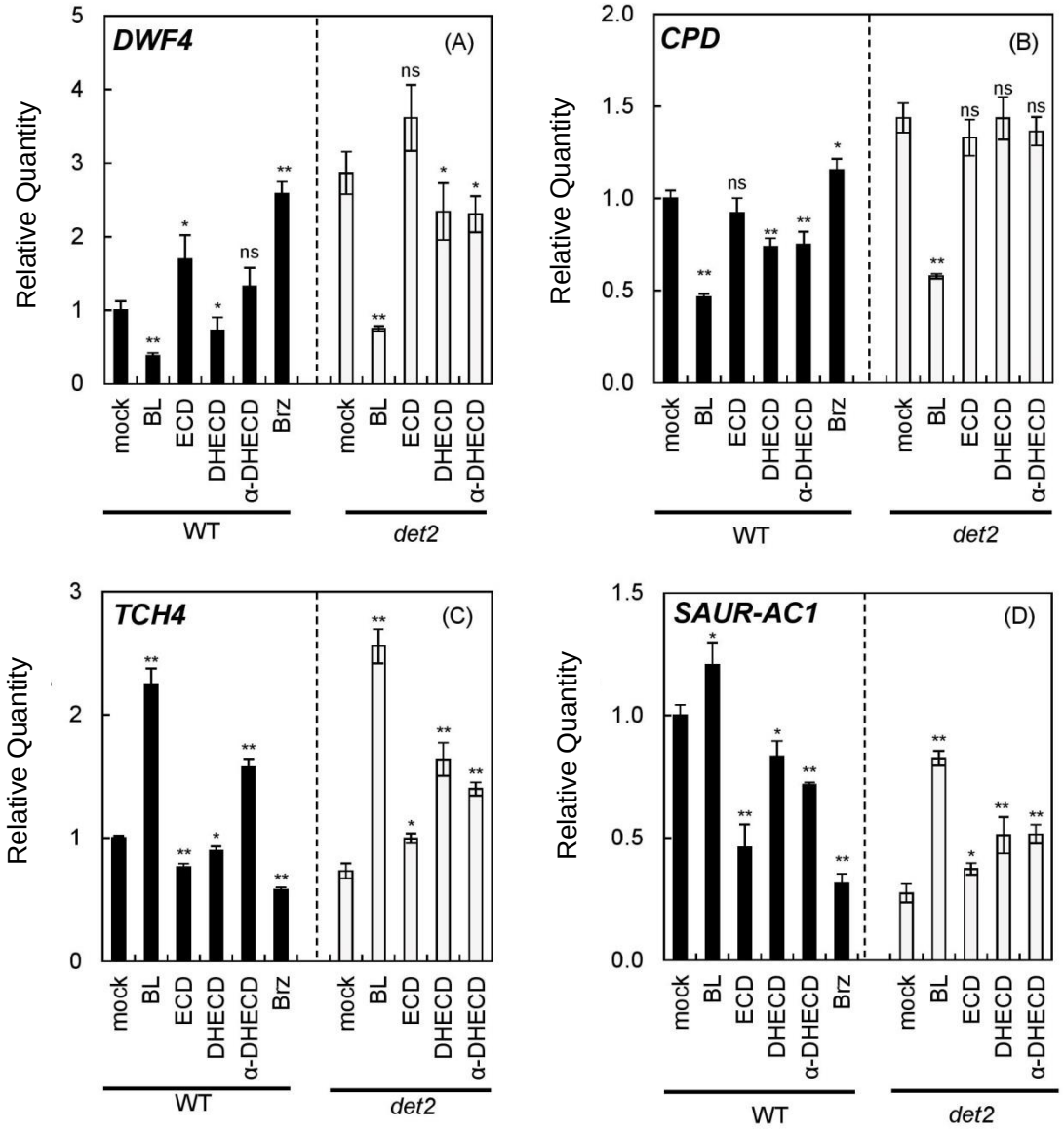

Fig. 2-7 Effect of brassinolide and ecdysteroid analogues on BR-related genes expression

Quantitative real-time PCR analysis of *DWF4* (A), *CPD* (B), *TCH4* (C), and *SAUR-AC1* (D) expression in wild-type *Arabidopsis* (WT) and the BR-biosynthesis *det2* mutant (*det2*) as controls or in plants treated with 10^{-8} M BL, 10^{-6} M ECD, 10^{-6} M DHECD, or 10^{-6} M α-DHECD. Data are the means of four replicates. Standard deviations are shown as vertical error bars. Statistically significant differences relative to the control are $^{**}p \leq 0.01$, $^{*}p \leq 0.05$, and ns: nonsignificant by Student's *t* test.

2.2.4 The phosphorylation status of BIL1/BZR1 protein under treatment of ecdysteroid analogues

Phosphorylation status of BIL1/BZR1 (hereafter BIL1) is generally used to identify BR-related signaling. BR-treatment induces the dephosphorylation of BIL1 that can be detected as a decrease of BIL1 molecular weight [26]. To reveal whether ECD, DHECD and α-DHECD mimic BR effects through BR signaling pathway, the phosphorylation states of BIL1-GFP protein with these three hydroxysteroidal compounds was analyzed by immune blotting using anti-GFP antibody.

The result showed that 10^{-8} M BL treatment exhibited a higher ratio of dephosphorylated BIL1 to phosphorylated BIL1 (de P-BIL1/P-BIL1) than control treatment (Fig. 2-8). The 10^{-6} M α-DHECD-treated plants exhibited the slightly higher ratio of de P-BIL1/P-BIL1 than control treatment (Fig. 2-8). ECD and DHECD treatment did not show the increase of de P-BIL1/P-BIL1 ratio (Fig. 2-8). Since BR-deficient mutants such as *det2* or BR-deficient plants caused by Brz treatment were more sensitive to BR than wild-type *Arabidopsis* or by control treatment respectively, I also checked the effect of these compounds on the status of BIL1-GFP protein in Brz-treated plants. Moreover, three hydroxysteroidal compounds were used at higher concentrations than in former experiments at 10^{-5} M and 10^{-4} M in expectation of the clear result. Control treatment of *BIL1-GFP Arabidopsis* gave a low ratio of de P-BIL1/P-BIL1. On the other hand, 10^{-8} M BL treatment exhibited a higher ratio of de P-BIL1/P-BIL1 than control treatment (Fig. 2-9). At 10^{-5} M, the de P-BIL1/P-BIL1 ratio of DHECD- or α-DHECD-treated plants were slightly different form that of the control (Fig. 2-9), whereas at 10^{-4} M both treatments gave as high de P-BIL1/P-BIL1 ratios as BL treatment (Fig. 2-9). However, ECD did not show a clear effect on BR signaling even at 10^{-4} M (Fig. 2-9).

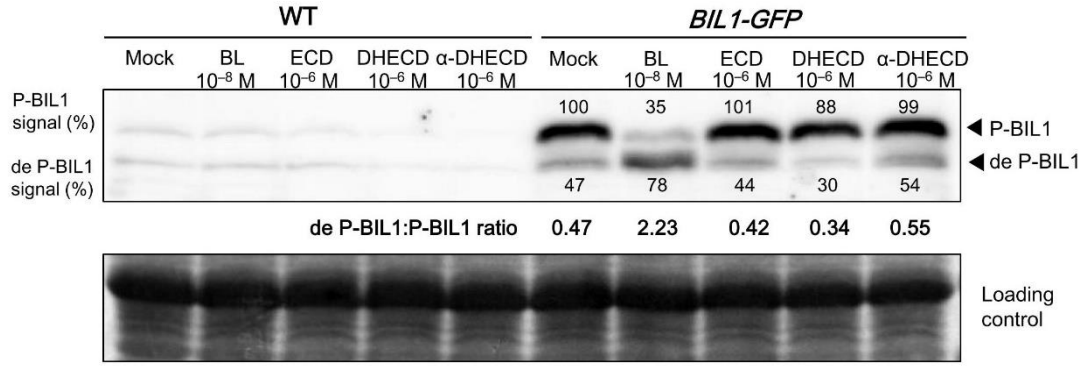

Fig. 2-8 Phosphorylation status of BIL1/BZR1 protein under the normal condition

DHECD and α-DHECD at 10^{-6} M showed the slightly higher ratio of dephosphorylated BIL1 to phosphorylated BIL1 (de P-BIL1:P-BIL1 ratio) than control (mock). The signal intensities of P-BIL1 and de P-BIL1 are shown by the top and below arrowheads, respectively. Gel was stained with Ponceau to indicate total proteins used as loading control.

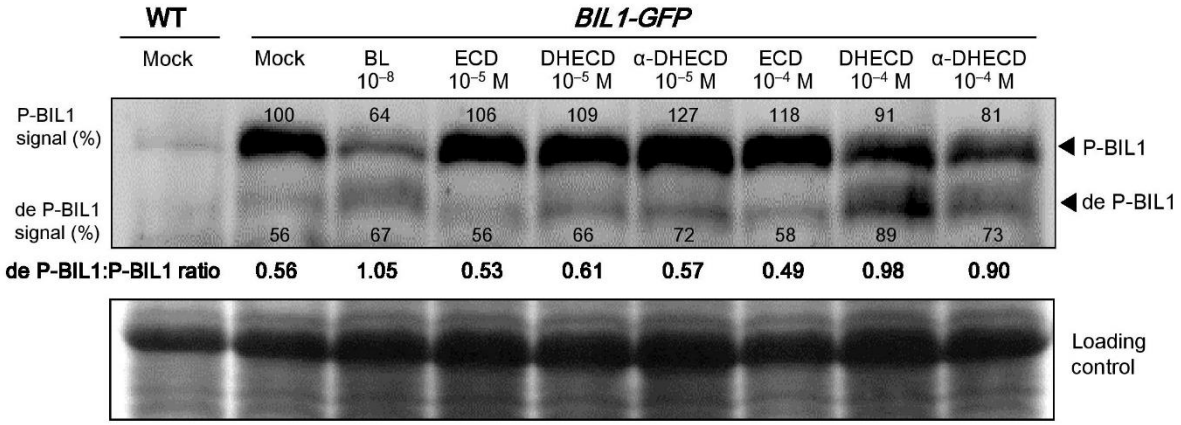

Fig. 2-9 Phosphorylation status of BIL1/BZR1 protein under the treatment of brassinazole

DHECD and α-DHECD at 10^{-4} M have the same dephosphorylated BIL1 to phosphorylated BIL1 ratios (de P-BIL1:P-BIL1 ratio) as BL. The signal intensities of P-BIL1 and de P-BIL1 are shown by the top and below arrowheads, respectively. Gel was stained with Ponceau to indicate total proteins used as loading control.

2.3 Discussion

Since the discovery of BRs and their potential applications, several BR analogues have been synthesized, allowing their large-scale economic production. In this study, I has demonstrated that the hydroxysteroidal compounds, DHECD and α-DHECD mimicked the function of BRs, promoting the rice lamina bending (Fig. 2-3) and reversing BR-deficient dwarfism in dark-grown *Arabidopsis* seedlings (Tables 2-1B, C and Table 2-2). The rice lamina inclination test is a very sensitive bioassay for BRs, so it is useful for assessing whether test compounds have BR-like activity [27, 28]. Therefore, both DHECD and α-DHECD were found to have a BR-like effect on lamina inclination, but were less active than BL (Fig. 2-3).

The hypocotyl length of the wild-type *Arabidopsis* treated with BL, DHECD, or α-DHECD was significantly increased (Table 2-1). Low concentrations of BR at nM concentrations have been reported to enhance hypocotyl elongation [6, 29], resulting from cell enlargement [3]. I found that high concentrations of BL significantly reduced root elongation in wild-type *Arabidopsis*, which differed from the results for both DHECD and α-DHECD (Table 2-1). Previous reports have suggested that the exogenous application of BR at low concentrations promotes root elongation, but at high concentrations BRs inhibit root growth [30, 31]. Müssig et al. [31] reported that 24-epibrassinolide concentrations that higher than 10^{-9} M exhibited the inhibition of root growth in wild-type *Arabidopsis*. Moreover, IC_{50} of each chemicals showed that BL had higher IC_{50} considering from root inhibition than DHECD and α-DHECD (Fig. 2-5). It implies that DHECD and α-DHECD concentration had the toxic on root growth lower than BL. This can explain why treatment with DHECD or α-DHECD promoted root elongation, even at high concentrations. As suggested by their effects on hypocotyl elongation, the effectiveness of DHECD and α-DHECD was less than that of BL. Therefore, at high concentrations, these two chemicals may have a similar effect as low concentrations of BR, and promote root elongation. When DHECD or α-DHECD was applied to hypocotyls in the presence of Brz, the hypocotyl shortening caused by 0.3 μM Brz was reversed (Table 2-1B), but in the presence of 3 μM Brz, the hypocotyl shortening

was not reversed (Table 2-1C). Brz is the specific BR biosynthesis inhibitor that inhibits C-22 hydroxylation in the BR biosynthesis pathway [23]. Brz induces dwarfism in many plants, including *Arabidopsis*, but this is reversible by the application of BRs [22, 23]. Therefore, my results suggest that DHECD and α-DHECD have the same functions as BRs. The *Arabidopsis det2* mutant was also used to clarify the functions of ECD, DHECD, and α-DHECD. The *det2* mutant is a BR-biosynthesis mutant that produces shorter hypocotyls in the dark than does the wild-type [32, 33]. The *det2* phenotype can be reversed by the addition of BRs [34]. The treatment of *det2* mutant plants with DHECD or α-DHECD significantly reversed their dwarfism, although to a lesser extent than BL, whereas treatment with ECD had no effect on their dwarfism (Table 2-2). These results also strongly suggest that DHECD and α-DHECD should mimic the effects of BR.

The regulatory effects of ECD, DHECD, and α-DHECD on the expression of four BR-responsive genes: *DWF4*, *CPD*, *TCH4*, and *SAUR-AC1* were investigated. The results showed that treatment with DHECD or α-DHECD significantly reduced *DWF4* mRNA expression in the *det2* mutant compared with that in the control, but ECD had no effect (Fig. 2-7A). DHECD and α-DHECD also significantly increased *TCH4* and *SAUR-AC1* expression in the *det2* mutant (Figs. 2-7C, D). *DWF4* and *CPD* are BR biosynthesis genes that are down-regulated by BR [1, 35], whereas *TCH4* and *SAUR-AC1* which are BR-specific expression genes are up-regulated by BR [36, 37]. These results suggest that DHECD and α-DHECD also regulate the expression of BR-related genes.

The phosphorylation status of the marker BIL1 protein was performed to demonstrate the efficacy of the hydroxysteroidal compounds on BR signaling. Phosphorylation status is modulated by BR signals showed on the increase of the dephosphorylated form of BR transcriptional factor such as BIL1 and BES1 [26, 38]. When plants were grown on Brz-containing medium, BL treatment clearly gave the high ratio of dephosphorylated BIL1 to phosphorylated BIL1 (Fig. 2-9). Among three hydroxysteroidal compounds, DHECD and α-DHECD treatments showed the higher ratios of dephosphorylated BIL1 to phosphorylated BIL1 than control and ECD treatment (Figs. 2-8 and 2-9). These results indicated that DHECD and α-DHECD should mimic

BR function mediated through the BR signal pathway while ECD should not. In this experiment effect of DHECD and α-DHECD were enhanced in BL deficient condition, as was the case in the recovery of hypocotyl elongation by DHECD or α-DHECD treatment in Brz-treated plants (Table 2-1B).

Among the three hydroxysteroid compounds, I found that DHECD and α-DHECD mimicked BRs in the biological assay systems tested in this study. Differences in the effectiveness of these compounds may be a consequence of their different structures, stability or plant species used for bioassays [39]. Generally, BRs consist of four rings (A, B, C, and D) forming a steroid nucleus and a side chain attached to C-17 of D ring as is the case with cholesterol [10, 40]. Studies of the structure–activity relationships of both natural and synthetic BR analogues have shown that the structures essential for high BR activity are: (1) an α-oriented hydroxyl group at either C-2 (2α-OH) or C-3 (3α-OH) in the A-ring; (2) a *trans* A/B ring junction; (3) oxygen at C-6, in the form of either a ketone or lactone in the B-ring; and (4) either a methyl or an ethyl group at C-24 in the side chain [40, 41].

The BR analogues displaying high BR activity will have a structure compatible with a binding site of the BR receptor. In *Arabidopsis*, BRI1 has been identified as the BR receptor, and consist of a leucine-rich repeat (LRR), a 70-amino-acid island domain in the N-terminal receptor-like kinase transmembrane domain, and a Ser/Thr kinase domain in the C-terminal region [42, 43]. BRI1 forms a heterodimer through its LRR repeat and Ser/Thr-type transmembrane kinase domain with members of the somatic embryogenesis receptor kinase (SERK) family, such as SERK1 and SERK3 [44, 45]. SERK3 was also identified as a functionally cooperative receptor of BRI1 which is referred to as BAK1 [46, 47]. BR is folded between the N-terminal capping domain of SERK1 and the 70-amino-acid island domain binding pocket of BRI1. The histidine residue of SERK1 also establishes hydrogen bonds with both the 2α- and 3α-hydroxyl groups of BR [45]. Lee et al. [48] reported that 2-epicastasterone (2-epiCS) and 2,3-diepicastasterone (2,3-diepiCS), which have 2β,3α- and 2β,3β-diol moieties, respectively, but lack the 2α,3α-diol moiety that is assumed to be important for potent BR activity,

showed 50 and 500 times less activity, respectively, than castasterone. This indicates that the 2α,3α-diol moiety in the A-ring of BR is necessary for its binding to the SERK co-receptor, which induces BR responses. However, it is important that 2-epiCS and 2,3-diepiCS are still active.

DHECD was synthesized by catalytic hydrogenation, which is a *cis*-reduction of the unsaturated bond on the B-ring of ECD [15]. The α-orientation of the H-8 was established by the splitting pattern and coupling constants of H-7α, H-7β and H-8 and the *cis*-relation of H-8 and H-9 in the ^{1}H NMR spectra of DHECD. The *cis*-A/B ring junction was evident from the *cis*-nature of the H-5 and the methyl group at C-10 (19-Me group) which was confirmed by the nuclear overhauser effect (NOE) correlation between H-5 and 19-Me at C-10 [15] (Fig. 2-2C). Base-catalyzed epimerization of H-5 yielded α-DHECD. The α-orientation of H-5 in α-DHECD was established by the large coupling constant of H-5 and the NOE correlation between H-5 and H-3 (Fig. 2-2D). Both DHECD and α-DHECD have a saturated ketone group at the B-ring, which is similar to that in the active BR castasterone. The major difference between castasterone and the three hydroxysteroids considered in this study are: 1) the B/C ring junctions of DHECD and α-DHECD are *cis*, whereas those of castasterone are *trans*; and 2) ECD, DHECD, and α-DHECD have 2β,3β-dihydroxyl groups at the A-ring, whereas castasterone has 2α,3α-dihydroxyl groups. The 3D structures show that the reduction of the unsaturated bond in the B-ring of ECD to form DHECD and/or α-DHECD causes a change in the spatial relationship between the 2β,3β-diol moiety and the methyl group in the C10 position which was confirmed by NOE (Figs. 2-2B, C, D). In the case of DHECD and α-DHECD, the altered configuration differs from that of ECD (Figs. 2-2B, C, D). This difference in chemical structure may explain why ECD shows no BR-like activity, whereas DHECD and α-DHECD show a weak but appreciable BR-like activity. Treatment with α-DHECD caused a significant increase in hypocotyl elongation in both wild-type *Arabidopsis* treated with 0.3 μM Brz and the *det2* mutant, and had a little bigger effect than did treatment with DHECD (Tables 2-1B and 2-2). The difference between DHECD and α-DHECD is in the structure of the A/B ring junction. DHECD has a *cis* A/B ring junction, whereas α-DHECD has a *trans* A/B ring junction, as occurs in BL (Figs. 2-1 and 2-2) and

castasterone. An evaluation of the biological activity of BR analogs showed that compounds possessing *trans* A/B ring junction were active than compounds possessing *cis* A/B ring junction [49, 50]. However, DHECD induced the ratio of dephosphorylated BIL1 to phosphorylated BIL1 as same as α-DHECD under both normal condition and Brz treatment (Figs. 2-8 and 2-9) indicating that they rather had similar activity on BR signaling.

Another way in which ECD, DHECD, and α-DHECD differ structurally from BR is in the side chain. The three hydroxysteroids have more hydroxyl groups in the side chain than does BL (Fig. 2-1). Analysis of the 3D structure of the BRI1 receptor showed that BR binds to a hydrophobic surface and maps inside the BRI1 superhelix [43]. Because the BRI1 pocket is hydrophobic, BR-like structures including too much hydroxyl groups in the side chain, such as 25-hydroxyBL, a catabolite of BL, can result in a lack of biological activity in plants [43, 51, 52]. This explanation is partly supported by the study by Mazorra et al. [53], who synthesized two spirostanic analogues of castasterone (MH5 and BB6) by substituting a typical BR side chain with a spiroketalic ring. This ring had a less-charged side chain than the side chain in my three hydroxysteroids. MH5 and BB6 exhibited BR mimic effect, but they were less active than BL. In this context no BR-like activity for ECD and the weak activity of DHECD and α-DHECD may be attributable to the hydrophilic side chains in these analogues, especially to the hydroxyl group at 25 position. Based on the above data, combination of 2α,3α-hydroxyl groups and a moderately charged side chain of BR could be important for binding to BRI1/BAK1 receptor complex. However, in my data DHECD and α-DHECD are still active though they have 2β,3β-OH and 25-OH. At present I cannot clearly confirm the reason why both DHECD and α-DHECD are active, but I think that it can be a good clue to design new BR mimics. For example, reducing the polarity of the side chains of DHECD and α-DHECD could be a good try to increase their BR-like activity in a future study.

2.4 Materials and Methods

2.4.1 Chemicals preparation

Brassinolide (BL, Figs. 2-1A and 2-2A), and the hydroxysteroids, ECD (Figs 2-1B and 2-2B), DHECD (Figs. 2-1C and 2-2C), and α-DHECD (Figs. 2-1D and 2-2D) were used as the test chemicals in this study. BL was purchased from Brassino Co., Toyama, Japan. The hydroxysteroidal compounds used in this study were performed by Prof. Dr. Apichart Suksamrarn's group, Department of Chemistry and Center of Excellence for Innovation in Chemistry, Faculty of Science, Ramkhamhaeng University, Thailand. ECD was a natural hydroxysteroid compound obtained from *Vitex glabrata* stem bark [14]. Then, the catalytic hydrogenation was used to reduce the 7,8-unsaturated bond in the B-ring of ECD. The hydrogenating ECD in ethanol and in the presence of sodium nitrite ($NaNO_2$) by using Pd-C as a catalyst gave 7,8-dihydro-8α-20-hydroxyecdysone (DHECD) [15]. Then, 7,8-dihydro-5α,8α-20-hydroxyecdysone (α-DHECD) was obtained in 77% yield by base-catalyzed (2% aqueous Na_2CO_3) epimerization of DHECD. Stock solutions of each chemical prepared by dissolving appropriate amounts of the compound in dimethyl sulfoxide (DMSO), were stored at –20 °C. The test concentrations were prepared from the stock solution, as required.

2.5.2 Rice lamina inclination bioassay

Rice (*Oryza sativa* L.) seeds were grown in the dark over a period of 9 days, and leaf sections consisting of the lamina joint, the lamina 1 cm above the lamina joint, and the leaf sheath 1 cm below the lamina joint were excised for using in the experiment. Solutions (10^{-8}, 10^{-7}, and 10^{-6} M) of BL, ECD, DHECD, and α-DHECD were prepared in 0.1% (v/v) DMSO, and the leaf sections were soaked for 48 h in each BR-related solution. Leaf sections soaked in 0.1% (v/v) DMSO were used as the control. The inclination angle of the lamina joint was measured with a semicircular protractor, and the concentrations of ECD, DHECD, and α-DHECD causing the greatest inclination angle were selected for use in subsequent experiments.

2.4.3 Plant materials, growth conditions, and morphological measurements

Arabidopsis thaliana ecotype Columbia (Col) was used as the wild-type plant. The *Arabidopsis* BR-biosynthesis *det2* mutant was selected as a BR mutant plant showing dwarfism. Seeds were germinated on 1/2 Murashige and Skoog (MS) medium containing 0.8% phytoagar (Duchefa, Haarlem, The Netherlands) and 1.5% sucrose. The medium was supplemented with 0.1% (v/v) DMSO (as the control) or the test chemicals 10^{-8} M BL, 10^{-6} M ECD, 10^{-6} M DHECD, or 10^{-6} M α-DHECD. Plants were grown in the control or treatment medium at 22 °C in the dark for 10 days. The hypocotyl and root lengths were measured with the ImageJ software.

2.4.4 Quantitative real-time PCR

Wild-type *Arabidopsis* and *det2* mutant plants were grown in the dark for 7 days in 1/2 MS medium contained 0.8% phytoagar and 1.5% sucrose. The plants were soaked for 3 h in 0.1% (v/v) DMSO as control, 10^{-8} M BL, 10^{-6} M ECD, 10^{-6} M DHECD, or 10^{-6} M α-DHECD solutions prepared in 1/2 MS medium without phytoagar and sucrose. Plant samples were removed and stored in liquid nitrogen for later RNA extraction. Total RNA was extracted from the samples with the RNeasy Plant Mini Kit (QIAGEN GmbH, Hilden, Germany). The complementary DNA (cDNA) was synthesized using PrimeScript (Takara, Kyoto, Japan), and was used in qRT–PCR. The qRT–PCR was performed according to the instructions provided with the PCR Thermal Cycler Dice (Takara, Tokyo, Japan), using the SYBR Premix ExTaq system (Takara, Shiga, Japan). *ACT2* was used as the constitutively expressed control gene. List of used primers are following;

DWF4-forward: 5′-CATAAAGCTCTTCAGTCACGA-3′
DWF4-reverse: 5′-CGTCTGTTCTTTGTTTCCTAA-3′
CPD-forward: 5′-CACTTCAAAGATGCTCGCACTT-3′
CPD-reverse: 5′-CAGCTCGTAACCGGGACATAG-3′
TCH4-forward: 5′-CGAGTCTTGGAACGCTGAT-3′
TCH4-reverse: 5′-CTTCTTGTTGAAAGCCACGG-3′

SAUR-AC1-forward: 5′-GAGATATGTGGTGCCGGTTT-3′
SAUR-AC1-reverse: 5′-GTATTGTTAAGCCGCCCATT-3′
ACT2-forward: 5′-CGCCATCCAAGCTGTTCTC-3′
ACT2-reverse: 5′-TCACGTCCAGCAAGGTCAAG-3′

2.4.5 Western blot analysis

Wild-type and *BIL1-GFP* transgenic plants were grown under light condition for 7 days in 1/2 MS medium without Brz or with 1 μM Brz. The plants were treated with 0.1% (v/v) DMSO (control), 10^{-8} M BL, 10^{-6} M, 10^{-5} M and 10^{-4} M of ECD, DHECD, or α-DHECD prepared in 1/2 MS medium for 3 h. Then, plants were collected to extract protein by boiling with twice volume per fresh weight of 1×Laemmli buffer (50 mM Tris-HCl, pH 6.8, 100 mM DTT, 2% (w/v) SDS, 0.1% (w/v) bromophenol blue, and 10% (w/v) glycerol). The proteins were separated by electrophoresis using SDS-PAGE (10% acrylamide gel). The electrophoretical proteins were transferred to a nitrocellulose blotting membrane (Amersham, Buckinghamshire, UK) and were blocked in TBS (Tris-Buffered Saline) containing 3% skim milk at room temperature. The nitrocellulose membrane was incubated overnight at 4°C in Western Blot Immuno Booster Solution I (Takara, Tokyo, Japan) with a polyclonal antibody (1:20,000) against GFP (Molecular Probes). After that membrane was washed in TBS containing 1% skim milk at room temperature and was incubated in Western Blot Immuno Booster Solution II (Takara, Tokyo, Japan) with horseradish peroxidase-conjugated secondary antibody (1:50,000; Promega) for 1 h at room temperature. The BIL1-GFP polypeptide was detected by the LAS-4000 mini (Fujifilm, Tokyo, Japan). Images were analyzed by using Multi Gauge Ver3.0 software (Fujifilm, Tokyo, Japan) to determine the relative signal intensity. Dephosphorylated BIL1 to phosphorylated BIL1 ratios (de P-BIL1/P-BIL1) were calculated from their signal intensities.

2.5 References

[1] Fujioka S, Yokota T, Biosynthesis and metabolism of brassinosteroids. Annu Rev Plant Biol. 2003;54:137–164.

[2] Sasse JM. Physiological actions of brassinosteroids: an update. J Plant Growth Regul. 2003;22:276–288.

[3] Müssig C. Brassinosteroid-promoted growth. Plant Biol (Stuttg). 2005;7:110–117.

[4] Asahina M, Tamaki Y, Sakamoto T, Shibata K, Nomura T, Yokota T. Blue light-promoted rice leaf bending and unrolling are due to up-regulated brassinosteroid biosynthesis genes accompanied by accumulation of castasterone. Phytochemistry. 2014;104:21–29.

[5] Singh I, Shono M. Physiological and molecular effects of 24-epibrassinolide, a brassinosteroid on thermotolerance of tomato. Plant Growth Regul. 2005;47:111–119.

[6] Clouse SD, Sasse JM. Brassinosterids: essential regulators of plant growth and development. Annu Rev Plant Physiol Plant Mol Biol. 1998;49:427–451.

[7] Krishna P. Brassinosteroid-mediated stress responses. J Plant Growth Regul. 2003;22:289–297.

[8] Fariduddin Q, Hasan SA, Ali B, Hayat S, Ahmad A. Effect of modes of application of 28-homobrassinolide on mung bean. Turk J Biol. 2008;32:17–21.

[9] Cao Y, Zhao H. Protective roles of brassinolide on rice seedlings under high temperature stress. Rice Sci. 2008;15:63–68.

[10] Grove MD, Spencer GF, Rohwedder WK, Mandava N, Worley JF, Warthen JD, et al. Brassinolide, a plant growth-promoting steroid isolated from *Brassica napus* pollen. Nature. 1979;281:216–217.

[11] Yokota T, Arima M, Takahashi N. Castasterone, a new phytosterol with plant hormone potency from chestnut insect gall. Tetrahedron Lett. 1982;23:1275–1278.

[12] Dinan L. Phytoecdysteroids: biological aspects. Phytochemistry. 2001;57:325–339.

[13] Dinan L, Harmatha J, Volodin V, Lafont R. Phytoecdysteroids: Diversity, biosynthesis and distribution, in: Smagghe G (Ed), Ecdysone: Structures and Functions., Springer Science + Business Media, 2009, pp. 3–45.

[14] Werawattanametin K, Podimuang V, Suksamrarn A. Ecdysteroids from *Vitex*

glabrata. J Nat Prod. 1986;49:365–366.

[15] Suksamrarn A, Tanachatchairatana T, Sirigarn C. Stereoselective catalytic hydrogenation of Δ^7-6-ketosteroids in the presence of sodium nitrite. Tetrahedron. 2002;58:6033–6037.

[16] Festucci-Buselli RA, Contim LAS, Barbosa LCA, Stuart J, Otoni WC. Biosynthesis and potential functions of the ecdysteroid 20-hydroxyecdysone — a review. Botany. 2008;86:978–987.

[17] Golovatskaya IF. Effect of ecdysterone on morphological and physiological processes in plants. Russ J Plant Physiol. 2004;51:407–413.

[18] Katsumi M. Interaction of a brassinosteroid with IAA and GA_3 in the elongation of cucumber hypocotyl sections. Plant Cell Physiol. 1985;26:615–625.

[19] Thussagunpanit J, Jutamanee K, Kaveeta L, Chai-arree W, Pankean P, Suksamrarn A. Effects of brassinosteroid and ecdysone analogue on pollen germination of rice under heat stress. J Pestic Sci 2013;38:105–111.

[20] Thussagunpanit J, Jutamanee K, Kaveeta L, Chai-arree W, Pankean P, Homvisasevongsa S, et al. Comparative effects of brassinosteroid and brassinosteroid mimic on improving photosynthesis, lipid peroxidation, and rice seed set under heat stress. J Plant Growth Regul. 2015;34:320–331.

[21] Thussagunpanit J, Jutamanee K, Sonjaroon W, Kaveeta L, Chai-arree W, Pankean P, et al. Effects of brassinosteroid and brassinosteroid mimic on photosynthetic efficiency and rice yield under heat stress. Photosynthetica. 2015;53:312–320.

[22] Asami T, Min YK, Nagata N, Yamagishi K, Takatsuto S, Fujioka S, et al. Characterization of brassinazole, a triazole-type brassinosteroid biosynthesis inhibitor, Plant Physiol. 2000;123:93–99.

[23] Asami T, Mizutani M, Fujioka S, Godai H, Min YK, Shimadai Y, et al. Selective interaction of triazole derivatives with DWF4, a cytochrome P450 monooxygenase of the brassinosteroid biosynthetic pathway, correlates with brassinosteroid deficiency. J Biol Chem. 2001;276:25687–25691.

[24] Bancos S, Nomura T, Sato T, Molnár G, Bishop GJ, Koncz C, et al. Cytochrome P450 genes involved in brassinosteroid biosynthesis. Plant Physiol. 2002;130:504–513.

[25] Goda H, Shimada Y, Asami T, Fujioka S, Yoshida S. Microarray analysis of

brassinosteroid-regulated genes in Arabidopsis. Plant Physiol. 2002;130:1319–1334.
[26] Shimada S, Komatsu T, Yamagami A, Nakazawa M, Matsui M, Kawaide H, et al. Formation and dissociation of the BSS1 protein complex regulates plant development via brassinosteroid signaling. Plant Cell. 2015;27:375–390.
[27] Maeda E. Rate of lamina inclination in excised rice leaves. Physiol Plantarum. 1965;18:813–827.
[28] Wada K, Marumo S, Abe H, Morishita T, Nakamura K, Uchiyama M, et al. A rice lamina inclination test-a micro-quantitative bioassay for brassinosteroids. Agric Biol Chem. 1984;48:719–726.
[29] Sasse JM. Physiological actions of brassinosteroids, in: Sakurai A, Yokota T, Clouse SD (Eds). Brassinosteroids Steroidal Plant Hormones. Springer-Verlag, Tokyo, 1999, pp. 137–161.
[30] Clouse SD. Molecular genetic studies confirm the role of brassinosteroids in plant growth and development. Plant J. 1996;10:1–8.
[31] Müssig C, Shin GH, Altmann T. Brassinosteroids promote root growth in Arabidopsis. Plant Physiol. 2003;133:1261–1271.
[32] Chory J, Nagpal P, Peto CA. Phenotypic and genetic analysis of *det2*, a new mutant that affects light-regulated seedling development in *Arabidopsis*. Plant Cell Physiol. 1991;3:445–459.
[33] Li J, Nagpal P, Vitart V, McMorris TC, Chory J. A role for brassinosteroids in light-dependent development of *Arabidopsis*. Science. 1996;272:398–401.
[34] Fujioka S, Li J, Choi YH, Seto H, Takatsuto S, Noguchi T, et al. The Arabidopsis *deetiolated2* mutant is blocked early in brassinosteroid biosynthesis. Plant Cell. 1997;9:1951–1962.
[35] Tanaka K, Asami T, Yoshida S, Nakamura Y, Matsuo T, Okamoto S. Brassinosteroid homeostasis in Arabidopsis is ensured by feedback expressions of multiple genes involved in its metabolism. Plant Physiol. 2005;138:1117–1125.
[36] Iliev EA, Xu W, Polisensky DH, Oh M, Torisky RS, Clouse SD, et al. Transcriptional and posttranscriptional regulation of Arabidopsis *TCH4* expression by diverse stimuli. Roles of cis regions and brassinosteroids. Plant Physiol. 2002;130:770–783.
[37] Nakamura A, Shimada Y, Goda H, Fujiwara MT, Asami T, Yoshida S. AXR1 is

involved in BR-mediated elongation and *SAUR-AC1* gene expression in Arabidopsis, FEBS Lett. 2003;553:28–32.

[38] Ryu H, Kim K, Cho H, Park J, Choe S, Hwang I. Nucleocytoplasmic shuttling of BZR1 mediated by phosphorylation is essential in *Arabidopsis* brassinosteroid signaling. Plant Cell. 2007;19:2749–2762.

[39] Gomes MMA. Physiological effects related to brassinosteroid application in plants, in: Hayat S, Ahmad A (Eds.), Brassinosteroids: A Class of Plant Hormone, Springer Science+Business Media, New York, 2011, pp. 193–242.

[40] Mandava NB. Plant growth-promoting brassinosteroids. Annu Rev Plant Physiol Plant Mol Biol. 1988;39:23–52.

[41] Brosa C. Structure-activity relationship, in: Sakurai A, Yokota T, Clouse SD (Eds), Brassinosteroids Steroidal Plant Hormones., Springer-Verlag, Tokyo, 1999, pp. 191–222.

[42] Li, J, Chory J. A putative leucine-rich repeat receptor kinase involved in brassinosteroid signal transduction. Cell. 1997;90:929–938.

[43] Hothorn M, Belkhadir Y, Dreux M, Dabi T, Noel JP, Wilson IA, et al. Structural basis of steroid hormone perception by the receptor kinase BRI1. Nature. 2011;474:467–471.

[44] Bojar DD, Martinez J, Santiago J, Rybin V, Bayliss R, Hothorn M. Crystal structures of the phosphorylated BRI1 kinase domain and implications for brassinosteroid signal initiation. Plant J. 2014;78:31–43.

[45] Santiago J, Henzler C, Hothorn M. Molecular mechanism for plant steroid receptor activation by somatic embryogenesis co-receptor kinases. Science. 2013;341:889–892.

[46] Li J, Wen J, Lease KA, Doke JT, Tax FE, Walker JC. BAK1, an *Arabidopsis* LRR receptor-like protein kinase, interacts with BRI1 and modulates brassinosteroid signaling. Cell. 2002;110:213–222.

[47] Nam KH, Li J. BRI1/BAK1, a receptor kinase pair mediating brassinosteroid signaling Cell. 2002;110:203–212.

[48] Lee SC, Joo S, Kim S. Stereoisomers of castasterone, 3-epicastasterone and 2,3-diepicastasterone, in immature seeds of *Phaseolus vulgaris*. J Plant Biol. 2011;54:10–14.

[49] Seto H, Hiranuma S, Fujioka S, Koshino H, Suenaga T, Yoshida S. Preparation, conformational analysis, and biological evaluation of 6a-carbabrassinolide and related compounds. Tetrahedron. 2002;58:9741–9749.

[50] Brosa C, Capdevila JM, Zamora I. Brassinosteroids: A new way to define the structural requirements. Tetrahedron. 1996;52:2435–2448.
[51] Wang ZY, Seto H, Fujioka S, Yoshida S, Chory J. BRI1 is a critical component of a plasma-membrane receptor for plant steroids. Nature. 2001;410:380–383.
[52] Neff MM, Nguyen SM, Malancharuvil EJ, Fujioka S, Noguchi T, Seto H, et al. BAS1: A gene regulating brassinosteroid levels and light responsiveness in *Arabidopsis*. Proc Natl Acad Sci USA. 1999;96:15316-15323.
[53] Mazorra LM, Núñez M, Nápoles MC, Yoshida S, Robaina C, Coll F, et al. Effects of structural analogs of brassinosteroids on the recovery of growth inhibition by a specific brassinosteroid biosynthesis inhibitor. Plant Growth Regul. 2004;44:183–185.

Remark: This chapter already published in;

Thussagunpanit J, Jutamanee K, Homvisasevongsa S, Suksamrarn A, Yamagami A, Nakano T, Asami T. Characterization of synthetic ecdysteroid analogues as functional mimics of brassinosteroids in plant growth. J Steroid Biochem Mol Biol. 2017;172:1–8. DOI: 10.1016/j.jsbmb.2017.05.003

CHAPTER 3: Strigolactone and Karrikin Promote Light-adapted Development of *Arabidopsis thaliana* in a STH7 Function Dependent Manner

3.1 Chapter introduction

Light induces transitions from dark-grown (etiolated) to light-grown (de-etiolated) morphology [1]. In dicotyledonous plants, etiolated seedlings grown in the dark have elongated hypocotyls, closed apical hooks, unopened cotyledons and undeveloped chloroplasts [2, 3]. When plants are grown under light conditions, seedlings show light-adapted development characterized by a decrease of hypocotyl elongation, an opened cotyledons, inducing of true leaf expansion and biosynthesis of chlorophyll and anthocyanin [1, 2]. This process is called de-etiolation or photomorphogenesis [3–5]. Light-adapted development during de-etiolation is regulated by several phytohormones such as gibberellins, auxins, ethylene, brassinosteroids and strigolactones [4, 6–8]. However, how plant hormone signal transduction pathways interact with light signals and activate the photomorphogenesis process is not fully understood.

Multiple genes regulate photomorphogenesis. The B-box zinc-finger protein or BBX protein family is one of the main downstream effectors of seedling photomorphogenesis. BBX proteins contain a box domain with one or two B-box motifs at the N-terminal, and some subfamilies have a CCT (CO-COL-TOC1) domain at the C-terminal [9, 10]. The BBX protein family is composed of five main subfamilies divided by their protein sequences [11]. BBX subfamily IV has been reported as the major regulator of photomorphogenesis and light signaling. Subfamily IV B-box proteins consist of eight members including BBX18–BBX25. This subfamily carries only B-box B1 and B2 without a CCT domain [10]. STH7/BBX20 has been described as a positive regulator of photomorphogenesis and a negative regulator of BR function [4]. Genome-wide analysis of gene expression revealed that the transcriptional expression of *STH7* was up-regulated by strigolactone (SL) [12] and karrikin (KAR) [13]. Moreover, among BBX IV members only *STH7* transcription was up-regulated by SL [14].

SLs are terpenoidal lactone-type plant hormones that are classified as seed germination stimulants of root-parasitic weeds of the Orobanchaceae [15]. SLs are involved in the regulation of various phenomena such as suppression of shoot branching, regulation of root morphology, control of secondary growth and so on [15–19]. KARs are a class of seed germination stimulant containing a methyl-butenolide moiety that is a common structure in SLs [13, 15]. Both SLs and KARs can promote seed germination of *Arabidopsis* and inhibit hypocotyl elongation in the light which is one of the photomorphogenetic processes [13, 20–22]. As SL and KAR can enhance *STH7* expression level and STH7 is reported as a positive regulator of photomorphogenesis [4], STH7 could be a possible candidate protein that functions in linking SL and KAR to induce light-adapted development *in planta*.

Here, I employed *STH7*-overexpressing (*STH7ox*) lines and functionally defective *STH7* (*STH7-SRDX*) mutants to investigate roles of SLs and KARs in photomorphogenesis of *Arabidopsis*, and found that SL- and KAR-induced photomorphogenesis of *Arabidopsis* depends on STH7.

3.2 Results

3.2.1 Effect of strigolactone and karrikin on *Arabidopsis* hypocotyl elongation

GR24 or KAR_1 at 0, 1, 5 and 10 μM were applied to wild-type *Arabidopsis* ecotype Col (hereafter wild-type) as a synthetic SL analogue and a KAR, respectively. The results showed that 5 and 10 μM of GR24 significantly decreased *Arabidopsis* hypocotyl length under weak light condition when compared with their control (Figs. 3-1A, C). Only the highest concentration of KAR_1 could significantly reduce hypocotyl elongation (Figs. 3-1B, D). The effect of light qualities among dark, weak light and light conditions were compared. The highest concentration of GR24 and KAR_1 treatment slightly decreased hypocotyl length of wild-type *Arabidopsis* either dark or light but, both two conditions did not show the statistic difference. Under weak light condition, GR24 and KAR_1 clearly showed the inhibition of hypocotyl elongation (Figs. 3-1 and 3-2).

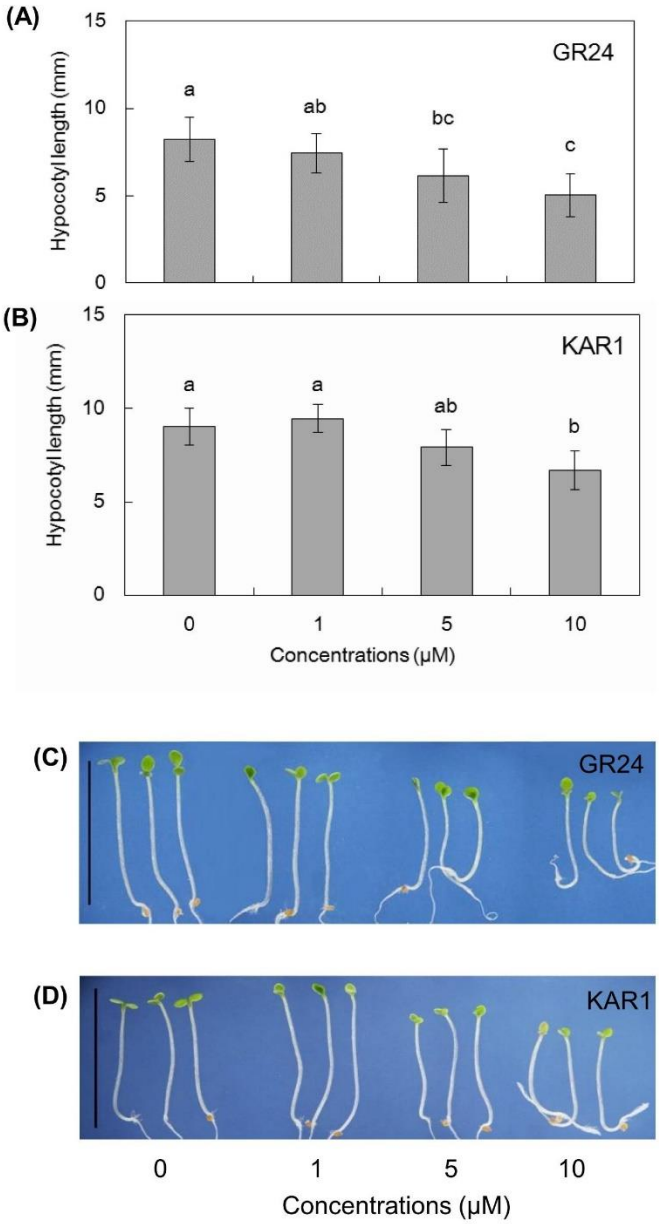

Fig. 3-1 Strigolactone and karrikin inhibit the hypocotyl length of wild-type *Arabidopsis*

Wild-type *Arabidopsis* were planted 4 days under weak light condition. Response of various concentrations of GR24 (A, C) and KAR_1 (B, D) on hypocotyl elongation. Data are means ± SD shown by vertical error bars ($n \geq 17$). Means with the same letter are not significantly different at $p \leq 0.05$ according to Tukey–Kramer's honestly significant difference test. Scale bars represent 10 mm.

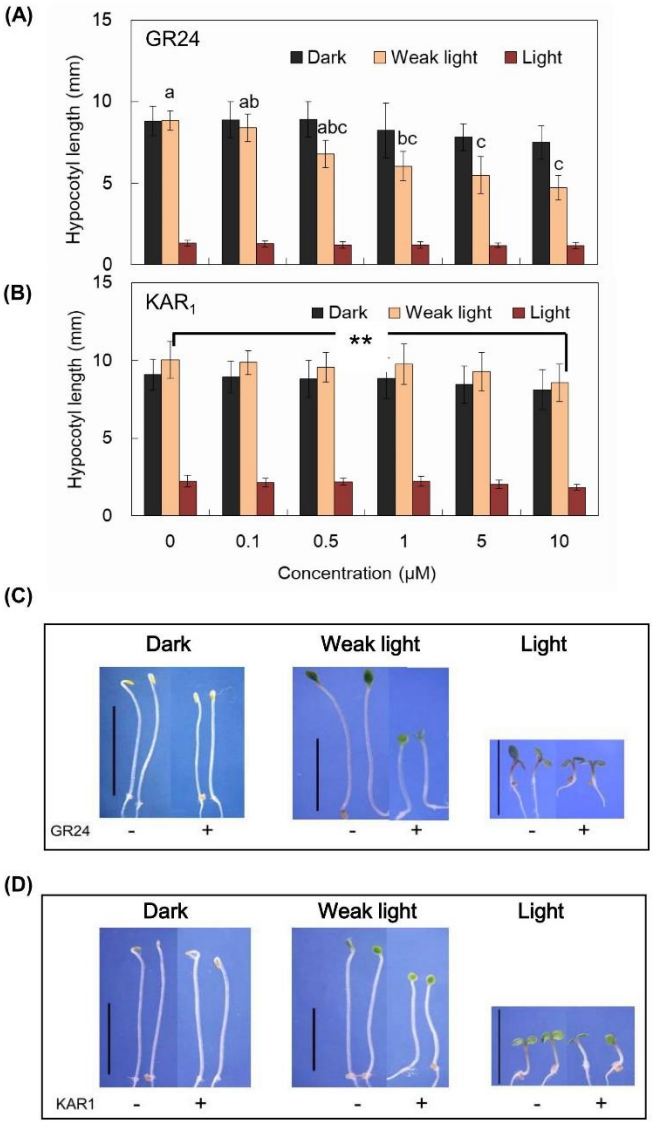

Fig. 3-2 Effect of strigolactone and karrikin on hypocotyl elongation under various light qualities

Wild-type *Arabidopsis* were planted 4 days under separately in dark, weak light, and light conditions. Plants were treated with various concentrations of GR24 (A, C) and KAR_1 (B, D). Treatments without GR24 or KAR_1 are described as "–"whereas treatments with 10 μM GR24 or 10 μM KAR_1 are described as "+". Data are means ± SD shown by vertical error bars ($n \geq 18$). Means with the same letter shown in (A) are not significantly different at $p \leq 0.05$ according to Tukey–Kramer's honestly significant difference test. Statistically significant difference shown in (B) relative to the control is $^{**}p \leq 0.01$ by Student's *t* test. Scale bars represent 5 mm.

3.2.2 Roles of STH7 on the light-adapted development

Wild-type *Arabidopsis* were grown under weak light conditions and incubated with 10 μM GR24 or 10 μM KAR_1 for 3 h. Treatments of both GR24 and KAR_1 up-regulated the expression of *STH7* (*At4G39070*); however, GR24 induced *STH7* expression at a level significantly higher than KAR_1 (Fig. 3-3A). *STH7* transcriptions were also determined in *Arabidopsis* SL-related mutants including *max2-1* (a SL signaling mutant), *max3-1* (a SL biosynthesis mutant) and *d14-1* (a SL receptor mutant) as well as *kai2-1* which is a KAR receptor mutant. The SL signaling mutant, *max2-1*, significantly down-regulated *STH7* expression comparing with wild-type *Arabidopsis* ecotype Col (Fig. 3-3B). However, SL receptor mutant, *d14-1*, and KAR receptor mutant, *kai2-1*, displayed the transcription of *STH7* as high as wild-type *Arabidopsis* ecotype Col and Ler, respectively (Fig. 3-3B).

Moreover, transgenic *Arabidopsis* which is the *STH7* promoter region fused to β-glucuronidase (GUS) was employed. After GUS staining, the *STH7pro::GUS* transgenic plant showed the expression of *STH7* at the shoot apex and the basal leaf blade of mature leaves whereas the vector control could not be observed the histochemical GUS stain (Fig. 3-4A). Treating with GR24 for 2 days, the *STH7* expression presented in the leaf apex and the basal leaf blade of young leaves as well as the apex of leaf indentation in mature leaves (Fig. 3-4B). Moreover, GR24 application induced the expression of *STH7* in lateral roots (Fig. 3-4B).

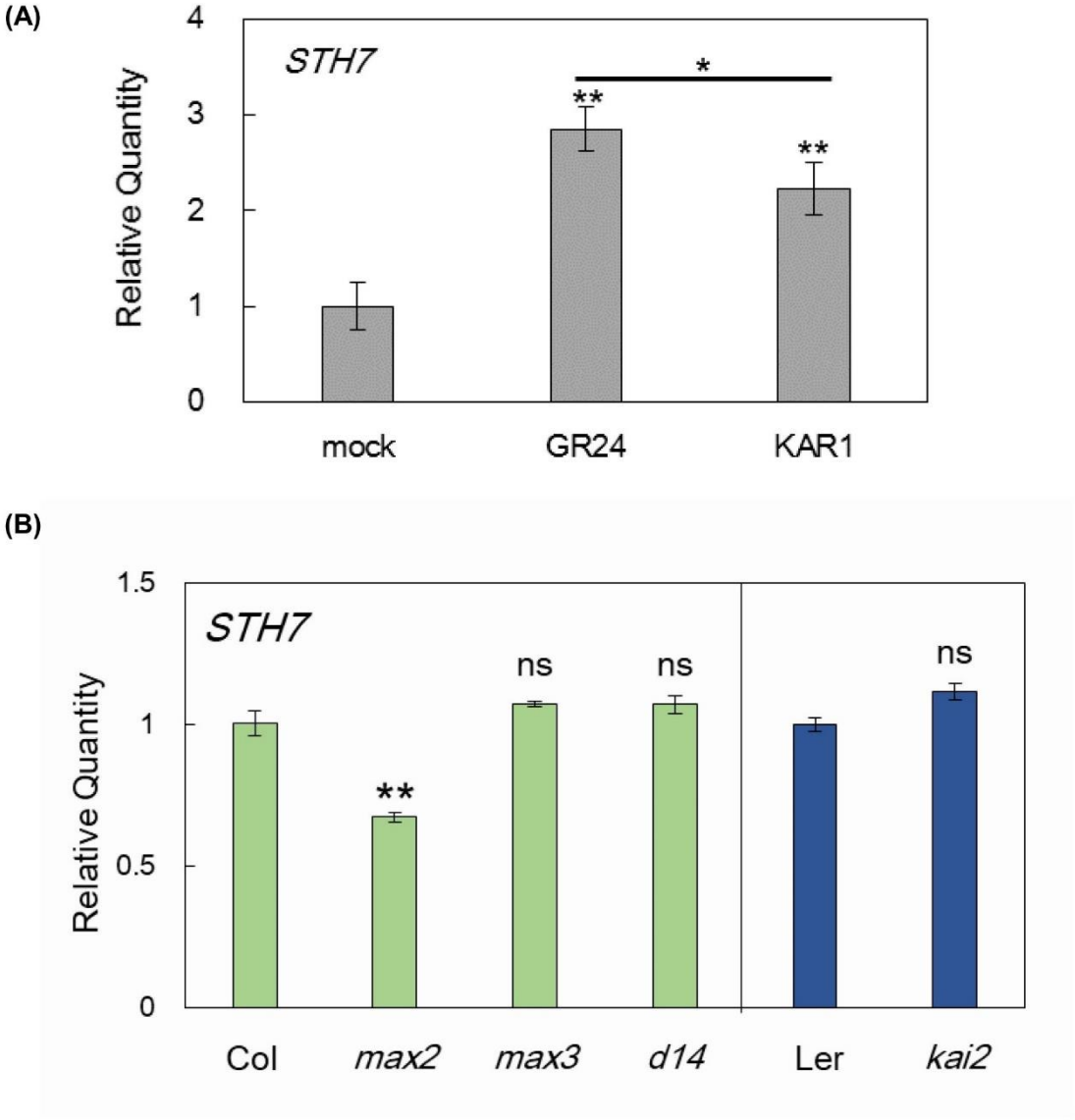

Fig. 3-3 Quantitative RT-PCR analysis of *STH7* expression level

Relative transcript levels of *STH7* in wild-type *Arabidopsis* treated with 0.1% (v/v) DMSO as a control, 10 µM GR24 or 10 µM KAR_1 (A). Relative transcript levels of *STH7* in *max2-1* (SL signaling mutant), *max3-1* (SL biosynthesis mutant), *d14-1* (SL receptor mutant), and *kai2-1* (KAR receptor mutant) (B). Plants were grown in 1/2 MS medium under weak light conditions for 4 days. The transcript levels were normalized to those of *ACT7*. Data are means ± SD shown by vertical error bars (n = 3). Standard deviations are shown as vertical error bars. Statistically significant differences relative to the control are $^{**}p \leq 0.01$ and $^{*}p \leq 0.05$ by Student's *t* test.

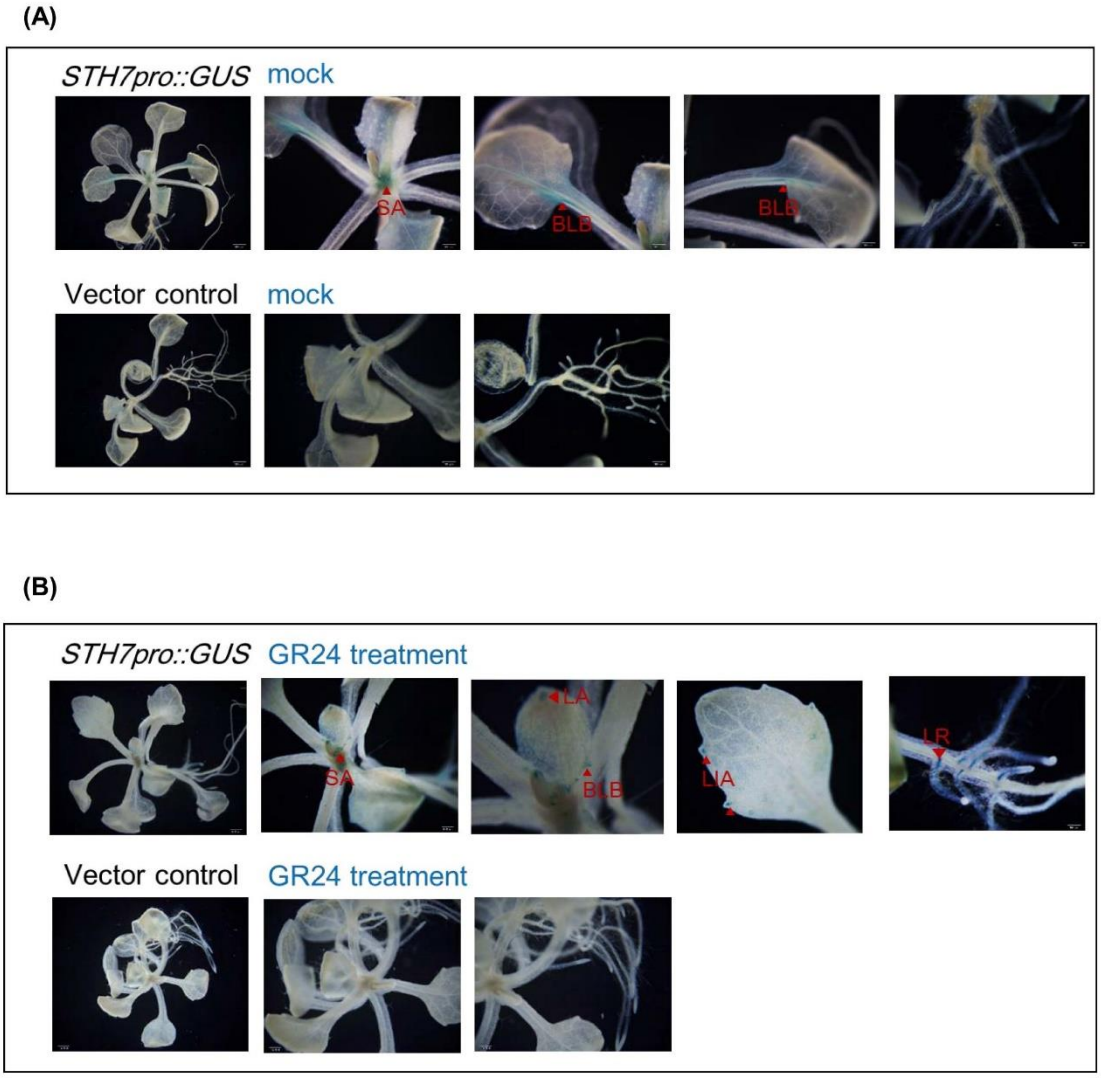

Fig. 3-4 *STH7* promoter (*STH7pro*)*::GUS* expression pattern

STH7pro::GUS transgenic plants were selected from plants that could germinate on 1/2 MS medium containing 50 μg/ml kanamycin. Plant samples were treated with 0.1% DMSO (mock or control) (A) or 10 μM GR24 (B) for 2 days before histochemical GUS stain. SA = Shoot apex, BLB = Basal leaf blade, LA = Leaf apex, LIA = Leaf indentation apex, and LR = Lateral root.

As it was reported that SL and KAR reduced *Arabidopsis* hypocotyl elongation [13, 21], and the inhibition of hypocotyl elongation is as one of the light-adapted responses [1, 2], I assumed that there should have been a crosstalk among SL, KAR and light-adapted development. Moreover, STH7 might relate this process. To understand how STH7 functions in photomorphogenesis, *STH7ox* and *STH7-SRDX* lines were used in this study. Three lines of *STH7ox (STH7ox-2*, *STH7ox-3* and *STH7ox-5*) and three lines of *STH7-SRDX* (*STH7-SR-2*, *STH7-SR-4* and *STH7-SR-5*) were grown on 1/2 MS media under 16/8 light/dark cycle for 7 days. All lines of *STH7-SRDX* exhibited longer hypocotyls than the wild-type. On the other hand, the hypocotyl length of *STH7ox-5* was shorter than that of the wild-type and the hypocotyl lengths of the other lines, *STH7ox-2* and *STH7ox-3*, were at the same level as that of the wild type (Figs. 3-5A, C). When *Arabidopsis* was grown under 16/8 light/dark cycle, the petiole lengths of 14-day-grown *STH7-SR2* and *STH7-SR4* were longer than those of wild-type. After 21 days planting, all lines of *STH7-SRDX* showed the longer petiole than wild-type. Meanwhile, the petiole lengths of *STH7ox-2* and *STH7ox-3* were similar to those of the wild-type except for the petiole length of *STH7ox-5* which was shorter than that of the wild-type (Figs. 3-5B, D).

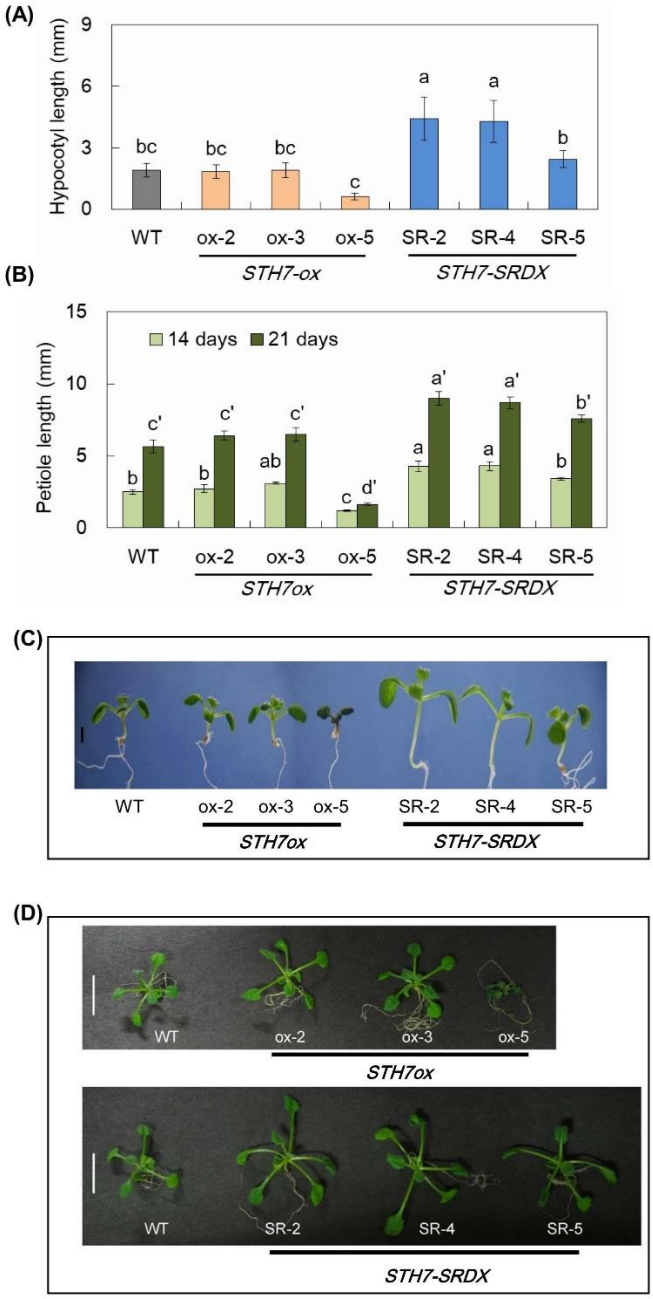

Fig. 3-5 Phenotype of *STH7ox* and *STH7-SRDX* mutants

Hypocotyl length at 7 days old under light conditions (A); petiole length at 14 and 21 days old under light conditions (B); 7-day-old seedlings, scale bars represent 1 mm (C); 21-day-old plants, a scale bar represents 10 mm (D). Data are means ± SD shown by vertical error bars ($n \geq 28$). Means with the same letter are not significantly different at $p \leq 0.05$ according to Tukey–Kramer's honestly significant difference test.

3.2.3 Effect of strigolactone and karrikin on the hypocotyl elongation of *Arabidopsis* strigolactone or karrikin mutants

Arabidopsis SL and KAR mutants were used to investigate the effect of SL and KAR on light-adapted development. Firstly, I compared the hypocotyl elongation response of *STH7ox* and *STH7-SRDX* on SL or KAR treatment. Not only GR24 and KAR_1 could reduce hypocotyl elongation in wild-type but they also decreased the hypocotyl length of *STH7ox* mutants (Fig. 3-6). The hypocotyl lengths of all *STH7ox* mutants (*STH7ox-2*, *STH7ox-3* and *STH7ox-5*) were significantly reduced by GR24 treatment in a concentration-dependent manner. Among the three *STH7ox* lines, the hypocotyl length of *STH7ox-5* was the shortest even without application of GR24 (Fig. 3-6A). The extent of the reduction of hypocotyl length by GR24 treatment was lower in all *STH7-SRDX* lines than in the wild-type. In particular, the *STH7-SR-5* line was clearly insensitive to GR24 (Fig. 3-6A). KAR_1 treatment of *STH7* mutants at both 5 and 10 μM reduced the hypocotyl length of all *STH7ox* and *STH7-SRDX* lines; however, *STH7-SRDX* lines were less sensitive to KAR_1 than *STH7ox* lines and the wild-type (Fig. 3-6B).

Arabidopsis SL-related mutants including *max2-1*, *max3-1*, *d14-1*, and KAR-related mutant, *kai2-1*, were used to investigate the effects of SL or KAR on hypocotyl elongation. The result showed that the hypocotyl elongation of the *Arabidopsis* signaling mutant *max2-1* was not affected either by treatment with GR24 or with KAR_1. On the other hand, GR24 significantly reduced the hypocotyl length of the *Arabidopsis* SL biosynthesis mutant *max3-1* (Fig. 3-7A). These data imply that MAX2 is important for both SL and KAR signal transduction. Next, SL receptor mutant *d14-1* and KAR receptor mutant *kai2-1* were used to examine the response of SL and KAR. KAR_1 treatment significantly induced the reduction of *d14-1* hypocotyl length under weak light conditions, while GR24 was not significantly decreased *d14-1* hypocotyl length. In contrast, GR24 application slightly reduced *kai2-1* hypocotyl length but KAR_1 did not (Fig. 3-7B). These results suggest that D14 mediates the SL response, whereas KAI2 mediates the KAR response in hypocotyl elongation of weak light-grown *Arabidopsis*.

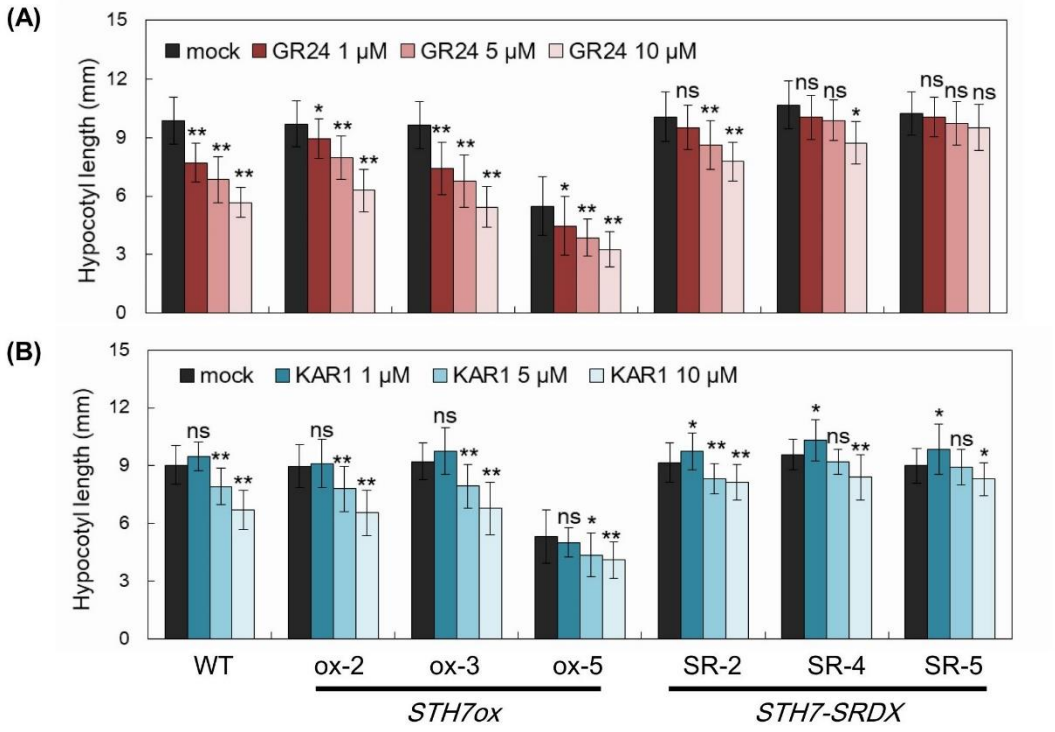

Fig. 3-6 Concentrations of strigolactone and karrikin on the hypocotyl elongation of *STH7ox* and *STH7-SRDX*

Wild-type *Arabidopsis*, *STH7-ox* and *STH7-SRDX* mutants were grown in 0.1% DMSO as control and in various concentrations of GR24 (A) or KAR_1 (B) under weak light condition for 4 days. All data are means ± SD shown by vertical error bars ($n \geq 18$). Statistically significant differences relative to each control are $^{**}p \leq 0.01$, $^{*}p \leq 0.05$ and ns: nonsignificant by Student's *t* test.

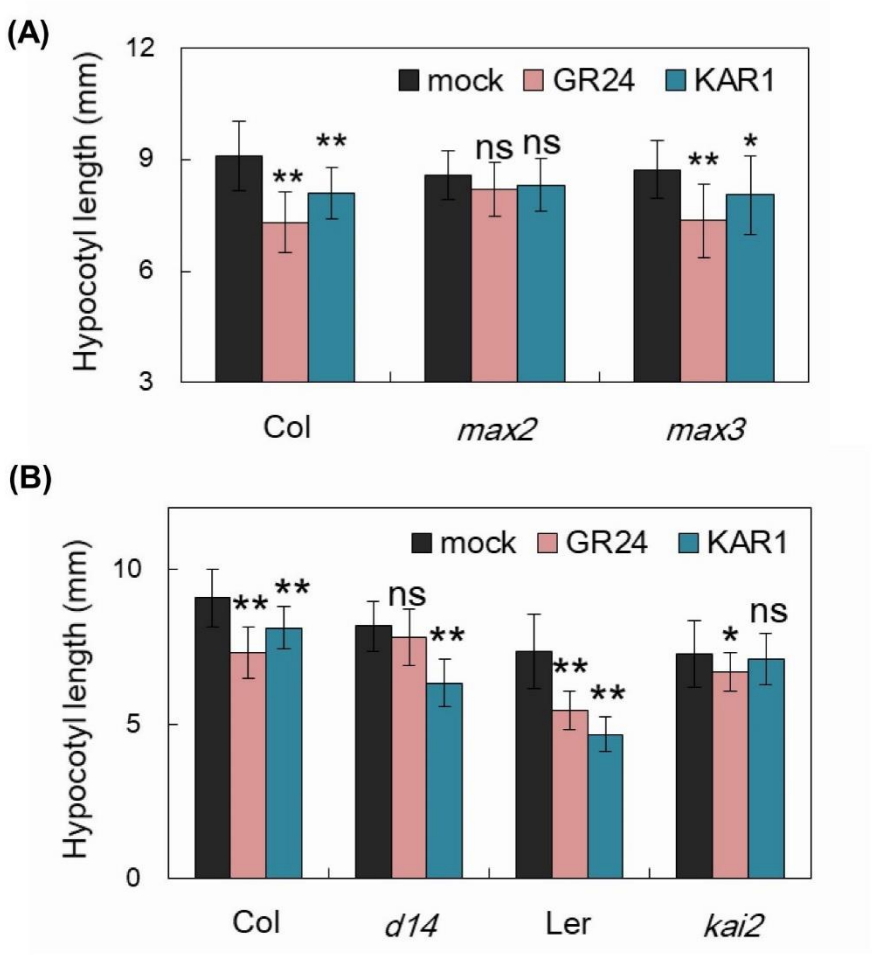

Fig. 3-7 Response of *Arabidopsis* SL- or KAR- mutants on strigolactone and karrikin treatment

Comparison of hypocotyl elongation in wild-type *Arabidopsis* ecotype Col, *max2-1* and *max3-1* mutants (A); comparison of hypocotyl elongation in wild-type *Arabidopsis* ecotype Col and Ler, *d14-1* and *kai2-1* mutants (B). Plants were treated with 0.1% DMSO as control, 10 μM GR24 or 10 μM KAR_1. Data are means ± SD shown by vertical error bars ($n \geq 18$). Statistically significant differences relative to each control are $^{**}p \leq 0.01$, $^{*}p \leq 0.05$ and ns: nonsignificant by Student's *t*-test.

The GR24 used in this study was a racemic mixture of two stereoisomers of chemically synthesized SLs consisting of $GR24^{5DS}$ and $GR24^{ent\text{-}5DS}$. The 5-deoxystrigol (5DS) is a natural form of SL but, the *ent*-5-deoxystrigol (*ent*-5DS) form is not. These two stereoisomers of GR24 were separately applied to check the effect on hypocotyl inhibition. Both of $GR24^{5DS}$ and $GR24^{ent\text{-}5DS}$ are inhibit hypocotyl elongation of the wild-type and *STH7ox* (Fig. 3-8A). On the other hand, *STH7-SRDX* was insensitive to any stereoisomer of GR24 (Fig. 3-8A). In SL- and KAR-receptor mutants, only $GR24^{ent\text{-}5DS}$ showed a significant reduction of *d14-1* hypocotyl elongation while only $GR24^{5DS}$ significantly inhibited *kai2-1* hypocotyl elongation under weak light condition (Figs. 3-8B, C). These results support that $GR24^{5DS}$ and $GR24^{ent\text{-}5DS}$ which is the stereoisomer of the GR24 racemic mixture (*rac*-GR24) is received separately by D14 and KAI2, respectively. The photomorphogenesis was activated via STH7 after the recognition of GR24 by D14 and/or KAI2. In contrast, KAR_1 could not reduce the hypocotyl length of the *kai2-1* mutant (Fig. 3-7B), indicating that KAR is thoroughly perceived by KAI2 and activates photomorphogenesis through STH7.

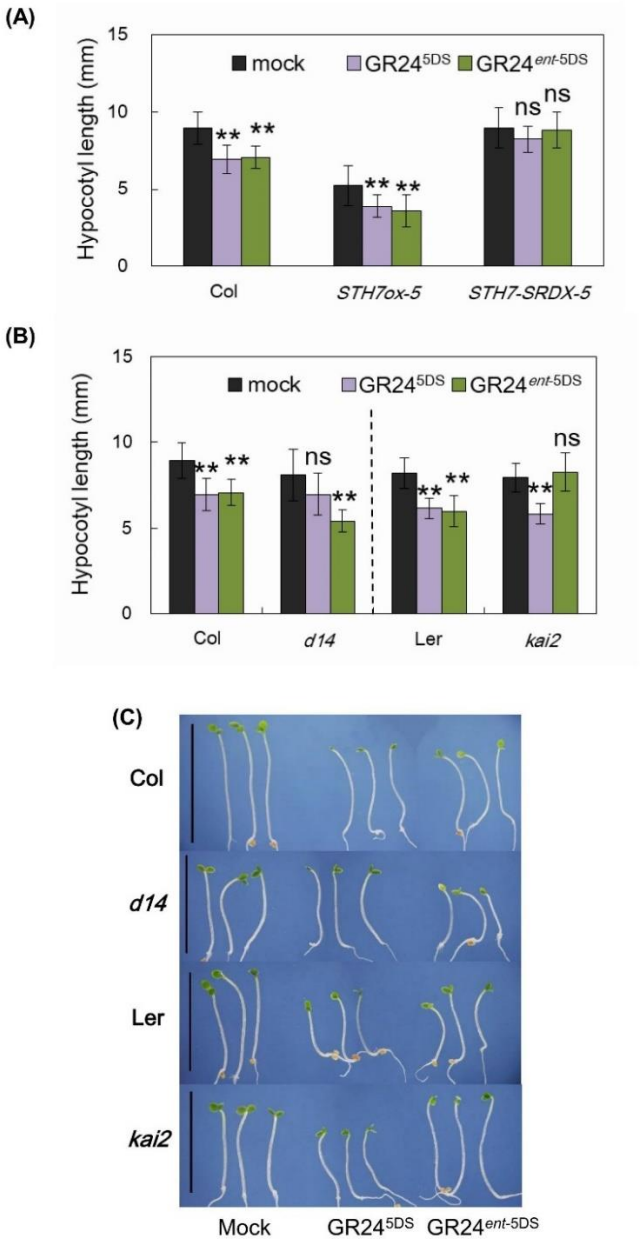

Fig. 3-8 Response of *Arabidopsis* SL- or KAR- mutants on two stereoisomers of GR24 treatment

Hypocotyl elongation of *STH7ox* and *STH7-SRDX* (A). Hypocotyl elongation of *d14-1* and *kai2-1* (B, C). Plants were treated with 0.1% DMSO as control, 10 μM $GR24^{5DS}$ or 10 μM $GR24^{ent\text{-}5DS}$. Data are means ± SD shown by vertical error bars (n ≥ 18). Statistically significant differences relative to each control are $^{**}p \leq 0.01$, $^{*}p \leq 0.05$ and ns: nonsignificant by Student's *t*-test.

3.2.4 Effect of strigolactone and karrikin on the production of anthocyanin and chlorophyll

Increases of anthocyanin and chlorophyll content are well-known parameters for detection of plant responses to light [2, 5]. When wild-type, *STH7ox* and *STH7-SRDX* mutants were grown in the dark, the anthocyanin content of all of them was undetectable. After seedlings were de-etiolated by light irradiation for 6 or12 h, anthocyanin levels in *STH7ox-3* and *STH7ox-5* mutants were significantly higher than those in the wild-type and all *STH7-SRDX* mutant lines (Fig. 3-9A). The accumulation of a larger amount of anthocyanin in *STH7ox-3* and *STH7ox-5* mutants was also observed under both weak light and light conditions (Fig. 3-10A). Furthermore, the chlorophyll content in de-etiolated *Arabidopsis* was investigated. The results showed that the total chlorophyll (total Chl), chlorophyll *a* (Chl *a*) and chlorophyll *b* (Chl *b*) content in the de-etiolated seedlings after 6 h of light irradiation was non-significantly different among wild-type *Arabidopsis*, *STH7ox* and *STH7-SRDX* mutants (Fig. 3-9B). When *Arabidopsis* seedlings were placed in the light for 12 h, the *STH7ox-5* mutant had a clearly increased total Chl content. Furthermore, total Chl content in *STH7ox-2* and *STH7ox-3* mutants was slightly higher than that in the wild-type and *STH7-SRDX* (Fig. 3-9B). The results showed that Chl *a* and Chl *b* content of *STH7ox* mutants was slightly higher and significantly higher than the wild-type, respectively, and the increase of total Chl in *STH7ox* was associated with the changes of Chl *a* and Chl *b*. On the other hand, in all *STH7-SRDX* lines, Chl *a* and Chl *b* content was almost at the same level as the wild-type (Figs. 3-9C, D). Significant accumulation of total Chl in *STH7ox* mutants compared to the wild-type and *STH7-SRDX* was also found in 7-day-grown *Arabidopsis* under weak light and normal light conditions (Fig. 3-10B). The higher production of total Chl in all *STH7ox* mutants under weak light conditions was related to the higher content of Chl *b*. Under weak light conditions, Chl *b* content in *STH7-SR-5* was lower than in the wild-type whereas Chl *a* content in this mutant was similar to that in wild-type *Arabidopsis* (Figs. 3-10C, D). When *Arabidopsis* was grown in the light for 14 days, *STH7-SRDX* mutants had increased total Chl, Chl *a* and Chl *b* content rather similar to wild-type *Arabidopsis* (Figs. 3-10B, C, D).

Because the anthocyanin content was strongly enhanced in *STH7ox-3* and *STH7ox-5* lines (Figs. 3-9A and 3-10A), SL and KAR functions might be associated with the increase of anthocyanin production. To check the involvement of SL and KAR in this process, wild-type *Arabidopsis*, *STH7ox* and *STH7-SRDX* mutants were grown in medium containing GR24 or KAR_1 under light conditions. *STH7ox-3*, *STH7ox-5* were selected because these lines showed the enhanced accumulation of the anthocyanin content in response to light. Since there was no significant difference between three *STH7-SRDX* mutants in the extent of the accumulation of the anthocyanin contents, I selected one *STH7-SRDX* line, *STH7-SR-5* as a representative. The results showed that both GR24 and KAR_1 significantly enhanced the anthocyanin content in the wild-type. However, the increase of anthocyanin content by GR24 was more than by KAR_1 (Fig. 3-11). In *STH7ox* and *STH7-SRDX* mutants, only the addition of GR24 significantly increased the anthocyanin content. Although SL enhanced the anthocyanin content in the *STH7-SRDX* mutant, its production was still lower than that in *STH7ox-3* and *STH7ox-5* (Fig. 3-11).

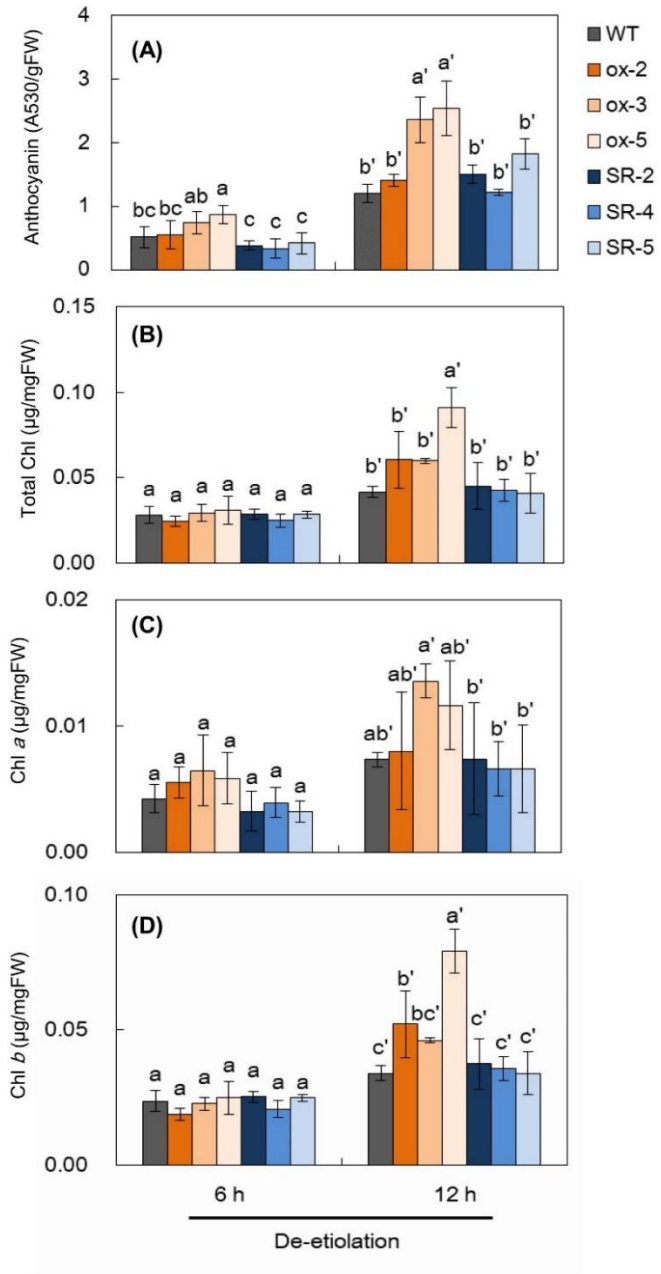

Fig. 3-9 Anthocyanin and chlorophyll content in various lines of the de-etiolated *STH7* mutants

Anthocyanin (A), total chlorophyll (B), chlorophyll *a* (C) and chlorophyll *b* (D) content in wild-type *Arabidopsis* and various lines of *STH7-ox* and *STH7-SRDX* mutants. Plants were grown under darkness for 7 days and exposed to light for 6 or 12 h to de-etiolate. Data are means ± SD shown by vertical error bars ($n \geq 3$). Means with the same letter are not significantly different at $p \leq 0.05$ according to Tukey–Kramer's honestly significant difference test.

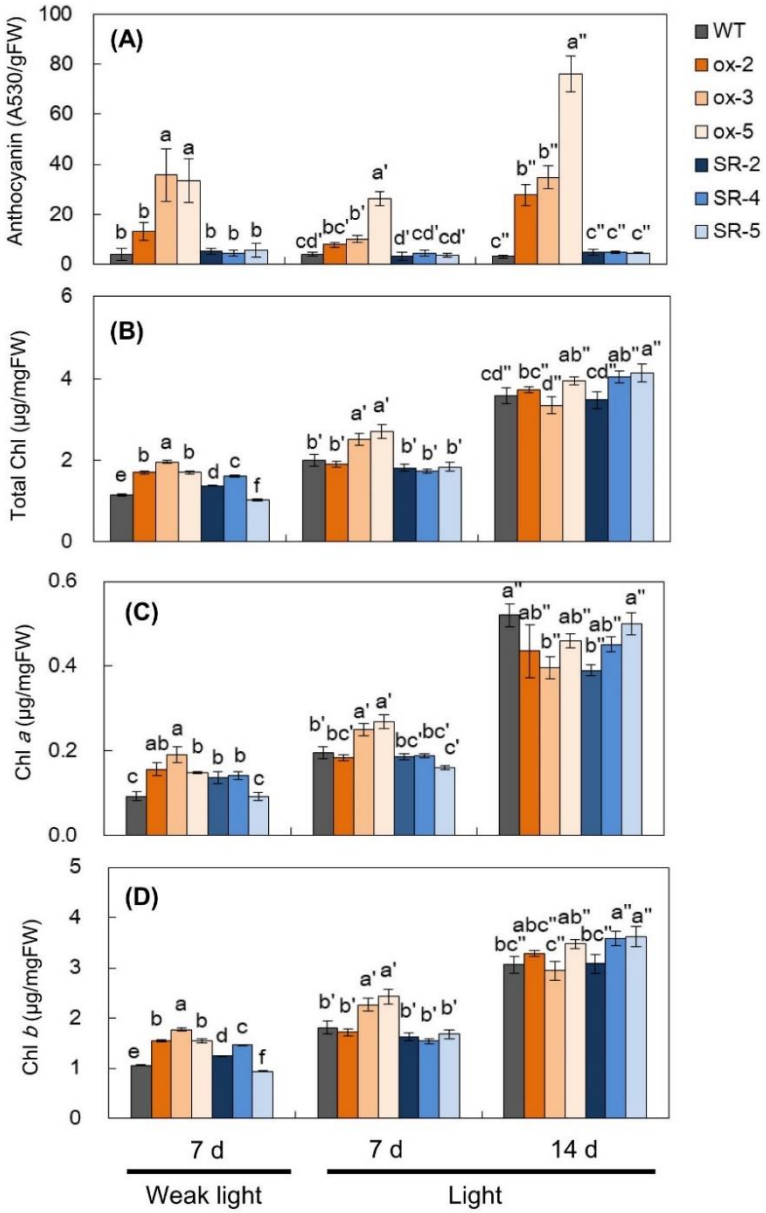

Fig. 3-10 Anthocyanin and chlorophyll content in various lines of weak light-grown and light-grown *STH7* mutants

Anthocyanin (A), total chlorophyll (B), chlorophyll *a* (C) and chlorophyll *b* (D) content in wild-type *Arabidopsis* and various lines of *STH7-ox* and *STH7-SRDX* mutants. Plants were grown under weak light conditions for 7 days, and under light conditions for 7 or 14 days. Data are means ± SD shown by vertical error bars (n ≥ 3). Means with the same letter are not significantly different at $p \leq 0.05$ according to Tukey–Kramer's honestly significant difference test.

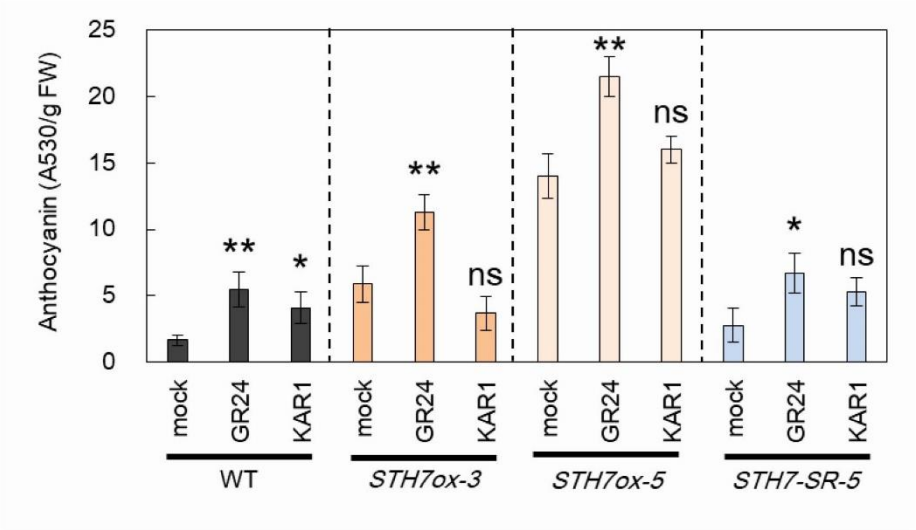

Fig. 3-11 Effect of strigolactone and karrikin on the accumulation of the anthocyanin content

Wild-type *Arabidopsis*, *STH7-ox* and *STH7-SRDX* mutants were grown in 1/2 MS medium containing 0.1% DMSO as control, 10 μM GR24 or 10 μM KAR_1 under light conditions for 7 days. Data are means ± SD shown by vertical error bars ($n \geq 3$). Statistically significant differences relative to each control are $^{**}p \leq 0.01$, $^{*}p \leq 0.05$ and ns: nonsignificant by Student's *t* test.

3.2.5 STH7 regulates the expression of photosynthesis-related genes that are induced by strigolactone and karrikin

Similarly to the accumulation of the anthocyanin content, Chl *a* and Chl *b* content was higher in *STH7ox-3* and *STH7ox-5* lines than in the wild-type, and was almost at the same level in all *STH7-SRDX* lines as in the wild-type after 12 h de-etiolation by light (Fig. 3-9). Therefore, *STH7ox-3*, *STH7ox-5* and *STH7-SR-5* were selected to examine the expression level of photosynthesis-related genes. *Arabidopsis* were grown in the dark for 4 days and then incubated with 1/2 MS media with 0.1% DMSO (control), 10 µM GR24 or 10 µM KAR_1 for 24 h. *LHCB1*, encoding the light-harvesting chlorophyll a/b binding protein, and *rbcS*, encoding the *small subunit* of RuBisCO, were selected as representative of photosynthesis-related genes, and *CHS* encoding chalcone synthase was selected as an anthocyanin synthesis gene. The qRT-PCR showed that GR24 treatment significantly increased *LHCB1*, *rbcS* and *CHS* expression levels in *STH7ox-3*, *STH7ox-5* and wild-type *Arabidopsis* compared with each of their controls. On the other hand, in the GR24-treated *STH7-SR-5* mutant, transcription levels of photosynthesis-related genes were similar to the control groups (Fig. 3-12). Moreover, in the GR24-treated *STH7ox-3* mutants, the expression levels of *LHCB1* and *rbcS* were significantly higher than those in wild-type *Arabidopsis* (Figs. 3-12A, B). When wild-type, *STH7ox-3* and *STH7ox-5* were treated with KAR_1, the expression levels of *LHCB1* and *rbcS* were significantly higher than in each of their controls (Figs. 3-12A, B). In *STH7ox-5* the expression level of *CHS* was the highest among the mutants, while in *STH7-SR-5* the expression level of *CHS* was similar to wild-type *Arabidopsis* in all treatments (Fig. 3-12C). When GR24 or KAR_1 was added to *Arabidopsis*, GR24 could up-regulate the expression level of *CHS* in the wild-type, *STH7ox-3* and *STH7ox-5*, but KAR_1 could increase the expression level of *CHS* only in *STH7ox-5*. Moreover, GR24 was more effective than KAR_1 in the increase of *CHS* transcription (Fig. 3-12C).

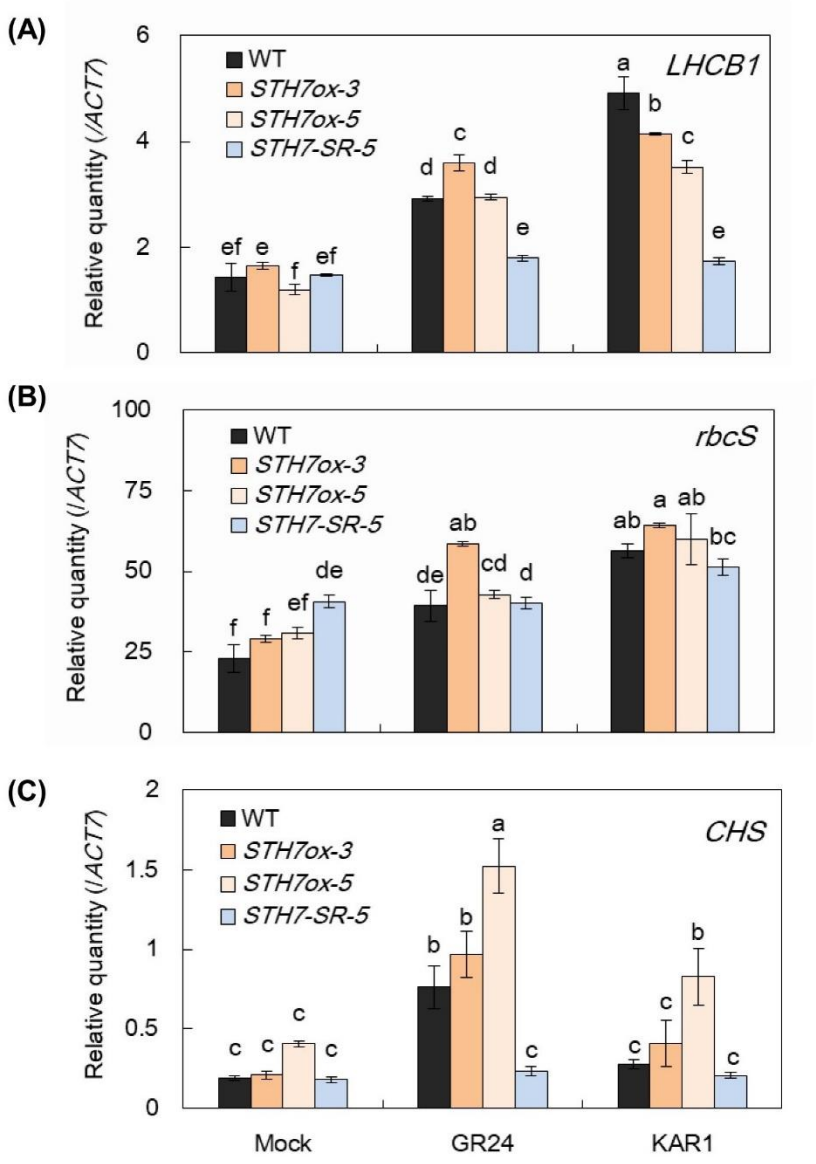

Fig. 3-12 Quantitative real-time PCR analysis of photosynthesis-related genes expression

Relative transcript levels of *LHCB1* (A), *rbcS* (B) and *CHS* (C) in wild-type *Arabidopsis*, *STH7-ox* and *STH7-SRDX* mutants. Plants were grown in 1/2 MS medium under darkness for 4 days and treated with 0.1% (v/v) DMSO as a control, 10 μM GR24 or 10 μM KAR_1. Data are means ± SD shown by vertical error bars (n = 3). Means with the same letter are not significantly different at $p \leq 0.05$ according to Tukey–Kramer's honestly significant difference test.

3.3 Discussion

When seeds germinate and shoots appear above the soil surface, seedlings undergo de-etiolation or photomorphogenesis. Light sensing is the main signal that impacts on the photomorphogenesis process. Several genes are regulated by light to induce morphological changes in plants [23]. COP1 is a negative regulator and HY5 is a positive regulator of photomorphogenesis [24, 25]. By interacting with COP1, HY5 is degraded by 26s proteasomes and light-adapted development is interrupted [25]. Photomorphogenesis in seedling development is also controlled by multiple plant hormones [7, 8]. In this study, I investigated the involvement of SL and KAR in regulating photomorphogenetic development in *Arabidopsis*.

Consistent with a report that SL inhibits COP1 function similarly to light signaling [26], GR24 treatment inhibited hypocotyl elongation in wild-type *Arabidopsis* (Fig. 3-1A). In addition, KAR_1 treatment also inhibited hypocotyl elongation in wild-type *Arabidopsis* (Fig. 3-1B). Both light and SL suppress COP1 accumulation in the nucleus together with the accumulation of HY5, which then leads to a reduction of hypocotyl elongation. The decrease of nuclear COP1 by SL application strongly suggests that there should be crosstalk between SL and light [26]; however, as shown in Fig. 3-2, 10 μM GR24 little affected the hypocotyl length of wild-type *Arabidopsis* in the dark. It might be possible to think that SL could affect hypocotyl length not only by crosstalk with light signals but also by substituting light signals and then regulating photomorphogenesis. The deeper investigation is required to unveil the relation between SL and light signaling. In the case of KAR, there is a possibility that hypocotyls could be inhibited by KAR by the same mechanism as SL.

SLs are carotenoid-derived phytohormones containing a butenolide ring (D ring) in their structure [27, 28]. KARs, byproducts of smoke, also have the butenolide moiety and affect plant growth like SLs [29, 30]. Treatment with both GR24 and KAR_1 significantly decreased hypocotyl elongation under weak light conditions (Fig. 3-1). These results suggest that there should be the relation between SL and light-adapted

growth as well as between KAR and light-adapted growth. Moreover, GR24 and KAR_1 significantly up-regulated the *STH7* expression level in wild-type *Arabidopsis* grown under weak light conditions (Fig. 3-3A). The histochemical GUS stain exhibited that *STH7* expressed at the shoot apex of *STH7pro::GUS* (Fig. 3-4). The shoot apex growth is normally suppressed in darkness, but rapidly developed by light activation. Moreover, this region has the high dynamic of light-induced genes [31]. Therefore, it implies that STH7 might induce light-adapted growth in shoot apex. Because *STH7pro::GUS* transgenic plants used in this study is T_1 generation, they might showed the weak expression of GUS activity. These transgenic plants should be selected by kanamycin-resistant phenotype for screening homogenous lines and repeatedly determine GUS stain in the future. Since *STH7* encodes a transcription factor belonging to the double B-box zinc finger family, which is known as a positive regulator of photomorphogenesis [4, 9–11], SL and KAR might evoke light-adapted development through the function of STH7.

To clarify this hypothesis, phenotypes of *STH7ox* and *STH7-SRDX* lines were observed. *STH7-SRDX* mutants showed longer hypocotyls and longer petioles than wild-type (Fig. 3-5). Moreover, the hypocotyl elongation of *STH7-SRDXs* was less reduced by GR24 or KAR_1 treatment in contrast with that of wild-type and *STH7ox Arabidopsis* (Fig. 3-6). These data suggest that SL and KAR modulate the inhibition of hypocotyl elongation dependent on STH7 function. Among three lines of *STH7ox*, *STH7ox-5* exhibited shorter hypocotyls and petioles than wild-type *Arabidopsis* (Figs. 3-5A, C) indicating that the overexpression of *STH7* shortens the hypocotyls and petioles.

SL and KAR probably affect photomorphogenesis through different signal pathways although both SL and KAR signaling pathways require MAX2 [21, 32, 33] because SLs and KARs are perceived by the paralogous α/β-hydrolases D14 and KAI2, respectively [13, 21, 34, 35]. Waters and Smith [22] reported that the overexpression of KAI2 is enough to modulate the signaling response of both SLs and KARs in the hypocotyl developing state, and Scaffidi et al. [36] reported that only natural forms of SL such as 5-deoxystrigol (5DS) were active through D14, whereas non-natural enantiomers such as *ent*-5-deoxystrigol (*ent*-5DS) were active through KAI2. Here, I confirmed that

neither GR24 nor KAR_1 could inhibit hypocotyl elongation of the *max2* mutant (Fig. 3-7A) indicating that MAX2 is essential for both SL and KAR signal transduction (Fig. 3-13.). Moreover, *max2* mutant displayed the down-regulation of *STH7* transcription (Fig. 3-3B) suggesting that MAX2 is also important for STH7 function. While KAR_1 treatment reduced the hypocotyl length of *d14* under weak light conditions, GR24 addition decreased *kai2-1* hypocotyl elongation (Fig. 3-7B). However, the individual application of $GR24^{5DS}$ or $GR24^{ent\text{-}5DS}$ which is the stereoisomer of racemic GR24 showed the different result from GR24 (*rac*-GR24) treatment. $GR24^{ent\text{-}5DS}$ decreased *d14-1* hypocotyl elongation whereas $GR24^{5DS}$ reduced *kai2-1* hypocotyl elongation under weak light condition (Fig. 3-8B). Generally, *rac*-GR24 should decreased the hypocotyl length of both *d14-1* and *kai2-1* because it includes of those two stereoisomers. However, it is difficult to control the ratio of $GR24^{5DS}$ and $GR24^{ent\text{-}5DS}$ during the synthesis of *rac*-GR24. In my experiment, *rac*-GR24 could not significantly reduce hypocotyl elongation of *d14-1* (Fig. 3-7B) might because *rac*-GR24 which was used in this study contained the high ratio of $GR24^{5DS}$ to $GR24^{ent\text{-}5DS}$. SL regulates light-adapted growth mediated by D14 and KAI2 while KAR response is mediated by only KAI2 was confirmed (Fig. 3-13).

The biosynthesis of chlorophyll and anthocyanin is a process of de-etiolated development [2, 5]. BBX proteins play a role in photomorphogenesis by inducing chlorophyll and anthocyanin accumulation [9]. Close homologues of STH7 such as STH2/BBX21 and STH3/BBX22/LZF1 have been reported as positive regulators of light-adapted development [37–39]. STH7 shares amino-acid identity of 71.82% with STH2 and 54.13% with STH3 [4]. STH3 plays a role as a positive regulator of chloroplast development [38–40]. *STH3ox* exhibited the increase of anthocyanin and chlorophyll levels under red light while the *sth3* mutant showed the decrease of anthocyanin and chlorophyll levels as well as delayed chloroplast development [39]. Moreover, the absence of *STH2* in the *cop1* mutant partially repressed anthocyanin production [37]. The study demonstrated that de-etiolated *STH7ox* mutants accumulated more anthocyanin and chlorophyll than wild-type and *STH7-SRDX* mutants (Fig. 3-9). This suggests that STH7 mediates chlorophyll and anthocyanin accumulation during light-adapted processes (Fig. 3-13).

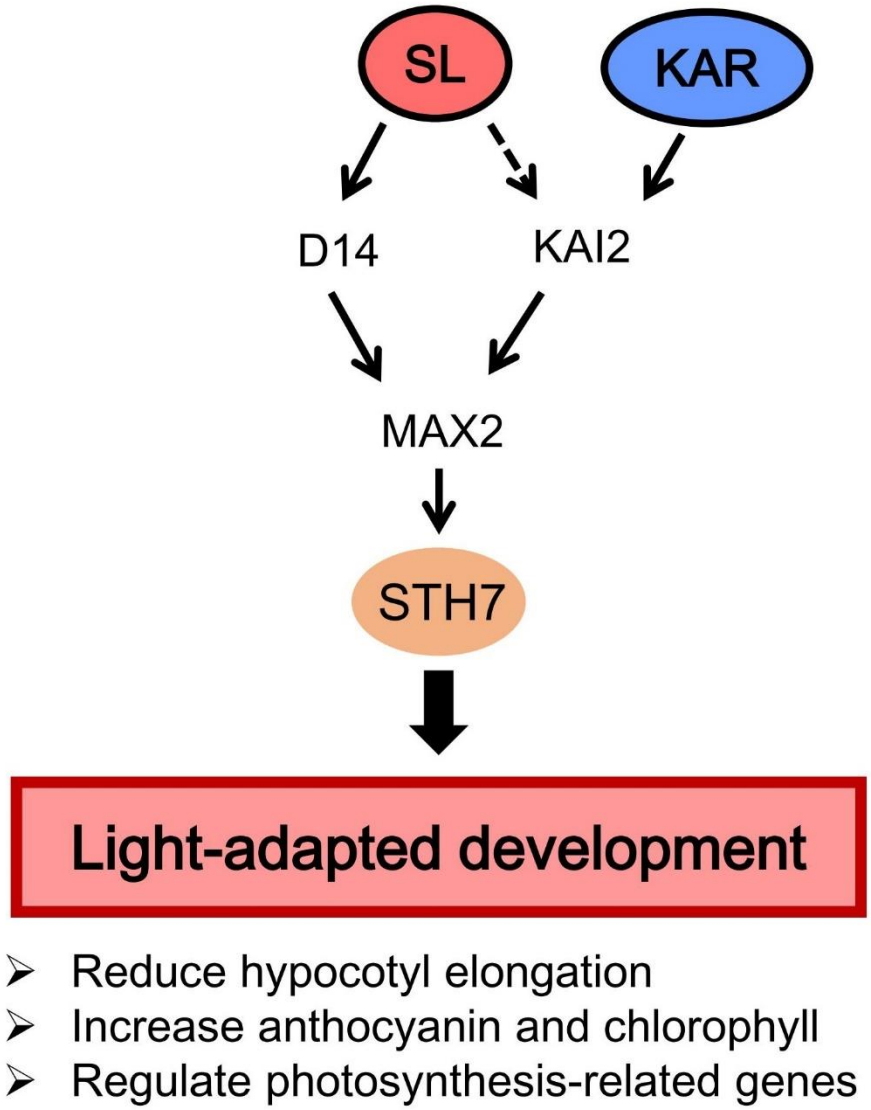

Fig. 3-13 Working model of strigolactone and karrikin effects on light-adapted development or photomorphogenesis

Strigolactone (SL) regulates light-adapted growth mediated by D14 and KAI2 while karrikin (KAR) response is mediated by only KAI2. MAX2 is important for both SL and KAR signaling in light-adapted development in the STH7-dependent manner. SL and KAR induce photomorphogenesis by the inhibition of hypocotyl elongation, the increase of anthocyanin and chlorophyll content and the up-regulation of photosynthesis-related genes. Dashed-line arrow indicates that non-natural SL can perceive in this way.

The expression levels of photosynthesis- and anthocyanin synthesis-related genes, such as *LHCB1*, *rbcS* and *CHS*, were up-regulated when plants were treated with GR24 or KAR_1 in wild-type *Arabidopsis* and *STH7ox* mutants (Fig. 3-12). These three genes are normally increased by light irradiation [26]. These results imply that SL and KAR modulate light-adapted development through the up-regulation of photosynthesis-related genes and STH7 is involved in this process (Fig. 3-13). *LHCB1* and *rbcS* are genes related to chlorophyll production [41, 42]. The up-regulation of these two genes by GR24 and KAR_1 treatment in *STH7ox* could be related to the increase of total chlorophyll content in this mutant (Fig. 3-9B). Moreover, the *CHS* gene is associated with anthocyanin biosynthesis [43, 44]. The fact that the expression level of *CHS* by GR24 addition was more than by KAR_1 addition (Fig. 3-12C) could be in accord with the result that the increase of anthocyanin content by GR24 addition was more than by KAR_1 addition (Fig. 3-11). Further analysis to investigate how expression of the *STH7* gene is regulated by SL and KAR and whether STH7 regulates the expression of these genes directly will provide deeper mechanistic insights into SL signaling in photomorphogenesis.

3.4 Materials and Methods

3.4.1 Plant materials and growth conditions

Arabidopsis thaliana ecotype Columbia (Col) or Landsberg erecta (Ler) were used as the wild-type plants. *Arabidopsis* SL-related mutants including *max2-1* (a SL signaling mutant), *max3-1* (a SL biosynthesis mutant) and *d14-1* (a SL receptor mutant) as well as *kai2-1* which is a KAR receptor mutant were used to investigate the effects of SL or KAR on hypocotyl elongation. Almost *Arabidopsis* mutants in this study are Col background excepted *kai2-1* is Ler background. Seeds were surface-sterilized by 70% and 99% ethanol for 30 min and 30 s, respectively. After that the sterilized seeds were germinated on 1/2 MS medium containing 3% sucrose and 0.8% phyto agar (Duchefa, Haarlem, The Netherlands). Seeds were sown in medium supplemented with different concentrations of GR24 (a racemic mixture of two stereoisomers – $GR24^{5DS}$ and $GR24^{ent\text{-}5DS}$) or KAR_1 in 0.1% (v/v) DMSO at 0, 1, 5 and 10 μM. Then, *Arabidopsis* were

transferred to 4 °C for 2 days and moved to grow at 22 °C in the dark, weak light (1.75 μmol m^{-2} s^{-1}) or light (23 μmol m^{-2} s^{-1}) for 4 days. The hypocotyl length was measured with ImageJ software.

3.4.2 Preformation of *Arabidopsis STH7* overexpression and *STH7-SRDX*

Arabidopsis STH7ox were obtained by overexpression of the B-box zinc finger protein *STH7* which was driven by a CaMV35S promoter in the wild-type *Arabidopsis* ecotype Col background. Functionally defective mutants of *STH7* were created by using chimeric repressor silencing technology [45]. The SRDX motif was fused to the C-terminal end of *STH7* and expressed under a CaMV35S promoter in wild-type *Arabidopsis* ecotype Col. Three homologous *STH7ox* lines (*STH7ox-2*, *STH7ox-3* and *STH7ox-5*) and three homologous *STH7-SRDX* lines (*STH7-SR-2*, *STH7-SR-4* and *STH7-SR-5*) were used as the representative lines. Various *STH7* mutant lines were planted at 22 °C under the 16/8 light/dark cycle for phenotype observation. The hypocotyl lengths were measured at 7 days old whereas petiole lengths were measured at 14 and 21 days old.

3.4.3 Quantitative real-time PCR

The qRT-PCR was performed as follows. Plant samples were frozen and homogenized in liquid nitrogen, and total RNA was extracted from the samples with a Total RNA Extraction Kit Mini for plants (RBC Bioscience, New Taipei City, Taiwan). Complementary DNA (cDNA) was synthesized using ReverTra Ace® qPCR RT Master Mix with gDNA remover (Toyobo, Osaka, Japan), and was used in qRT-PCR. The qRT-PCR was performed according to the instruction provided with the PCR Thermal Cycler Dice (Takara, Tokyo, Japan), using the SYBR Premix Ex Taq system (Takara, Shiga, Japan). Transcript levels were normalized to those of *ACT7*. To investigate the expression levels of *STH7* in wild-type *Arabidopsis* ecotype Col, *max2-1*, *max3-1*, *d14-1*, and *kai2-1*, plants were grown under weak light conditions for 4 days. Wild-type *Arabidopsis* were incubated in 0.1% (v/v) DMSO as a control, 10 μM GR24 or 10 μM KAR_1 solution

prepared in 1/2 MS medium without sucrose and phyto agar for 3 h. The *STH7* transcript levels were checked by using *STH7* primers;

STH7-forward: 5′-CCAATAAACTAGCCGGGAAA-3′
STH7-reverse: 5′-GCTCTGTCTTCTTGGCAAAAT-3′

To examine the effects of SL and KAR on the expression levels of photosynthesis-related genes, wild-type *Arabidopsis*, *STH7ox-3, STH7ox-5* and *STH7-SR-5* plants were grown under dark condition for 4 days. Then, plants were incubated in 0.1% (v/v) DMSO as a control, 10 μM GR24 or 10 μM KAR_1 solution prepared in 1/2 MS medium without sucrose and phyto agar for 24 h. Samples were collected to extract RNA and perform qRT-PCR in the same manner as described above. The photosynthesis-related primers and *ACT7* (used as the constitutively expressed control gene) were described as following;

LHCB1-forward: 5′-CCATTTGGGCCACTCAAGTTATC-3′
LHCB1-reverse: 5′-AGCCTCTGGGTCGGTAGCAAG-3′
rbcS-forward: 5′-GTTAGCTGCATGAAGGTGTGG-3′
rbcS-reverse: 5′-ACGGTACACAAATCCGTGCTCCA-3′
CHS-forward: 5′-GGCTATTGGCACTGCTAACCCTGAG-3′
CHS-reverse 5′:-GTGACGTTTCCGAATTGTCGACTTG-3′
ACT7-forward: 5′-GATATTCAGCCACTTGTCTGTGAC-3′
ACT7-reverse: 5′-CATGTTCGATTGGATACTTCAGAG-3′.

3.4.4 *STH7pro::GUS* construction and GUS staining

The *STH7* promoter region from the upstream of -2463 bp to +186 bp at the end of first exon was constructed by connecting to β-glucuronidase (GUS) in pBI101 vector. The *STH7pro::GUS* and pBI101 (vector control) were transformed into *Arabidopsis* ecotype Col by *Agrobacterium* using the floral dip transformation method. The seeds from transformed plants were collected and screened by kanamycin. Transgenic plants that could survive under 1/2 MS medium containing 50 μg/ml kanamycin were selected

to check GUS activity. Plant samples were transferred to 1/2 MS medium containing 0.1% DMSO as the control or 10 μM GR24 for 2 days. The plants expressing the *STH7 promoter::GUS* reporter gene fusion and the vector control were histochemical stained. Firstly, plant samples were soaked in 90% (v/v) acetone on ice for 15 min. Acetone was discarded and plant samples were washed by 100 mM PBS buffer (pH 7.0) for 3 times. The plant samples were stained in X-Gluc solution containing 40 mg/ml 5-bromo-4-chloro-3-indolyl-β-glucronide (X-Gluc) in dimethylformamide (DMF), 12.5 mM potassium ferrocyanide, 12.5 mM potassium ferricyanide, 0.5 M EDTA and 0.2 M PBS buffer (pH 7.0). The staining was conducted overnight at 37°C. Then, X-Gluc solution was discarded and chlorophyll in plant samples was removed by 70% (v/v) ethanol. Lastly, the histochemical GUS staining was observed under the stereomicroscope.

3.4.5 Anthocyanin and chlorophyll measurement

Wild-type *Arabidopsis* and various *STH7ox* and *STH7-SRDX* mutant lines were planted in 1/2 MS medium containing 3% sucrose and 0.8% phyto agar under dark or weak light conditions for 7 days and under light conditions for 7 and 14 days, respectively. *Arabidopsis* grown under darkness were transferred to the light for 6 or 12 h to de-etiolate. After that, 10–20 mg of cotyledons and leaves were collected for chlorophyll and anthocyanin extraction. The chlorophyll content was measured according to Porra et al. [46]. Plant samples were added to 1 mL DMF and kept at 4 °C overnight. After extraction, chlorophyll content was measured at 647 and 664 nM. Total Chl, Chl *a*, and Chl *b* were calculated by the following equations: total Chl = (17.67 × A647) + (7.17 × A664), Chl *a* = (12 × A664) − (3.11 × A647) and Chl *b* = (20.78 × A647) − (4.88 × A664). Anthocyanin content was measured according to Ito et al. [47]. Methanol in 1% HCl was used as the extraction solution. Plant samples were added to 300 μL of extraction solution and kept at 4 °C overnight. Then, 200 μL of distilled water and 200 μL of chloroform were added and the mixture was centrifuged at 10,000 × *g* for 1 min. The anthocyanin content was measured at 530 nm. The amount of anthocyanin was calculated by A530/fresh weight (FW). Moreover, wild-type *Arabidopsis*, *STH7ox-3*, *STH7ox-5* and *STH7-SR-5* plants were grown in 1/2 MS medium containing 0.1% (v/v) DMSO as a control, 10 μM GR24

or 10 µM KAR_1 under light conditions for 7 days. After that the cotyledons from each treatment were collected and anthocyanin was extracted in the same manner.

3.5 References

[1] Symons GM, Smith JJ, Nomura T, Davies NW, Yokota T, Reid JB. The hormonal regulation of de-etiolation. Planta. 2008;227:1115–1125.

[2] Chory J, Chatterjee M, Cook RK, Elich T, Fankhauser C, Li J, et al. From seed germination to flowering, light controls plant development via the pigment phytochrome. Proc Natl Acad Sci USA. 1996;93:12066–12071.

[3] Li Q-F, He J-X. BZR1 interacts with HY5 to mediate brassinosteroid- and light-regulated cotyledon opening in *Arabidopsis* in darkness. Mol. Plant. 2015;9:113–125.

[4] Fan XY, Sun Y, Cao DM, Bai MY, Luo XM, Yang HJ, et al. BZS1, a B-box protein, promotes photomorphogenesis downstream of both brassinosteroid and light signaling pathways. Mol Plant. 2012;5:591–600.

[5] Neff MM, Chory J. Genetic interactions between phytochrome A, phytochrome B, and cryptochrome 1 during *Arabidopsis* development. Plant Physiol. 1998;118:27–35.

[6] Feng S, Martinez C, Gusmaroli G, Wang Y, Zhou J, Wang F, et al. Coordinated regulation of *Arabidopsis thaliana* development by light and gibberellins. Nature. 2008;451:475–479.

[7] Lau OS, Deng XW. Plant hormone signaling lightens up: integrators of light and hormones. Curr Opin Plant Biol. 2010;13:571–577.

[8] Wang ZY, Bai MY, Oh E, Zhu JY. Brassinosteroid signaling network and regulation of photomorphogenesis. Annu Rev Genet. 2012;46:701–724.

[9] Gangappa SN, Botto JF. The BBX family of plant transcription factors. Trends Plant Sci. 2014;19:460–470.

[10] Sarmiento F. The BBX subfamily IV: additional cogs and sprockets to fine-tune light-dependent development. Plant Signal Behav. 2013;8:e23831-1–e23831-7.

[11] Khanna R, Kronmiller B, Maszle DR, Coupland G, Holm M, Mizuno T, et al. The *Arabidopsis* B-box zinc finger family. Plant Cell. 2009;21:3416–3420.

[12] Mashiguchi K, Sasaki E, Shimada Y, Nagae M, Ueno K, Nakano T, et al. Feedback-

regulation of strigolactone biosynthetic genes and strigolactone-regulated genes in *Arabidopsis*. Biosci Biotechnol Biochem. 2009;73:2460–2465.

[13] Nelson DC, Flematti GR, Riseborough JA, Ghisalberti EL, Dixon KW, Smith SM. Karrikins enhance light responses during germination and seedling development in *Arabidopsis thaliana*. Proc Natl Acad Sci USA. 2010;107:7095–7100.

[14] Wei C, Chien C, Ai L, Zhao J, Zhang Z, Li KH, Burlingame AL, Sun Y, Wang Z. The *Arabidopsis* B-BOX protein BZS1/BBX20 interacts with HY5 and mediates strigolactone regulation of photomorphogenesis. J Genet Genomics. 2016;43:555–563.

[15] Cook CE, Whichard LP, Turner B, Wall ME, Egley GH. Germination of witchweed (*Striga lutea* Lour.): isolation and properties of a potent stimulant. Science. 1966;154:1189–1190.

[16] Akiyama K, Matsuzaki K, Hayashi H. Plant sesquiterpenes induce hyphal branching in arbuscular mycorrhizal fungi. Nature. 2005;435:824–827.

[17] Gomez-Roldan V, Fermas S, Brewer PB, Puech-Pages V, Dun EA, Pillot J-P, et al. Strigolactone inhibition of shoot branching. Nature. 2008;455:189–194.

[18] Seto Y, Kameoka H, Yamaguchi S, Kyozuka J. Recent advances in strigolactone research: chemical and biological aspects. Plant Cell Physiol. 2012;53:1843–1853.

[19] Umehara M, Hanada A, Yoshida S, Akiyama K, Arite T, Takeda-Kamiya N, et al. Inhibition of shoot branching by new terpenoid plant hormones. Nature. 2008;455:195–200.

[20] Nelson DC, Riseborough JA, Flematti GR, Stevens J, Ghisalberti EL, Dixon KW, et al. Karrikins discovered in smoke trigger *Arabidopsis* seed germination by a mechanism requiring gibberellic acid synthesis and light. Plant Physiol. 2009;149:863–873.

[21] Waters MT, Nelson DC, Scaffidi A, Flematti GR, Sun YK, Dixon KW, et al. Specialisation within the DWARF14 protein family confers distinct responses to karrikins and strigolactones in *Arabidopsis*. Development. 2012;139:1285–1295.

[22] Waters MT, Smith SM. KAI2- and MAX2-mediated responses to karrikins and strigolactones are largely independent of HY5 in *Arabidopsis* seedlings. Mol Plant. 2013;6:63–75.

[23] Wu SH. Gene expression regulation in photomorphogenesis from the perspective of the central dogma. Annu Rev Plant Biol. 2014;65:311–333.

[24] Eckardt NA. From darkness into light: factors controlling photomorphogenesis. Plant Cell. 2001;13:219–221.
[25] Osterlund MT, Hardtke CS, Wei N, Deng XW. Targeted destabilization of HY5 during light-regulated development of *Arabidopsis*. Nature. 2000;405:462–466.
[26] Tsuchiya Y, Vidaurre D, Toh S, Hanada A, Nambara E, Kamiya Y, et al. A small-molecule screen identifies new functions for the plant hormone strigolactone. Nat Chem Biol. 2010;6:741–749.
[27] Al-Babili S, Bouwmeester HJ. Strigolactones, a novel carotenoid-derived plant hormone. Annu Rev Plant Biol. 2015;66:161–186.
[28] Seto Y, Yamaguchi S. Strigolactone biosynthesis and perception. Curr. Opin. Plant Biol. 2014;21:1–6.
[29] Morffy N, Faure L, Nelson DC. Smoke and hormone mirrors: action and evolution of karrikin and strigolactone signaling. Trends Genet. 2016;32:176–188.
[30] Nelson DC, Flematti GR, Ghisalberti EL, Dixon KW, Smith SM. Regulation of seed germination and seedling growth by chemical signals from burning vegetation. Annu Rev Plant Biol. 2012;63:107–130.
[31] López-Juez E, Dillon E, Magyar Z, Khan S, Hazeldine S, de Jager SM, et al. Distinct light-initiated gene expression and cell cycle programs in the shoot apex and cotyledons of *Arabidopsis*. Plant Cell. 2008;20: 947–968.
[32] Nelson DC, Scaffidi A, Dun EA, Waters MT, Flematti GR, Dixon KW, et al. F-box protein MAX2 has dual roles in karrikin and strigolactone signaling in *Arabidopsis thaliana*. Proc Natl Acad Sci USA. 2011;108:8897–8902.
[33] Stanga JP, Morffy N, Nelson DC. Functional redundancy in the control of seedling growth by the karrikin signaling pathway. Planta. 2016;243:1397–1406.
[34] Nakamura H, Xue Y-L, Miyakawa T, Hou F, Qin H-M, Fukui K, et al. Molecular mechanism of strigolactone perception by DWARF14. Nat Commun. 2013;4:1–10.
[35] Zhou F, Lin Q, Zhu L, Ren Y, Zhou K, Shabek N, et al. D14-SCFD3-dependent degradation of D53 regulates strigolactone signalling. Nature. 2013;504:406–410.
[36] Scaffidi A, Waters MT, Sun YK, Skelton BW, Dixon KW, Ghisalberti EL, et al. Strigolactone hormones and their stereoisomers signal through two related receptor proteins to induce different physiological responses in Arabidopsis. Plant Physiol.

2014;165:1221–1232.

[37] Datta S, Hettiarachchi C, Johansson H, Holm M. SALT TOLERANCE HOMOLOG2, a B-box protein in *Arabidopsis* that activates transcription and positively regulates light-mediated development. Plant Cell. 2007;19:3242–3255.

[38] Datta S, Johansson H, Hettiarachchi C, Irigoyen ML, Desai M, Rubio V, et al. LZF1/SALT TOLERANCE HOMOLOG3, an *Arabidopsis* B-box protein involved in light-dependent development and gene expression, undergoes COP1-mediated ubiquitination. Plant Cell. 2008;20:2324–2338.

[39] Kumagai T, Ito S, Nakamichi N, Niwa Y, Murakami M, Yamashino T, et al. The common function of a novel subfamily of B-Box zinc finger proteins with reference to circadian-associated events in *Arabidopsis thaliana*. Biosci Biotechnol Biochem. 2008;72:1539–1549.

[40] Chang CS, Li YH, Chen LT, Chen WC, Hsieh WP, Shin J, et al. LZF1, a HY5-regulated transcriptional factor, functions in *Arabidopsis* de-etiolation. Plant J. 2008;54:205–219.

[41] Dhingra A, Portis AR, Daniell H. Enhanced translation of a chloroplast-expressed *RbcS* gene restores small subunit levels and photosynthesis in nuclear *RbcS* antisense plants. Proc Natl Acad Sci USA. 2004;101:6315–6320.

[42] Meehan L, Harkins K, Chory J, Rodermel S. *Lhcb* transcription is coordinated with cell size and chlorophyll accumulation (studies on fluorescence-activated, cell-sorter-purified single cells from wild-type and *immutans Arabidopsis thaliana*). Plant Physiol. 1996;112:953–963.

[43] Boss PK, Davies C, Robinson SP. Analysis of the expression of anthocyanin pathway genes in developing *Vitis vinifera* L. cv Shiraz grape berries and the implications for pathway regulation. Plant Physiol. 1996;111:1059–1066.

[44] Solfanelli C, Poggi A, Loreti E, Alpi A, Perata P. Sucrose-specific induction of the anthocyanin biosynthetic pathway in *Arabidopsis*. Plant Physiol. 2006;140:637–646.

[45] Hiratsu K, Matsui K, Koyama T, Ohme-Takagi M. Dominant repression of target genes by chimeric repressors that include the EAR motif, a repression domain, in *Arabidopsis*. Plant J. 2003;34:733–739.

[46] Porra RJ, Thompson WA, Kriedemann PE. Determination of accurate extinction

coefficients and simultaneous equations for assaying chlorophylls a and b extracted with four different solvents: verification of the concentration of chlorophyll standards by atomic absorption spectroscopy. Biochim Biophys Acta Bioenergetics. 1989;975:384–394.

[47] Ito S, Nozoye T, Sasaki E, Imai M, Shiwa Y, Shibata-Hatta M, et al. Strigolactone regulates anthocyanin accumulation, acid phosphatases production and plant growth under low phosphate condition in *Arabidopsis*. PLoS One. 2015;10:1–17.

Remark: This chapter already published in;

Thussagunpanit J, Nagai Y, Nagae M, Mashiguchi K, Mitsuda N, Ohme-Takagi M, Nakano T, Nakamura H, Asami T. Involvement of STH7 in light-adapted development in *Arabidopsis thaliana* promoted by both strigolactone and karrikin. Biosci Biotechnol Biochem. 2017;81:292–301. DOI: 10.1080/09168451.2016.1254536

CHAPTER 4: Coordination of STH7 and the Brassinosteroid Regulated Molecules Mediates the Crosstalk between Strigolactone and Brassinosteroid in Light-adapted Development

4.1 Chapter introduction

Growth and development in plants are not only regulated by the environment stimuli but also by several phytohormones [1]. Sometimes different plant hormones contribute to the inducing of the same plant phenomena indicating that they have the synergistic interaction [1–3]. Crosstalk among phytohormones usually occur at the gene network [4]. For example, the cell elongation is mediated by both BRs and GAs. The transcription repressor of GAs, DELLAs, stabilize and suppress the positive transcription regulator of BR, BIL1/BZR1 leading to inhibit the cell expansion [5]. GA application causes the degradation of DELLA and allows the initiation cell elongation response by BIL1/BZR1 [5, 6]. In this chapter, the crosstalk of plant hormones in the light-adapted growth was investigated.

Light is the important environmental factor that regulates plant growth and development from seed germination to seedling establishment [7]. After light perception, seedlings display the shortened hypocotyls, the opened cotyledons, the development of true leaves, and the biosynthesis of chlorophyll and anthocyanin. This process is called the light-adapted development or photomorphogenesis [8, 9]. Various transcription factors regulate this light-adapted development as positive or negative regulators such as, basic leucine zipper transcription factors (bZIPs), basic helix-loop-helix transcription factors (bHLHs), and B-box zinc-finger transcription factors (BBXs) [9]. One of the important positive regulators of photomorphogenesis is HY5, which is the member in bZIPs family [9]. In darkness, COP1, a negative regulator of photomorphogenesis, represses HY5 by inhibiting the binding of HY5 to the promoter regions of light-induced genes [8, 10]. Cytokinins have been reported to moderate light-adapted growth by activating the HY5 accumulation [11]. On the contrary, GAs induce COP1 activity leading to repress the HY5 accumulation [7]. Moreover, the treatment with SLs, a series

of terpenoidal lactone-type plant hormones [12, 13], reduce COP1 leading to promote HY5 function [14]. These evidences suggest that there should be the crosstalk between light signal and plant hormones. The previous study showed that SL could decrease hypocotyl elongation of *Arabidopsis* even if in darkness [chapter 3, ref. 15]. It implies that SL not only regulates the light-adapted development by crosstalk with light through HY5, but also substitutes for light signals through other components. Another group of transcription factors that regulate the photomorphogenesis is the subfamily IV of BBXs, which is compose of eight members consisting of BBX18–BBX25 [16]. Previous microarray analysis revealed that SL up-regulated the expression of BBX20/STH7 [17], and later demonstrated that among subfamily IV of BBXs, only the transcriptional level of *STH7* was up-regulated by GR24, a synthetic analogue of SL [18]. Moreover, STH7 was identified to exist in the downstream signaling of BRs [19].

BRs are the group of steroidal plant hormones that function in the cell elongation [20, 21] and the hypocotyl elongation [chapter 2, ref. 22]. On the other hand, SL inhibits the hypocotyl elongation of *Arabidopsis* [chapter 3, ref. 15]. Since the opposite function of SLs and BRs in the hypocotyl elongation which is one of light-adapted response [8, 9], the crosstalk between these two groups of plant hormone may play an important role in regulating the photomorphogenesis. Here, the mutually antagonistic effects of SLs and BRs were investigated by focusing on the STH7 function. The *STH7-overexpressing* (*STH7ox*), the defective function of *STH7* (*STH7-SRDX*) and their double mutants between BR-regulated molecules were used in this study.

4.2 Results

4.2.1 Effects of strigolactones and brassinosteroids on *Arabidopsis* hypocotyl elongation

A synthetic SL analogue, GR24, and the most potent BR, BL, at 10 μM and 10 nM, respectively, was applied to wild-type *Arabidopsis* ecotype Col (hereafter wild-type), *STH7ox* and *STH7-SRDX*. The results showed that GR24 significantly reduced hypocotyl elongation of wild-type and *STH7ox* under weak light condition. *STH7-SRDX* hypocotyls was not decreased with treatment of GR24 (Fig. 4-1). As described above, GR24 reduced the hypocotyl length, while BL treatment increased the hypocotyl elongation of wild-type and *STH7ox* (Fig. 4-1). The inhibitory activity of GR24 on hypocotyl elongation of wild-type and *STH7ox* was decreased with the co-treatment of BL, suggesting that BR can counteract SL. (Fig. 4-1). Considering shortened hypocotyls are one of light-adapted growth [8, 9], this result implies that SL and BR has the mutual antagonistic function in photomorphogenesis. To clarify this hypothesis, Brz, the BR biosynthesis inhibitor [23, 24], was applied to the plants. Brz significantly decreased hypocotyl elongation in all plants, but *STH7-SRDX* mutants were less sensitive to Brz comparing with wild-type and *STH7ox* (Fig. 4-2). These results supported that SL and BR play an opposite role in the hypocotyl growth and STH7 could be involved in the functions of both SL and BR. Moreover, co-treatment of GR24 and Brz induced shorter hypocotyls in wild-type and *STH7ox* than the individual application of either GR24 or Brz, and these shortened hypocotyls could not restore with treatment of BL (Fig. 4-2). That is, the effect of Brz was additive to that of SL and linked with the function of SL.

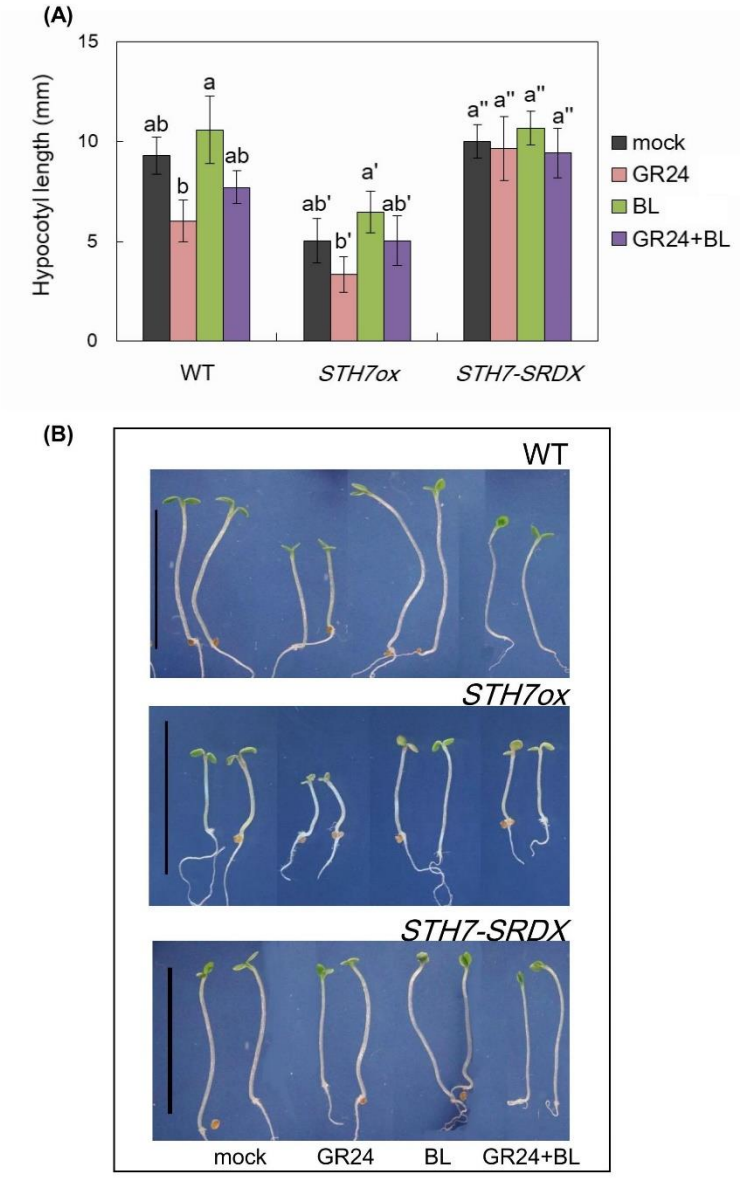

Fig. 4-1 Effects of strigolactone and brassinosteroid on the *Arabidopsis* hypocotyl elongation

Hypocotyl elongation of wild-type *Arabidopsis*, *STH7ox* and *STH7-SRDX* (A, B). Plants were grown on 1/2 MS medium containing 10 μM GR24, 10 nM BL or the mixture of GR24 and BL (GR24+BL) under weak light condition for 4 days. The 0.1% DMSO was used as control. Data shown in (A) are means ± SD shown by vertical error bars ($n \geq 20$). Means with the same letter are not significantly different at $p \leq 0.05$ according to Tukey–Kramer's honestly significant difference test. Scale bars in (B) represent 10 mm.

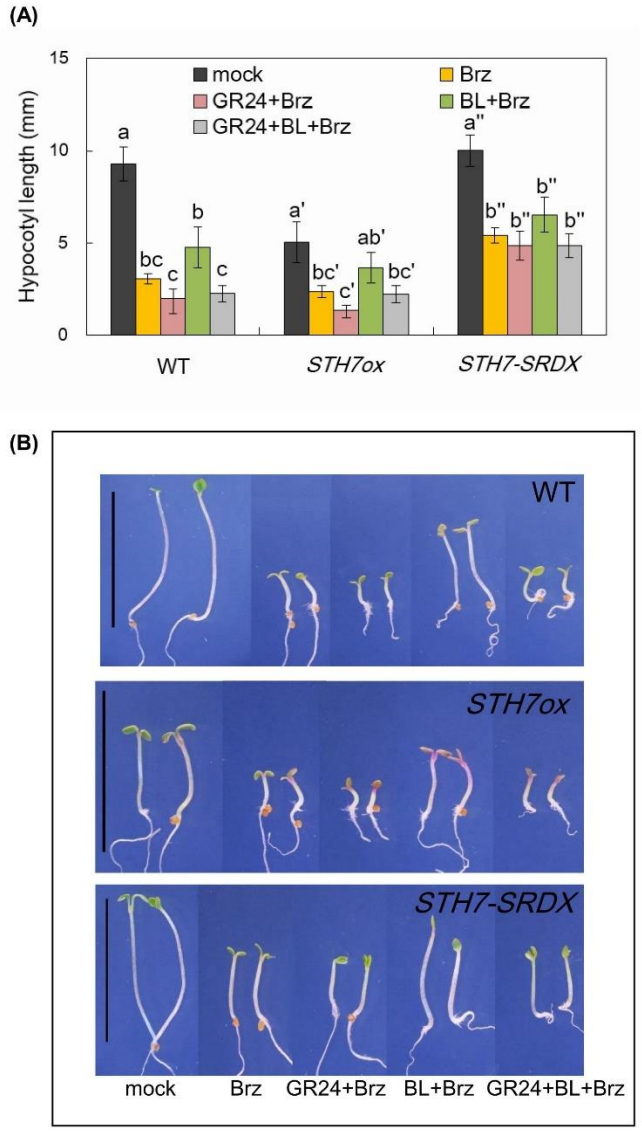

Fig. 4-2 Effects of strigolactone and brassinosteroid biosynthesis inhibitor on the *Arabidopsis* hypocotyl elongation

Hypocotyl elongation of wild-type *Arabidopsis*, *STH7ox* and *STH7-SRDX* (A, B). Plants were grown on 1/2 MS medium containing 10 μM GR24, 0.3 μM Brz or the mixture of GR24, Brz, and 10 nM BL (GR24+BL, BL+Brz and GR24+BL+Brz) under weak light condition for 4 days. The 0.1% DMSO was used as control. Data shown in (A) are means ± SD shown by vertical error bars ($n \geq 20$). Means with the same letter are not significantly different at $p \leq 0.05$ according to Tukey–Kramer's honestly significant difference test. Scale bars in (B) represent 10 mm.

4.2.2 Influences of strigolactones and brassinosteroids on STH7

In the chapter 3, it is confirmed that SL induces the light-adapted growth of *Arabidopsis* in the STH7-dependent manner. To investigate the involvement of STH7 in the responses of plants to SL- and/or BR-related photomorphogenesis, the expression of *STH7* was determined by qRT-PCT. GR24 treatment increased the *STH7* transcript level in wild-type and this up-regulation tended to decrease by BL treatment (Fig. 4-3). Interestingly, SL-upregulated transcription of *STH7* was significantly increased by the treatment of BR inhibitor, Brz (Fig. 4-3). It implies that SL and Brz can coordinately induce *STH7* transcription. Moreover, the 35S:STH7-GFP transgenic plant was performed to investigate behaviours of STH7 protein upon chemical treatments. STH7-GFP localized in nucleus and STH7-GFP signal was increased when plants were treated with GR24 for 3 h (Fig. 4-4). However, the increase of STH-GFP signal by GR24 was reduced by BL treatment (Fig. 4-4). This result suggested that BR attenuated the accumulation of STH7 in nucleus.

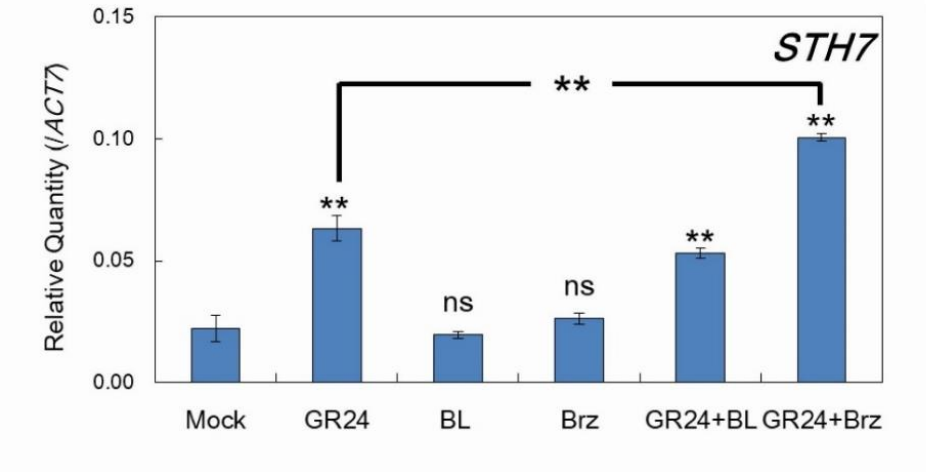

Fig. 4-3 Relative transcript levels of *STH7* in wild-type *Arabidopsis* treated with strigolactone, brassinosteroid, and brassinosteroid inhibitor

Plants were grown in 1/2 MS medium containing 0.1% (v/v) DMSO as a control, 10 μM GR24, 10 nM BL, 0.3 μM Brz, the mixture of GR24 with BL (GR24+BL) or Brz (GR24+Brz) under weak light conditions for 4 days. The transcript levels were normalized to those of *ACT7*. Data are means ± SD shown by vertical error bars (n = 3). Standard deviations are shown as vertical error bars. Statistically significant differences relative to the control are $^{**}p \leq 0.01$, and ns = nonsignificant by Student's *t* test.

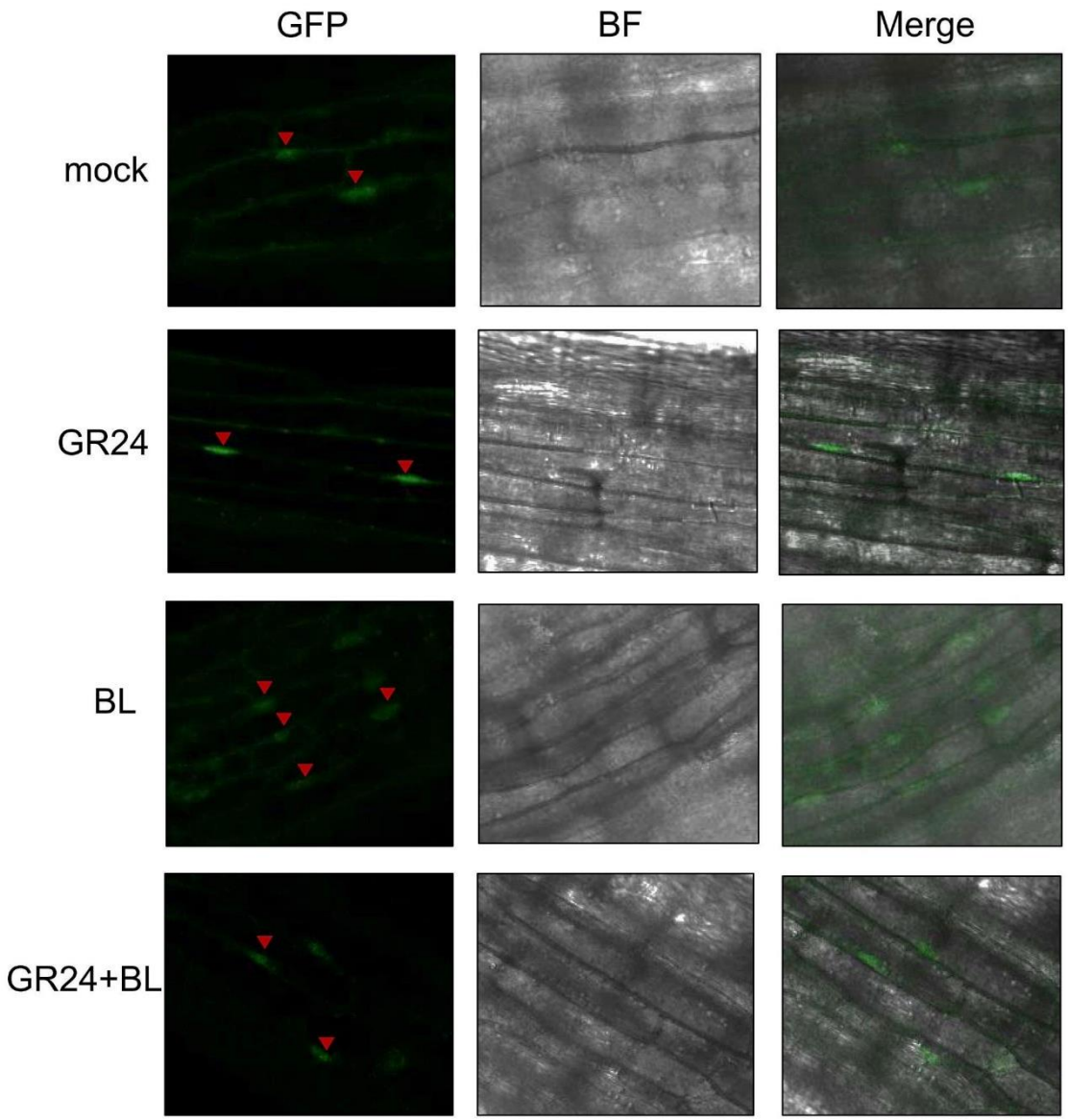

Fig. 4-4 STH-GFP signal in hypocotyl cells

35S:STH7-GFP seedlings were grown on 1/2 MS medium under weak light condition for 4 days. Then, plants were treated with 0.1% (v/v) DMSO as a control, 10 µM GR24, 10 nM BL, and the mixture of GR24 with BL (GR24+BL) for 3 h. STH7-GFP signals were observed in hypocotyl cells by laser scanning microscope. Red triangles indicate nucleus. BF means bright field.

To investigate the relationship between BR and SL, the studies were focused on STH7. The correlation analysis between BR-regulated genes and *STH7*-regulated genes from the previous published microarrays were performed [19, 25]. The data showed that 20 of *STH7*-upregulated genes overlapped with BR-repressed genes (Fig. 4-5A). Furthermore, half of these genes were the genes related to the light responses such as *STH7* and *ELIP2* (Fig. 4-5B), and the pigment biosynthesis such as *CHI* and *CHIL* (Fig. 4-5C). To understand the role of SL and BR in the *STH7*-upregulated and BR-repressed genes, some of the genes from those microarray data were selected to determine their expression levels. First group of selected genes was the Early Light-Induced Proteins (ELIPs) including *ELIP2* and its homolog, *ELIP1*. ELIPs are nuclear-encoded thylakoid membrane proteins belonging to the multigene family of light-harvesting complexes [26, 27]. They can be immediately expressed after light stimulation [26]. The second group of selected genes is the flavonoid biosynthesis-related genes including anthocyanin synthesis, *CHS* and its homolog, *CHI* [28]. Moreover, the expression of *FLS1* which is the *STH7*-upregulated gene encoding the favonol synthase [28] was also determined. All of those five genes, especially, *ELIP1* and *ELIP2*, exhibited the highest expression level in *STH7ox* mutant comparing with those in wild-type and *STH7-SRDX*, suggesting that they might the direct target of STH7 (Fig. 4-6). Moreover, GR24 and Brz were applied to investigate the expression levels of these genes. The results showed that all of those genes have the highest transcript levels when co-treated with GR24 and Brz (Fig. 4-7) in the same manner as *STH7* expression level (Fig. 4-3). The transcriptional quantity of *ELIP2* and *CHI*, which their expression were up-regulated by STH7 and down-regulated by BR, were significantly higher with co-treatment of GR24 and Brz than with single treatment of GR24 at 99% p-value (Figs. 4-7D, E). Whereas, the expression levels of *ELIP1* and *CHS*, which are the STH7-upregulated genes but are not BR-repressed genes (Fig. 4-5), exhibited significant increase at 95% p-value (Figs. 4-7A–C).

(A)

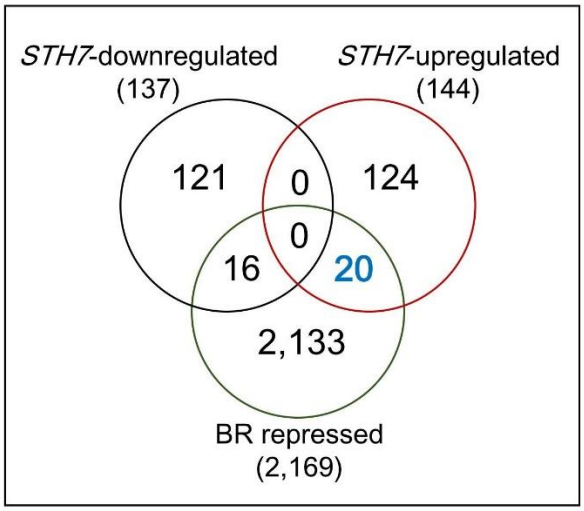

(B)

Gene	Biological process
STH7 (AT4G39070)	Positive regulation of photomorphogenesis
ELIP2 (AT4G14690)	Cellular response to light, Photoprotection, Photosynthesis
CHI (AT3G55120)	Response to UV-B
HBP2 (AT2G37970)	Red or far-red light signaling pathway
VQ12 (AT2G22880)	Response to UV-B
COL1 (*BBX2*, AT5G15850)	Response to light stimulus

(C)

Gene	Biological process
CHI (AT3G55120)	Anthocyanin biosynthetic process
CHIL (AT5G05270)	Anthocyanin biosynthetic process
UGT89C1 (AT1G06000)	Flavonoid biosynthetic process
AT3G56290	Chloroplast organization
AT4G25640	Flavonoid biosynthetic process

Fig. 4-5 The microarray data of brassinosteroid-regulated genes and *STH7*-regulated genes

Overlapping of BR-repressed gene from Sun et al. [19] with *STH7*-regulated genes from Fan et al. [25] (A). Some of genes overlapping *STH7*-upregulated and BR-repressed genes were the light response-related gene (B) or the pigment biosynthesis-related genes (C). The biological process of genes obtained from TAIR database (www.arabidopsis.org).

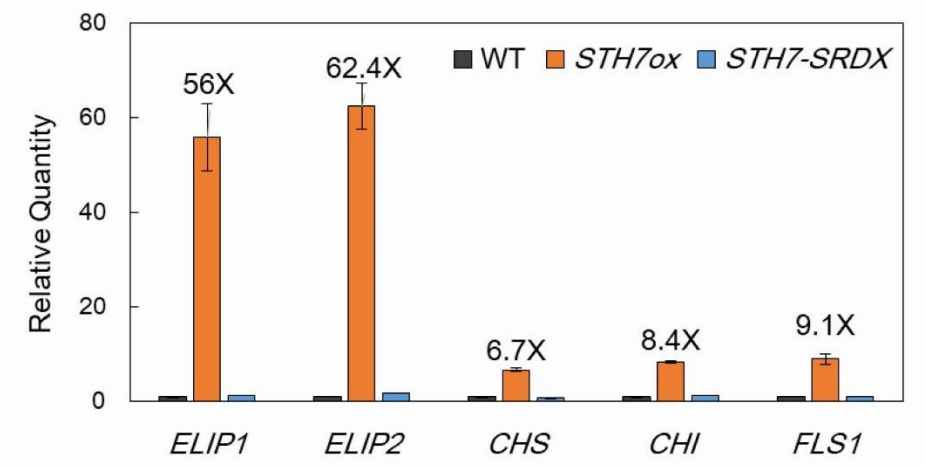

Fig. 4-6 Quantitative real-time PCR analysis of the *STH7*-upregulated genes

Relative transcript levels of *ELIP1*, *ELIP2*, *CHS*, *CHI* and *FLS1* in wild-type *Arabidopsis*, *STH7-ox* and *STH7-SRDX* mutants were analysed. Plants were grown in 1/2 MS medium under weak light for 4 days. The transcript levels were normalized to those of *ACT7*. The number above the expression levels of each gene in *STH7ox* mutant indicated their increasing times comparing with in wild-type. Data are means ± SD shown by vertical error bars (n = 3).

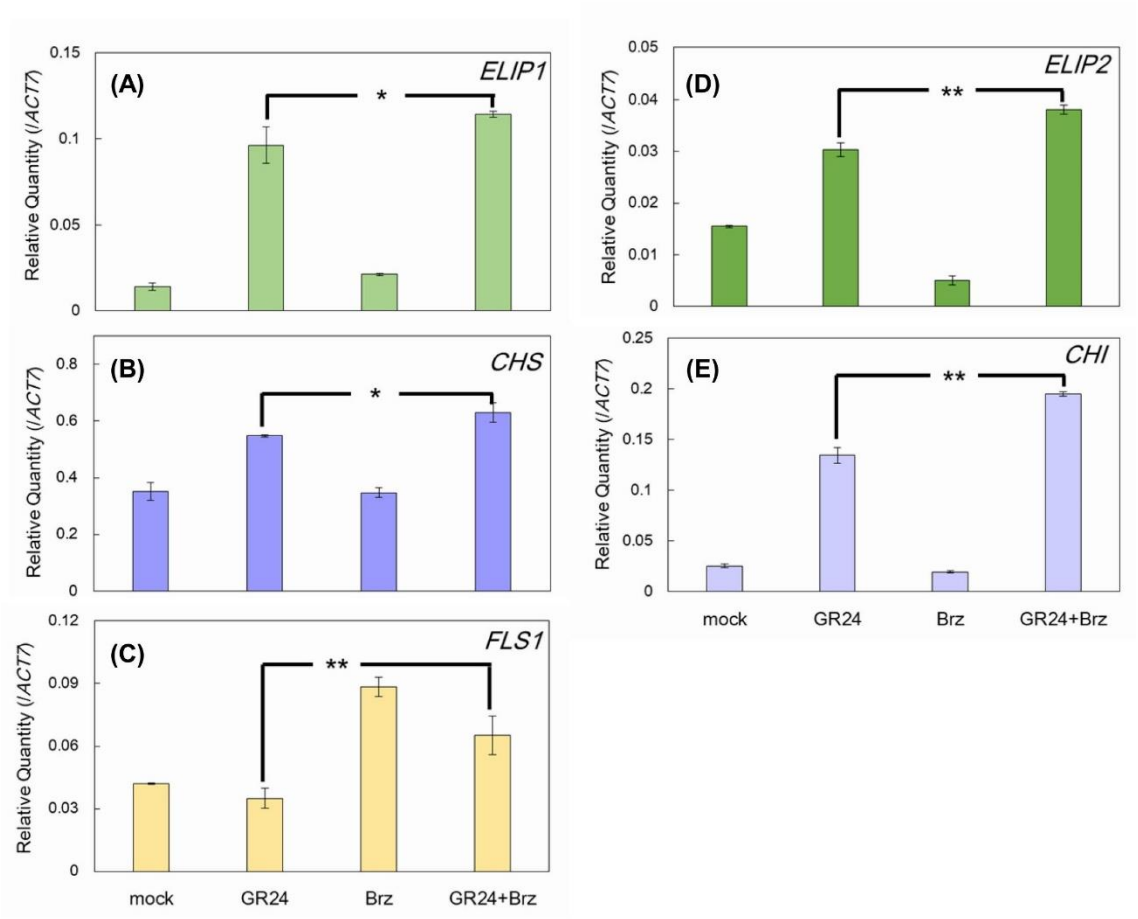

Fig. 4-7 Relative transcript levels of the *STH7*-upregulated genes in wild-type *Arabidopsis* treated with strigolactone and brassinosteroid inhibitor

Relative transcript levels of *ELIP1* (A), *CHS* (B), *FLS1* (C), *ELIP2* (D), and *CHI* (E) in wild-type *Arabidopsis* were analysed. Plants were grown in 1/2 MS medium containing 0.1% (v/v) DMSO as a control, 10 µM GR24, 0.3 µM Brz or the mixture of GR24 and Brz (GR24+Brz) under weak light for 4 days. The transcript levels were normalized to those of *ACT7*. Data are means ± SD shown by vertical error bars (n = 3). Statistically significant differences comparing between GR24 treatment and GR24+Brz co-treatment are $^{**}p \leq 0.01$ and $^{*}p \leq 0.05$ by Student's *t* test.

4.2.3 Integration of brassinosteroids positive regulators and STH7

Since the co-application of SL and BR inhibitor, Brz, clearly induced the high expression levels of *STH7* (Fig. 4-3) and possibly *STH7* downstream genes such as *ELIP1* and *ELIP2* (Fig. 4-7), it is likely that both SL and BR inhibitor positively act in the expression of STH7 functions. When BR is perceived by its receptor, the nuclear proteins including BIL1/BZR1 (hereafter BIL1) and its homolog, BES1 are accumulated in the dephosphorylation form and initiate BR responses. Thus, BIL1 and BES1 act as positive regulators of BR signaling [29, 30]. To clarify how BR and SL mediate the light-adapted development in the STH7-dependent manner, double mutants between BR gain-of-function *bil1-1D* or *bes1-D*, and *STH7ox* or *STH7-SRDX* were produced by hybridization. The *bil1-1D*×*STH7ox*, *bil1-1D*×*STH7-SRDX*, *bes1-D*×*STH7ox* and *bes1-D*×*STH7-SRDX* double mutants were used in this chapter. Among them, *bil1-1D*×*STH7ox* presented shorter petioles and smaller leaves than their wild-type similar to single mutant of *STH7* (Figs. 4-8A, B). Furthermore, the leaves of *bil1-1D*×*STH7ox* mutant displayed downward curling and dark green color (Fig. 4-8B). Leaves of *bil1-1D*×*STH7-SRDX* were larger than those of *bil1-1D*×*STH7ox* and exhibited round leaves as same as *bil1-1D* (Figs. 4-8A, C). All of *bes1-D*×*STH7ox* and *bes1-D*×*STH7-SRDX* double mutants exhibited the characteristics similar to their single mutant, *bes1-D*. That is, they had long petioles and some of petioles and leaf blades were curved (Figs. 4-8D, E). Moreover, leaf color of *bes1-D*-related double mutants and *bes1-D* single mutant appeared weaker green than their wild-type (Figs. 4-8A, D, E).

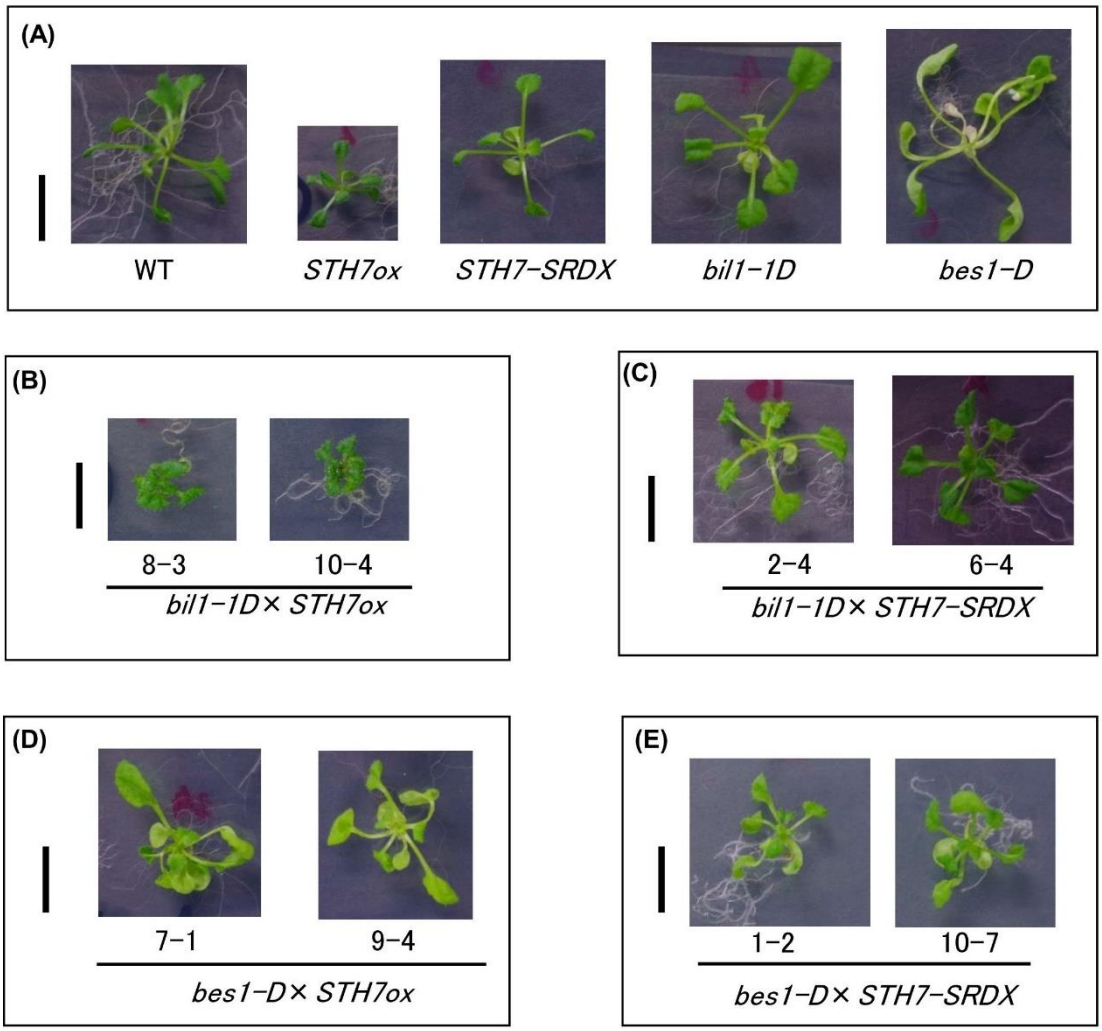

Fig. 4-8 Phenotype of the *bil1-1D*-related and *bes1-D*-related double mutants

Parent lines (A) including wild-type *Arabidopsis* (control), *STH7ox*, *STH7-SRDX*, *bil1-1D*, and *bes1-D* as well as *bil1-1D*×*STH7ox* (B), *bil1-1D*×*STH7-SRDX* (C), *bes1-D*×*STH7ox* (D) and *bes1-D*×*STH7-SRDX* (E) double mutants were grown in 1/2 MS medium at 22 °C under 22/8 light/dark cycle. The phenotypes were observed after 3-week-grown. Scale bars represent 1 cm.

Then, the effects of GR24 and BL on the hypocotyl elongation of *bil1-1D*-related and *bes1-D*-related double mutants were determined. Similarly to Fig. 4-2, co-treatment of GR24 and Brz caused shorter hypocotyl length in wild-type and *STH7ox* than single treatment of Brz (Figs. 4-9 and 4-10). In the *bil1-1D*-related double mutants, all lines of *bil1-1D×STH7ox* showed the responses to GR24 and Brz in a similar manner as their single mutant *STH7ox* did. Hypocotyl length of *bil1-1D×STH7ox* double mutant was decreased by the application of either GR24 or Brz. *bil1-1D×STH7ox* presented the shortest hypocotyls when co-treated with GR24 and Brz (Fig. 4-9). *STH7-SRDX* showed less but significant sensitivity to Brz, while *bil1-1D×STH7-SRDX* lines were insensitive to Brz in the inhibition of hypocotyl elongation. This response was similar to that of *bil1-1D* (Fig. 4-9). In the *bes1-D*-related double mutants, hypocotyl length of neither *bes1-D×STH7ox* nor *bes1-D×STH7-SRDX* double mutant was reduced by Brz, similarly to that presented in *bes1-D* (Fig. 4-10). Moreover, co-application of GR24 and Brz could not induce shorter hypocotyl length in *bes1-D×STH7ox* than single treatment of GR24 (Fig. 4-10). Taking account of the phenotype of *bil1-1D*-related double mutants, *bes1-D*-related double mutants and their responses to the application of SL and BR inhibitor, STH7 might be respectively regulated by BIL1 and BES1 in different manners.

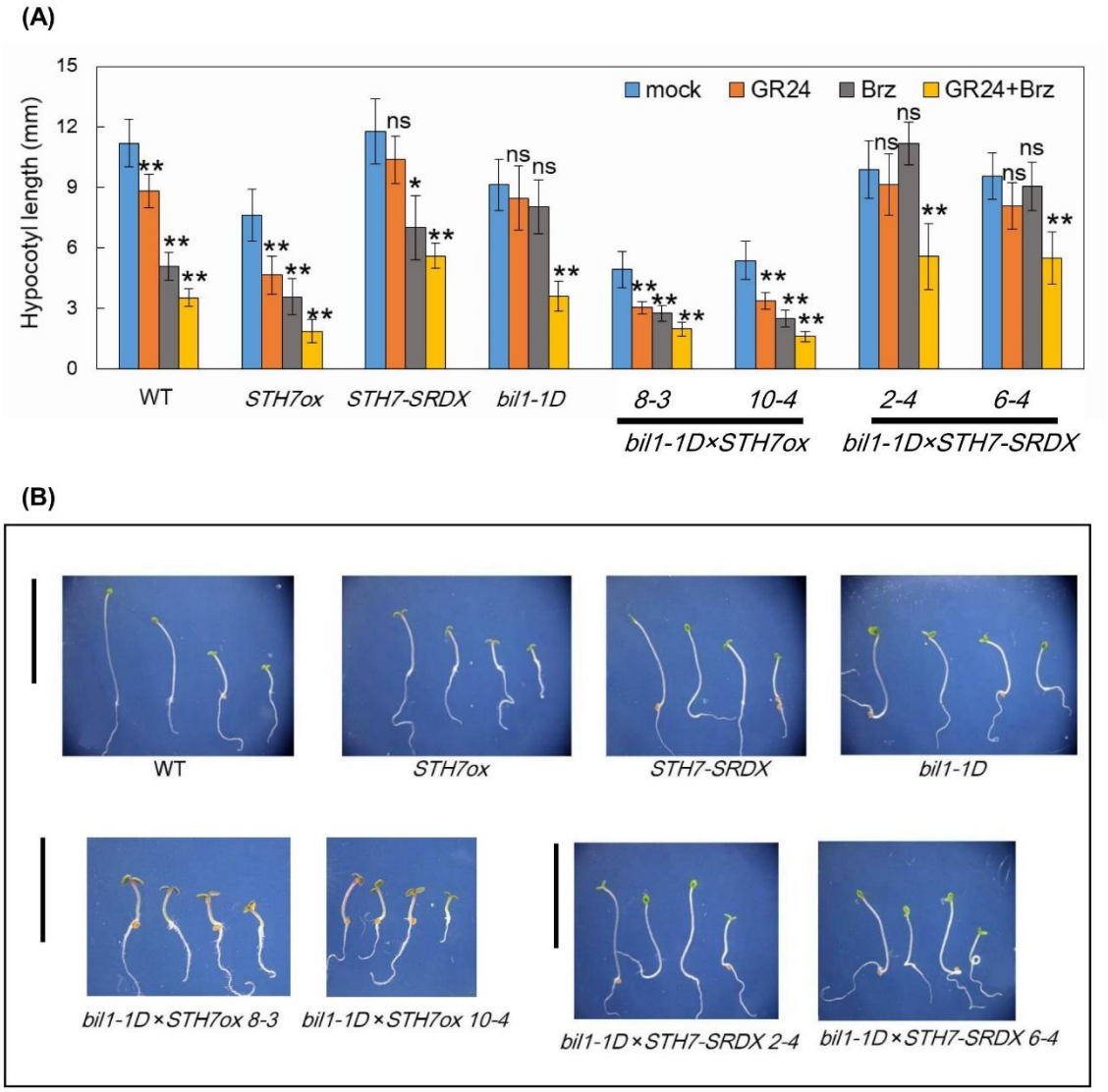

Fig. 4-9 Hypocotyl elongation of *bil1-1D*-related double mutants

Hypocotyl elongation of wild-type, *STH7ox*, *STH7-SRDX*, *bil1-1D*×*STH7ox*, and *bil1-1D*×*STH7-SRDX* (A, B). Plants were grown on 1/2 MS medium containing 10 μM GR24, 0.3 μM Brz or the mixture of GR24 and Brz (GR24+Brz) under weak light condition for 4 days. The 0.1% DMSO was used as control. Data shown in (A) are means ± SD shown by vertical error bars ($n \geq 15$). Statistically significant differences relative to each control are $^{**}p \leq 0.01$, $^{*}p \leq 0.05$, and ns = nonsignificant by Student's *t* test. Each frame of hypocotyl's picture in (B) represents control, GR24, Brz, GR24+Brz treatment from left to right, respectively. Scale bars represent 10 mm.

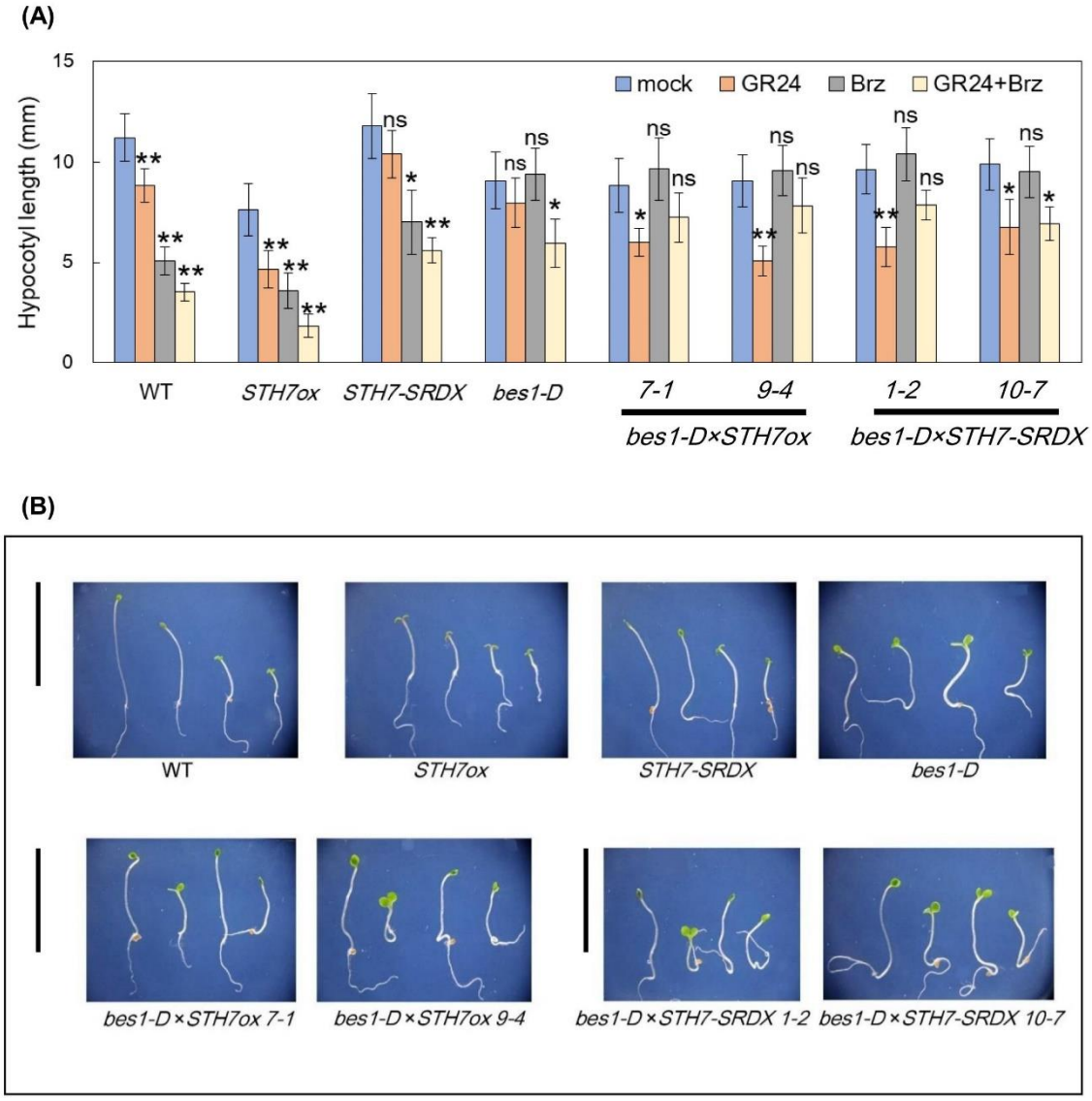

Fig. 4-10 Hypocotyl elongation of *bes1-D*-related double mutants

Hypocotyl elongation of wild-type, *STH7ox*, *STH7-SRDX*, *bes1-D*×*STH7ox*, and *bes1-D*×*STH7-SRDX* (A, B). Plants were grown on 1/2 MS medium containing 10 μM GR24, 0.3 μM Brz or the mixture of GR24 and Brz (GR24+Brz) under weak light condition for 4 days. The 0.1% DMSO was used as control. Data shown in (A) are means ± SD shown by vertical error bars ($n \geq 15$). Statistically significant differences relative to each control are $^{**}p \leq 0.01$, $^{*}p \leq 0.05$, and ns = nonsignificant by Student's *t* test. Each frame of hypocotyl's picture in (B) represents control, GR24, Brz, GR24+Brz treatment from left to right, respectively. Scale bars represent 10 mm.

Four kinds of double mutant were grown under weak light for 4 days and the chlorophylls and anthocyanins were extracted from the cotyledons to determine their contents. The result showed that *STH7ox* and all lines of *bil1-1D*×*STH7ox* accumulated higher amount of total Chl than wild-type (Fig. 4-11A). In *bes1-D*-related mutants, *bes1-D* and a line of *bes1-D*×*STH7-SRDX* had lower content of total Chl than wild-type. On the other hand, a line of *bes1-D*×*STH7ox* showed higher total Chl comparing to their wild-type and *bes1-D* (Fig. 4-11B). The accumulation of the anthocyanin was clearly higher in *bil1-1D*×*STH7ox* double mutants than in wild-type (Fig. 4-12A). On the other hand, the anthocyanin level in *bes1-D*×*STH7ox* was higher than that in wild-type (Fig. 4-12B) but lower than that in *bil1-1D*×*STH7ox* (Fig. 4-12).

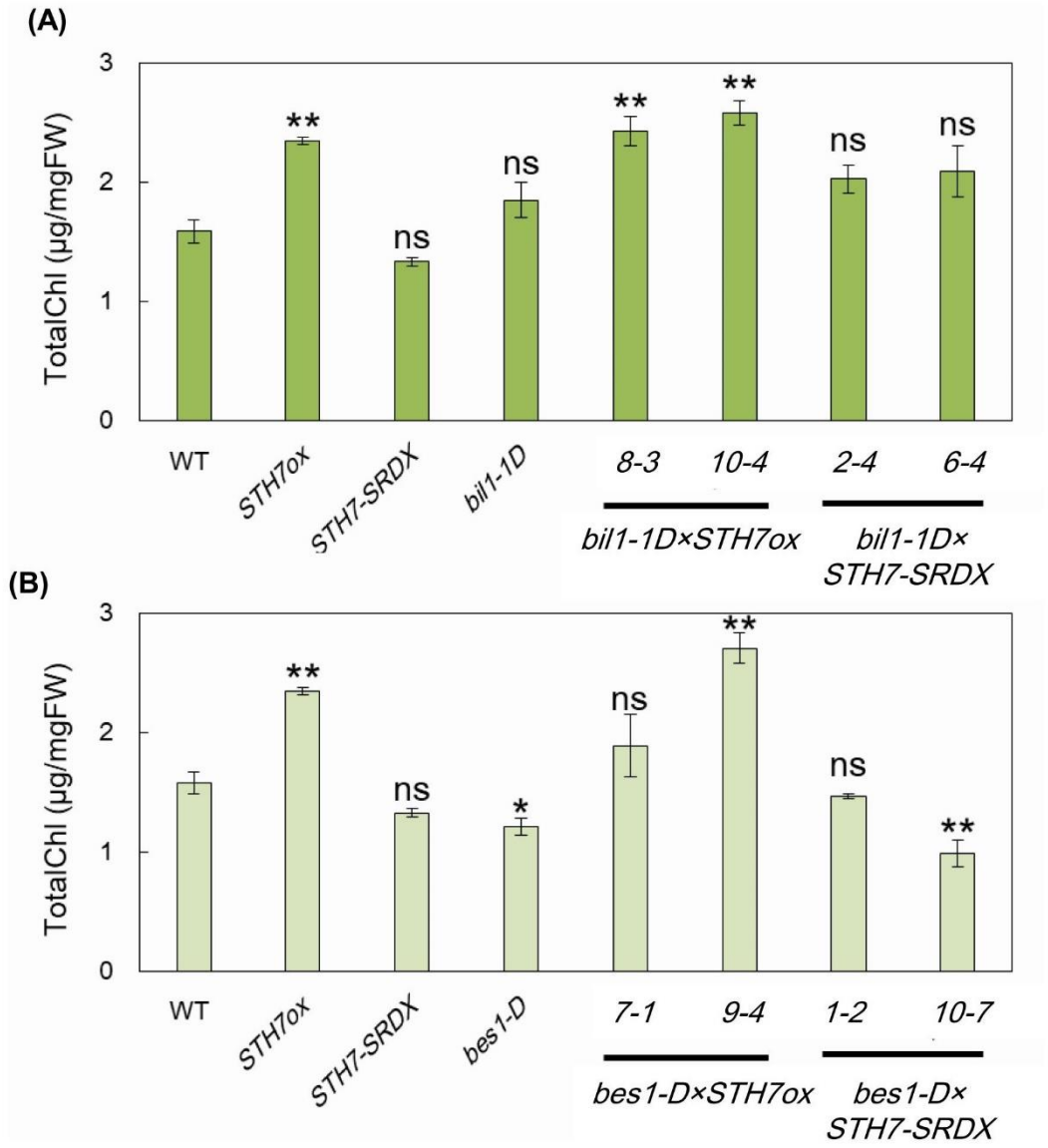

Fig. 4-11 Chlorophyll content in the *bil1-1D*-related and *bes1-D*-related double mutants

Total chlorophyll contents in *bil1-1D*-related double mutants (A) and *bes1-D*-related double mutants (B) were examined. Plants were grown under weak light conditions for 7 days and their cotyledons were collected for the chlorophyll extraction. Data are means ± SD shown by vertical error bars (n = 4). Statistically significant differences relative to wild-type (WT) are $^{**}p \leq 0.01$, $^{*}p \leq 0.05$, and ns = nonsignificant by Student's *t* test.

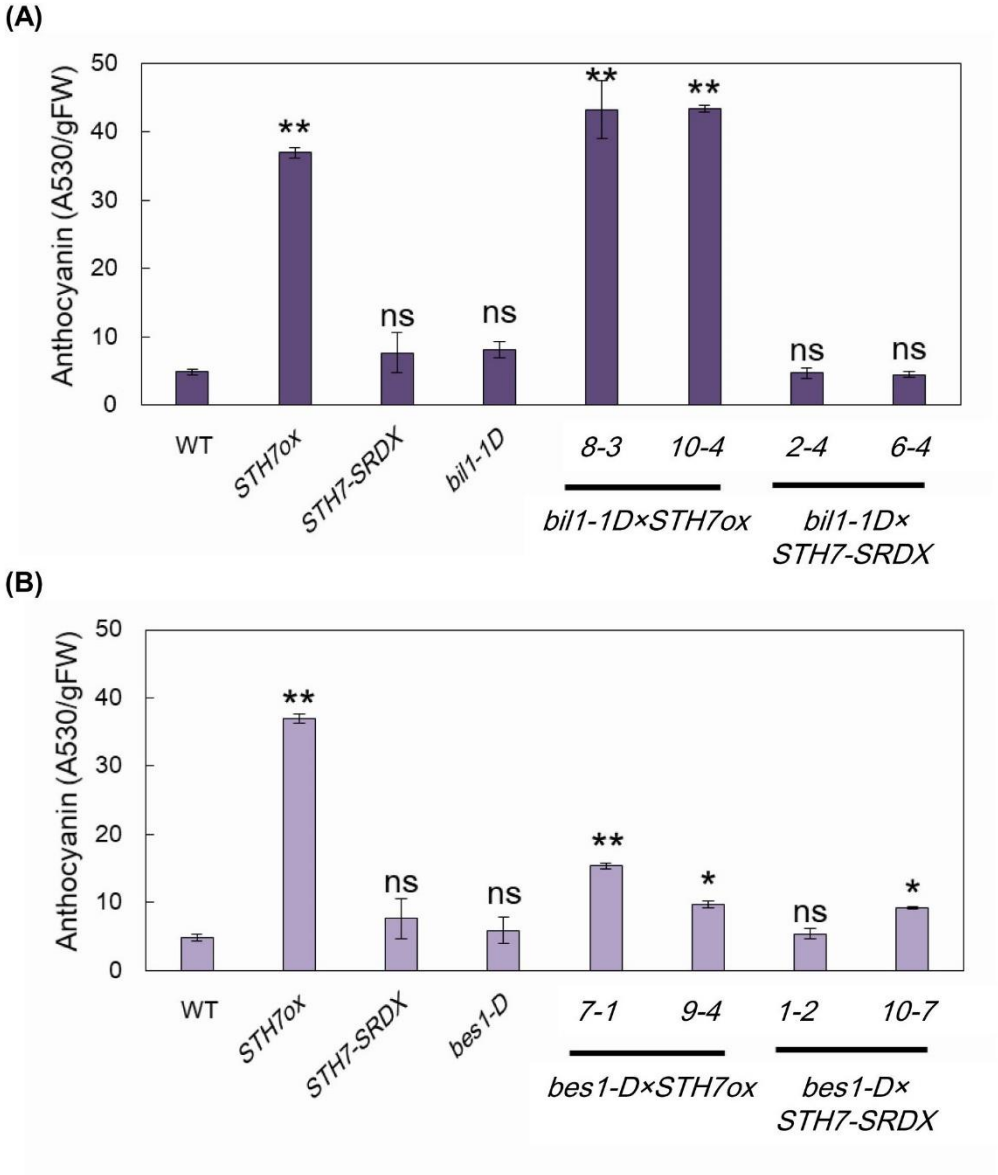

Fig. 4-12 Anthocyanin content in the *bil1-1D*-related and *bes1-D*-related double mutants

Anthocyanin contents in *bil1-1D*-related double mutants (A) and *bes1-D*-related double mutants (B) were examined. Plants were grown under weak light conditions for 7 days and their cotyledons were collected for the anthocyanin extraction. Data are means ± SD shown by vertical error bars (n = 4). Statistically significant differences relative to wild-type (WT) are $^{**}p \leq 0.01$, $^{*}p \leq 0.05$, and ns = nonsignificant by Student's *t* test.

4.2.4 Transcript levels of *STH7* and cell elongation-related genes

To examine the hypothesis that STH7, a transcription factor related to light-adapted growth, is differently regulated by BIL1 and BES1, *STH7* expression level in wild-type, *bil1-1D* and *bes1-D* were analyzed. While the *STH7* expression level increased 8.6-folds in wild-type plants co-treated with GR24 and Brz comparing to its control, the expression levels of *STH7* increased only 3.1-folds in *bil1-1D* by the same treatment (Fig. 4-13). That is, there was a 64% fall in the rate of increase. On the other hand, in *bes1-D* co-treated with GR24 and Brz the rate of increase in the expression level of *STH7* was at the same level as in wild-type (Fig. 4-13).

Since the study is focused on the light-adapted responses such as shortened hypocotyls in this research, a quantitative analysis of the expression levels of the cell elongation regulated genes should be a good tool to examine SL and BR crosstalk. In this context an early auxin-inducible gene (*SAUR-AC1*), a gene encoding a xyloglucan-endotransglycosylase (*TCH4*), an expansin gene (*EXP1*), and *PRE1* which is the gene that has been identified as a positive regulator of cell elongation [31] were analyzed as representatives of cell elongation-related genes. The qRT-PCR results showed that either GR24 or Brz treatment reduced the expression levels of *SAUR-AC1*, *TCH4*, *EXP1* and *PRE1* in wild-type comparing with control treatment. Moreover, GR24 and Brz coordinately down-regulated transcript levels of these genes as shown in the plants co-treated with GR24 and Brz (Figs. 4-14 and 4-15). Comparing with wild-type, *SAUR-AC1*, *TCH4* and *PRE1* were down-regulated in *bil1-1D×STH7ox* and these genes were up-regulated in *bil1-1D×STH7-SRDX* by both GR24 and Brz treatments (Figs. 4-14A, B, D). When plants were co-treated with GR24 and Brz, *SAUR-AC1* and *PRE1* were extremely down-regulated in *bil1-1D×STH7ox* (Figs. 4-14A, D) whereas *TCH4* was most up-regulated in *bil1-1D×STH7-SRDX* (Figs. 4-14B). Without the treatment of GR24 and Brz, *SAUR-AC1*, *TCH4* and *PRE1* were down-regulated in *bes1-D×STH7ox* but these genes were up-regulated in *bes1-D×STH7-SRDX* (Figs. 4-15A, B, D). However, the expression levels of *SAUR-AC1* were not significantly different in both *bes1-D×STH7ox* and *bes1-D×STH7-SRDX* double mutants treated with GR24 (Fig. 4-15A). Treated with Brz,

TCH4 and *PRE1* transcription levels in *bes1-D×STH7ox* and *bes1-D×STH7-SRDX* double mutants were not significantly different (Figs. 4-15B, D). The co-treatment of GR24 and Brz showed rather same expression levels of *TCH4* and *EXP1* in all *bes1-D*-related double mutants (Figs. 4-15B, C). Based on the different expression pattern of cell elongation-related genes in *bil1-1D*-related and *bes1-D*-related double mutants, the coordination mechanism between STH7 and BIL1 or STH7 and BES1 to control the light-adapted development might be different.

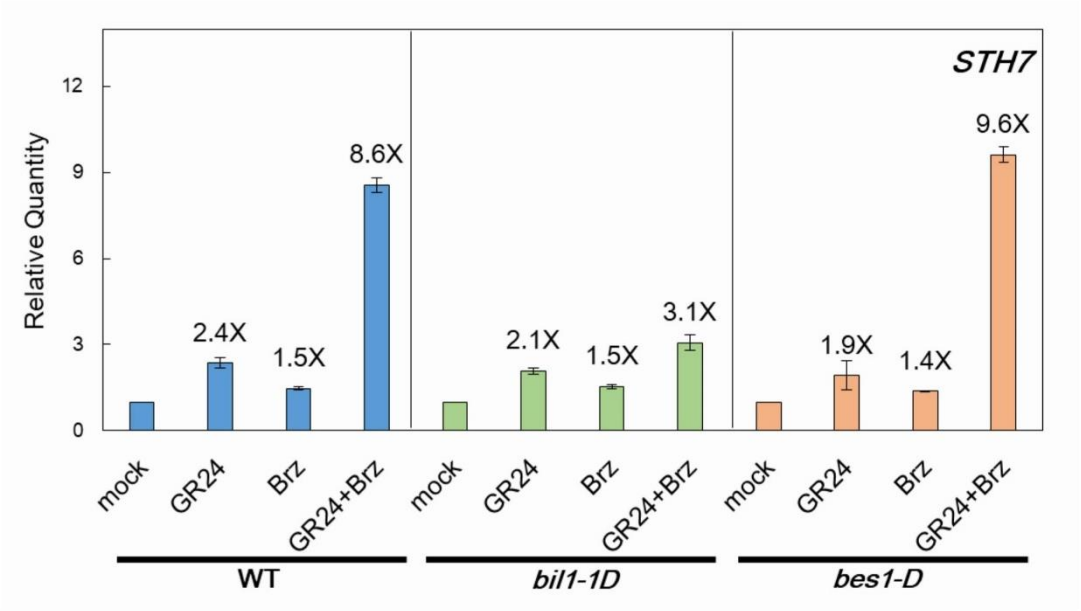

Fig. 4-13 Transcriptional expression of *STH7* in wild-type *Arabidopsis*, *bil1-1D*, and *bes1-D*

Relative transcript levels of *STH7* in wild-type *Arabidopsis*, the BR gain-of-function *bil1-1D* and *bes1-D* were analysed. Plants were grown in 1/2 MS medium containing 0.1% (v/v) DMSO as a control, 10 μM GR24, 0.3 μM Brz or the mixture of GR24 and Brz (GR24+Brz) under weak light for 4 days. The transcript levels were normalized to those of *ACT7*. The number above the expression levels of each treatment indicates their increasing times comparing with their control. Data are means ± SD shown by vertical error bars (n = 3).

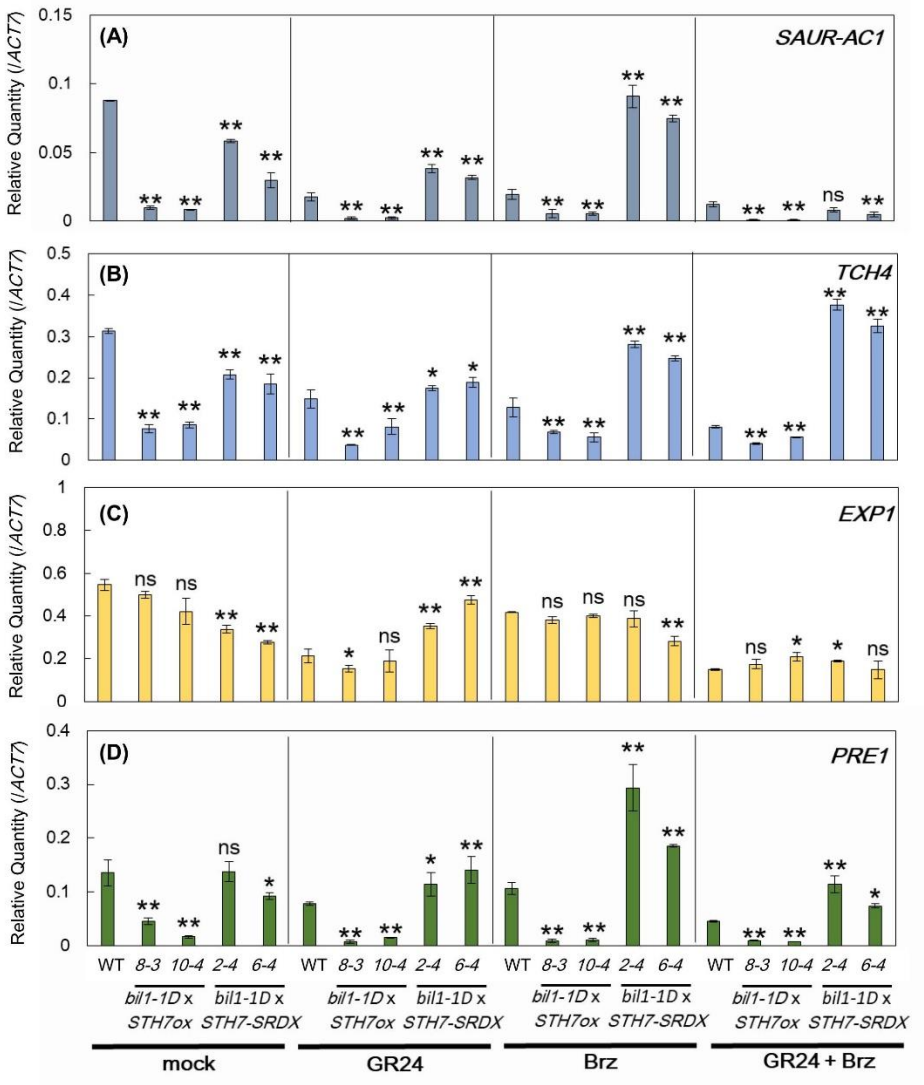

Fig. 4-14 Expression levels of cell elongation-related genes in *bil1-1D*-related double mutants

Relative transcript levels of *SAUR-AC1* (A), *TCH4* (B), *EXP1* (C), and *PRE1* (D) in wild-type *Arabidopsis*, *bil1-1D*×*STH7ox* and *bil1-1D*×*STH7-SRDX* double mutants were analysed. Plants were grown in 1/2 MS medium containing 0.1% (v/v) DMSO as a control, 10 µM GR24, 0.3 µM Brz or the mixture of GR24 and Brz (GR24+Brz) under weak light for 4 days. The transcript levels were normalized to those of *ACT7*. Data are means ± SD shown by vertical error bars (n = 3). Statistically significant differences relative to wild-type (WT) of each treatment are $^{**}p \leq 0.01$, $^{*}p \leq 0.05$, and ns = nonsignificant by Student's *t* test.

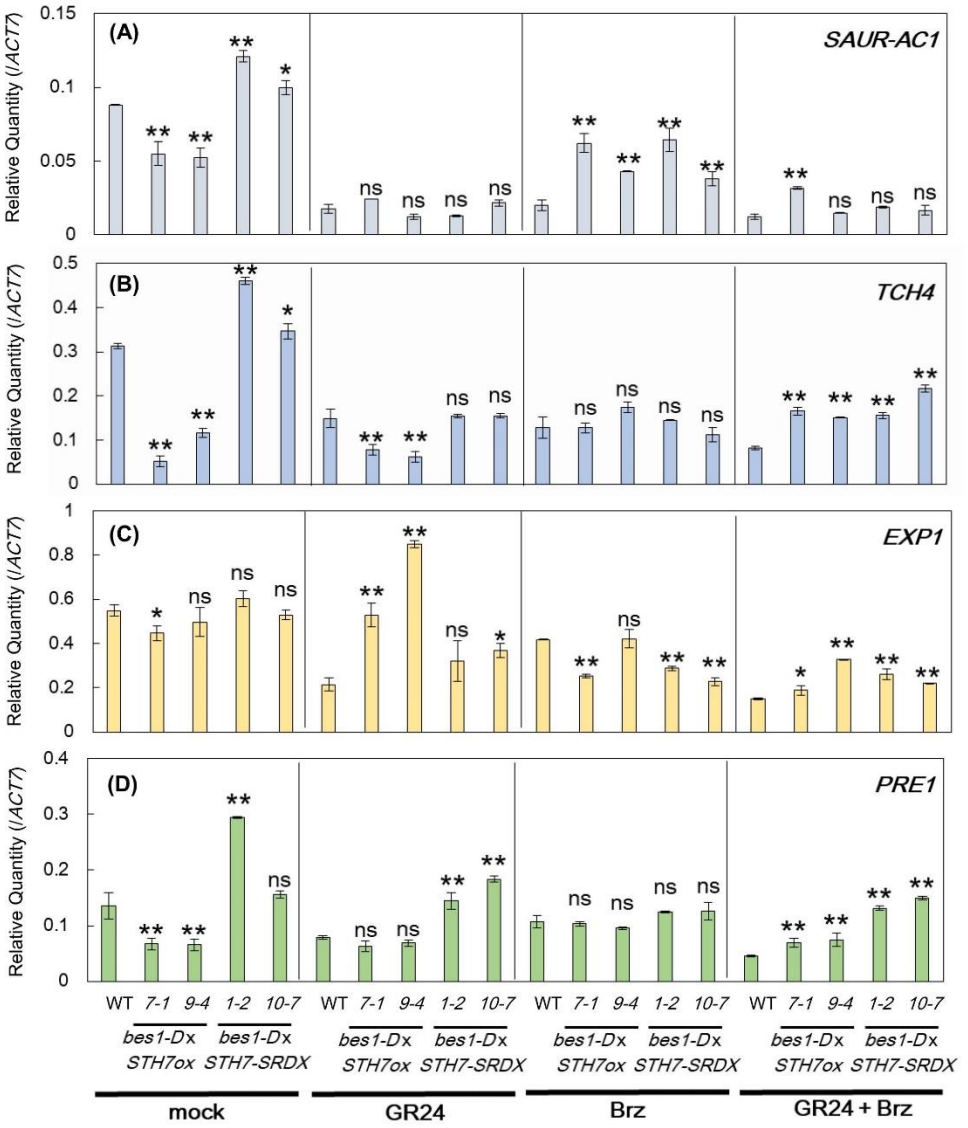

Fig. 4-15 Expression levels of cell elongation-related genes in *bes1-D*-related double mutants

Relative transcript levels of *SAUR-AC1* (A), *TCH4* (B), *EXP1* (C), and *PRE1* (D) in wild-type *Arabidopsis*, *bes1-D×STH7ox* and *bes1-D×STH7-SRDX* double mutants were analysed. Plants were grown in 1/2 MS medium containing 0.1% (v/v) DMSO as a control, 10 µM GR24, 0.3 µM Brz or the mixture of GR24 and Brz (GR24+Brz) under weak light for 4 days. The transcript levels were normalized to those of *ACT7*. Data are means ± SD shown by vertical error bars (n = 3). Statistically significant differences relative to wild-type (WT) of each treatment are $^{**}p \leq 0.01$, $^{*}p \leq 0.05$, and ns = nonsignificant by Student's *t* test.

4.2.5 Interaction of BIL1 protein or BES1 protein with the *STH7* promoter

To investigate the protein and DNA interaction, the electrophoretic mobility shift assay (EMSA) was performed. The recombinant BIL1 and BES1 protein was fused to the maltose binding protein (MBP) and the thioredoxin-histidine (Trx-His), respectively, and they were expressed and affinity-purified from *E. coli*. To check the efficiency of those recombinant proteins, the fragment of *CPD* promoter which is BR target gene containing BR-responsive element (BRRE) or 5′-CGTG-3′ was used as the positive control. The EMSA result exhibited that both MBP-BIL1 and Trx-His-BES1 could interact with *CPD* promoter region as indicated by the presence of shifted bands (Fig. 4-16). Next, various regions of *STH7* promoter were amplified by specific primers and the reverse primer was fused with 6-carboxyfluorescein (FAM) which is a fluorescent dye at the 5′ terminal. DNA probes from *STH7* promoter were performed in three lengths including 495 bp *(I)*, 340 bp *(II)* and 140 bp *(III)* from various upstream regions to the downstream region at +27 bp (Fig. 4-17). The EMSA result from *STH7* fragments and MBP-BIL1indicated that fragment *(I)* and *(II)* but not fragment *(III)* of *STH7* promoter could interact with MBP-BIL1 protein (Fig. 4-18). The binding efficiency of MBP-BIL1 to *STH7* regions *(I)* and *(II)* were decreased after their specific competitors were added (Fig. 4-18). On the other hand, in the experimental group of Trx-His-BES1 there was no specific shifted band with any *STH7* fragments (Fig. 4-19A). To confirm Trx-His-BES1 did not have the interaction with *STH7* promoter, the concentration of Trx-His-BES1 was 2-folds increased. Although, at the high concentration of Trx-His-BES1, only weak interaction between Trx-His-BES1 and region *(I)* and *(II)* of *STH7* promoter was observed (Fig. 4-19B). Based on EMSA results, it is predicted that BIL1 could directly bind to the *STH7* promoter at the region between upstream -313 bp to -113 bp or between region *(II)* and *(III)* (Fig. 4-17).

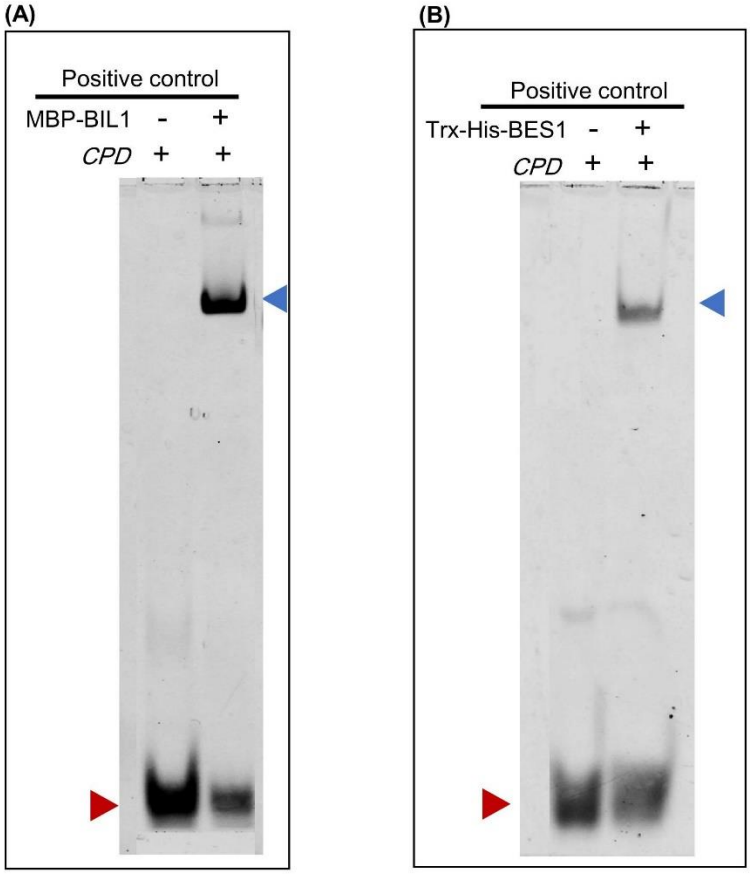

Fig. 4-16 The interaction of MBP-BIL1 and Trx-His-BES1 with *CPD* promoter

The electrophoretic mobility shift assay (EMSA) between the recombinant protein, MBP-BIL1 (A) or Trx-His-BES1 (B), and the fragment of *CPD* promoter containing BR-responsive element (BRRE, CGTG) used as the positive control. The final concentration of proteins and DNA probe were 5 μM and 35 nM, respectively. Red arrowheads indicate free DNA probe and blue arrowheads indicate the shifted band causing from the protein and DNA interaction.

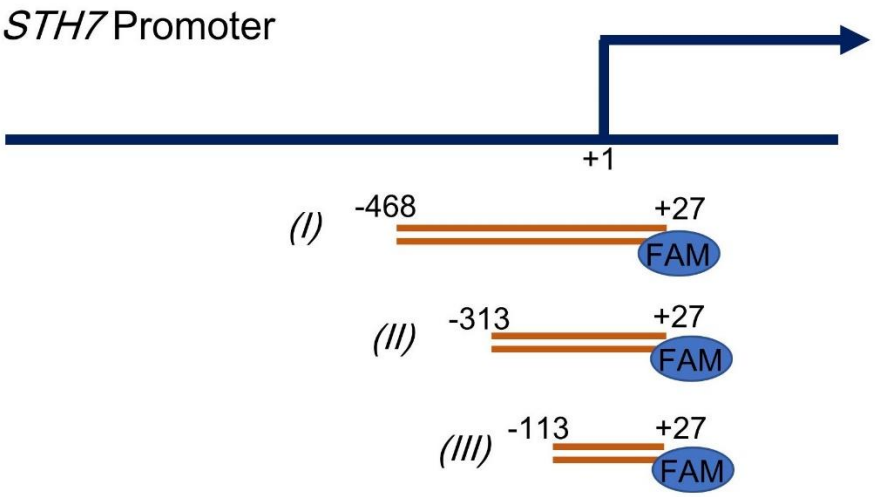

Fig. 4-17 The regions on *STH7* promoter for the production of DNA probe

The DNA probe from *STH7* promoter was performed in three lengths including 495 bp *(I)*, 340 bp *(II)* and 140 bp *(III)* from various upstream regions to the downstream region at +27 bp. The reverse primer was fused with FAM.

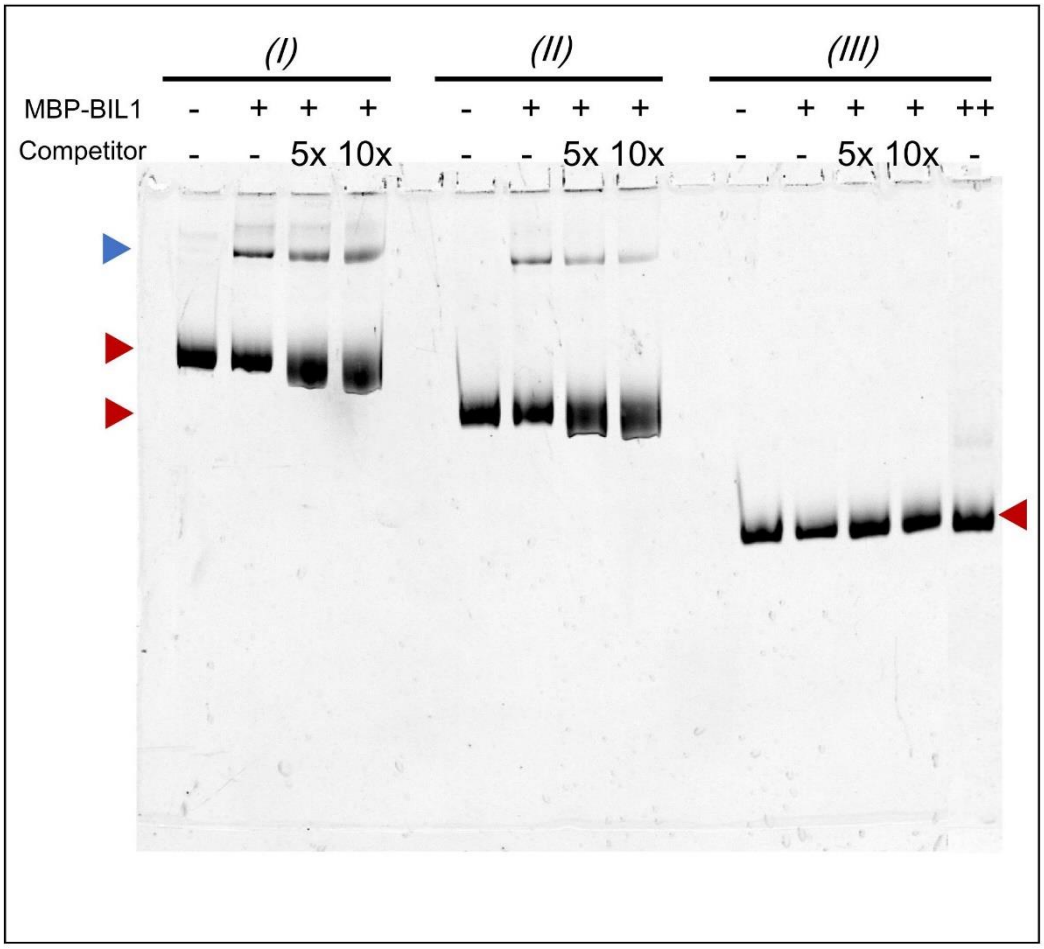

Fig. 4-18 The interaction of MBP-BIL1 with various upstream regions of *STH7* promoter

The electrophoretic mobility shift assay (EMSA) between the recombinant protein, MBP-BIL1, and various upstream regions of *STH7* promoter including -468 bp *(I)*, -313 bp *(II)* and -113 bp *(III)*. The final concentrations of MBP-BIL1 was 5 μM (+) or 10 μM (++). The final concentration of DNA probe was 35 nM. Red arrowheads indicate free DNA probe and blue arrowheads indicate the shifted band causing from the protein and DNA interaction.

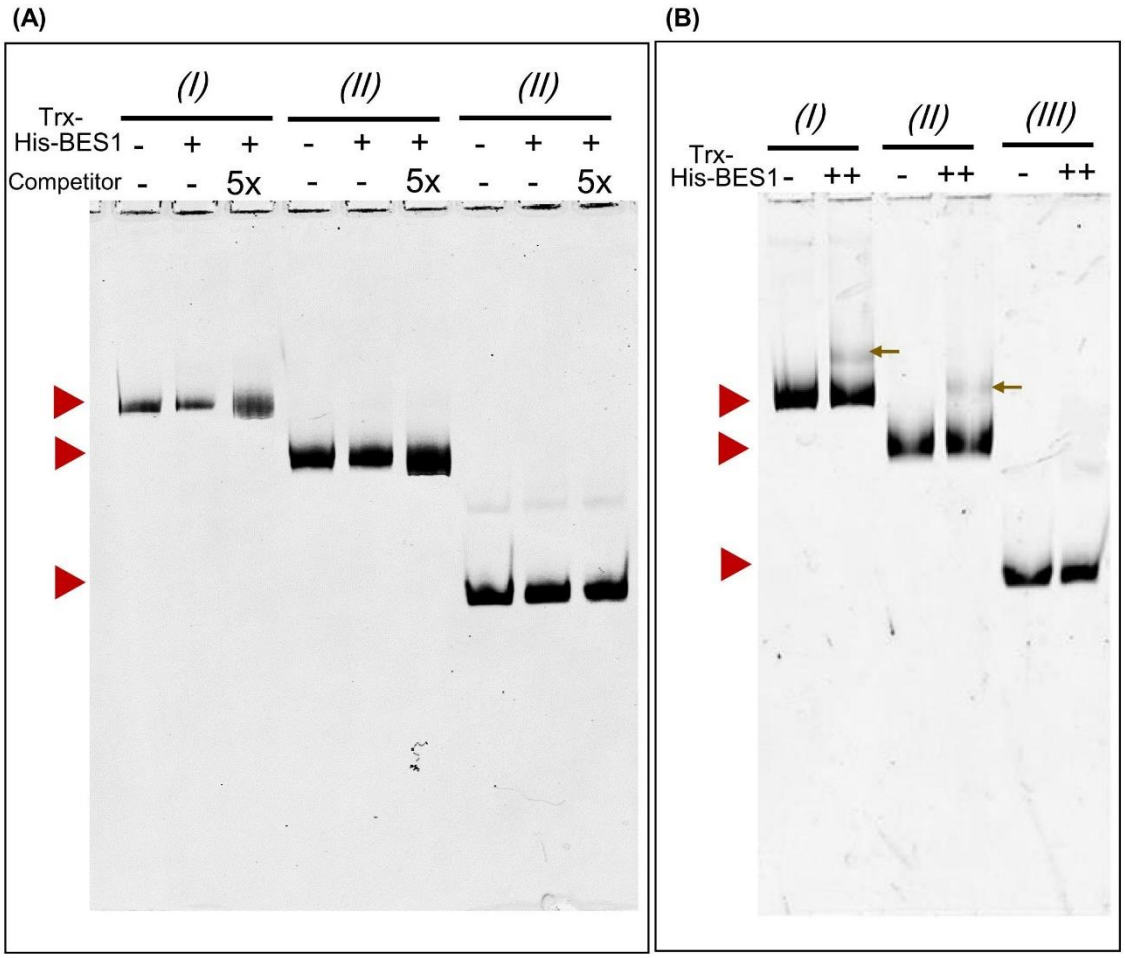

Fig. 4-19 The interaction of Trx-His-BES1 with various upstream regions of *STH7* promoter

The electrophoretic mobility shift assay (EMSA) between the recombinant protein, Trx-His-BES1, and various upstream regions of *STH7* promoter including -468 bp *(I)*, -313 bp *(II)* and -113 bp *(III)*. The final concentrations of BES-His was 5 µM (+) (A) or 10 µM (++) (B). The final concentration of DNA probe was 35 nM. Red arrowheads indicate free DNA probe and arrows indicate the weak shift band.

As the above results indicated the importance of the upstream region of *STH7* promoter at -313 bp to -113 bp for BIL1 binding, the database of plant cis-acting regulatory DNA elements (PLACE database, http://www.dna.affrc.go.jp/PLACE/) was used to investigate the important cis-element on this region. The data showed that the region from -313 bp to -113 bp had two of GATA boxes (TACA), a RAV1 box (CAACA) and an E-box (CACATG) belonging to the *STH7* promoter (Fig. 4-20). To identify the cis-element on *STH7* promoter bound by MBP-BIL1, four regions on *STH7* promoter consisting of the deletion of GATA box (GATA-Δ), the deletion of RAV1 box (RAV1-Δ), the E-box, and the deletion of E-box (E-box-Δ) were designed based on the data from PLACE database as shown in Fig. 4-20. Even if the GATA boxes and the RAV1 box were deleted, MBP-BIL1 can still bind to *STH7* probes implying that GATA and RAV1 might not be cis-acting regulatory elements for BIL1 (Figs. 4-21A, B). Next, E-box was focused as the cis-element of *STH7* promoter and EMSA was performed by *STH7* probes with or without E-box. The result showed that the deletion of E-box (E-box-Δ) inhibited the interaction between MBP-BIL1 and *STH7* promoter (Fig. 4-21D). Although the concentration of MBP-BIL1 was increased 2-folds, E-box-Δ probe did not exhibit any shifts (Fig. 4-21D). On the contrary, the presence of E-box in *STH7* promoter caused the shift of MBP-BIL1. The addition of the specific E-box competitor strengthened the band intensity of free DNA probe (Fig. 4-21C). These results supported that MBP-BIL1 bound to *STH7* promoter at the E-box.

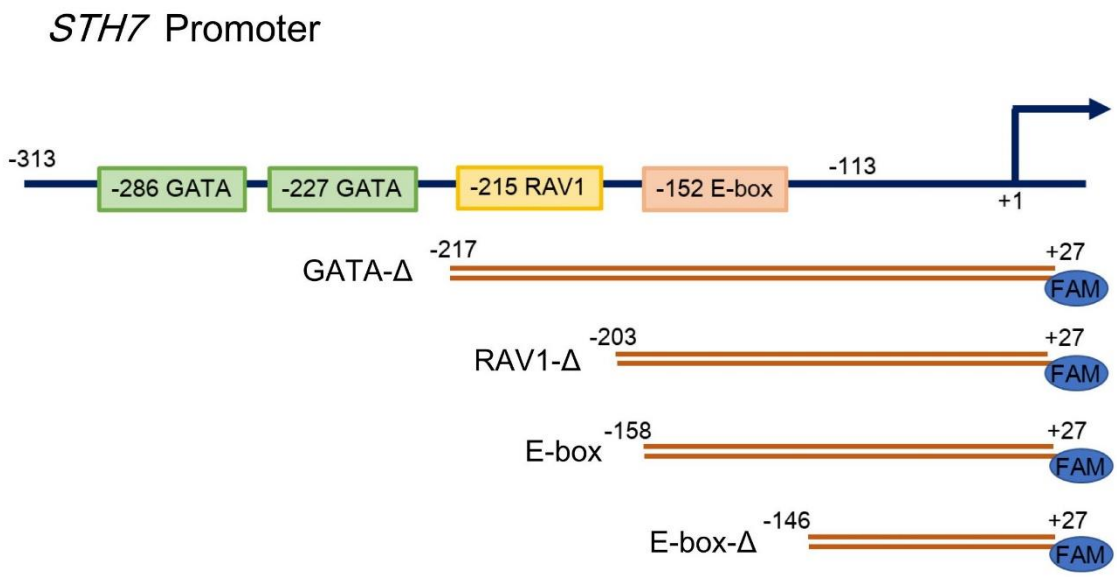

Fig. 4-20 The cis-element regulatory between -313 bp to -113 bp of the upstream region of *STH7* promoter

The 200 bp between the upstream region of *STH7* promoter between -313 bp to -113 bp is compose of two GATA boxes (TACA), a RAV1 box (CAACA) and an E-box (CACATG). The position of each cis-element on *STH7* promoter was shown in the diagram. Various upstream regions of *STH7* promoter were performed in four frangments including the deletion of GATA box (GATA-Δ), the deletion of RAV1 box (RAV1-Δ), the E-box and the deletion of E-box (E-box-Δ) to the downstream region at +27 bp. The reverse primer was fused with FAM.

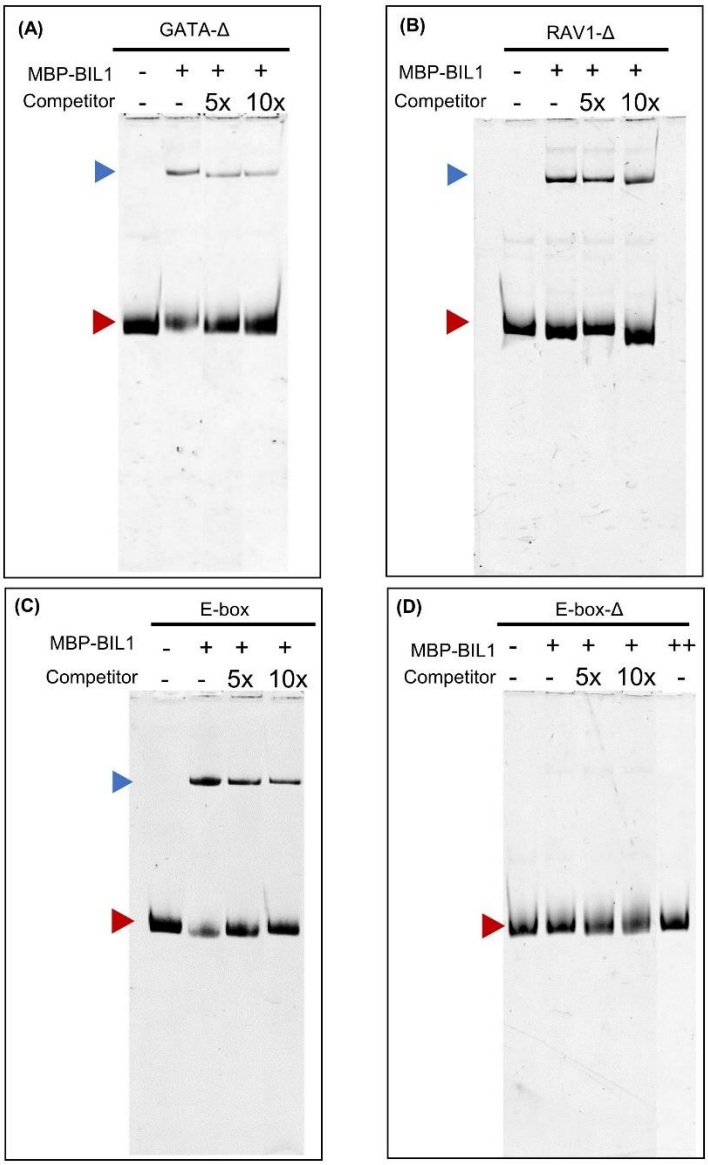

Fig. 4-21 The interaction of MBP-BIL1 with 200 bp between -313 bp to -113 bp of the upstream region of *STH7* promoter

The electrophoretic mobility shift assay (EMSA) between MBP-BIL1 and various upstream regions of *STH7* promoter including the deletion of GATA box (GATA-Δ) (A), the deletion of RAV1 box (RAV1-Δ) (B), the E-box (C), and the deletion of E-box (E-box-Δ) (D). The final concentrations of MBP-BIL1was 5 µM (+) or 10 µM (++). The final concentration of DNA probes were 35 nM. Red arrowheads indicate free DNA probe and blue arrowheads indicate the shifted band causing from the protein and DNA interaction.

4.3 Discussion

Since the photomorphogenesis is controlled by both light signals and various phytohormones, the study on how seedlings response to light is the key to investigate plant development. Previous chapters showed that BR increased hypocotyl elongation which is the negative response of the light-adapted growth (chapter 2), but SL played the positive roles in photomorphogenesis (chapter 3). In this chapter, it was demonstrated that by the co-treatment of SL with BR, the inhibition of *Arabidopsis* hypocotyl elongation induced by SL was attenuated by BR (Fig. 4-1). Moreover, the BR biosynthesis inhibitor, Brz, could enhance the shortened hypocotyl caused by SL (Fig. 4-2). These results supported that there should be a crosstalk between SL and BR in light-adapted development. Tsuchiya et al. [14] reported that SL promoted the light-adapted growth in *Arabidopsis* seedling throughout the increasing of *HY5* expression and HY5 protein accumulation. Since HY5 is the positive regulatory factor for the induction of light-adapted development, the light-grown *hy5* mutant displayed the long hypocotyl elongation [32, 33]. However, the application of SL could decrease hypocotyl of *hy5* mutants which were grown under red, far-red or blue light [32]. This evidences supported that SL can promote the photomorphogenesis through pathways other than HY5 signaling.

This study showed that GR24 not only reduces the hypocotyl elongation in wild-type *Arabidopsis* but it also shortens the hypocotyls of *STH7ox* mutant. On the other hand, GR24 could not decrease the hypocotyl length of *STH7-SRDX* (Fig. 4-1). STH7 is the transcription factor belonging to the B-box zinc-finger protein subfamily IV [25, 34]. This subfamily consists of eight members and they were reported as the regulatory factor of photomorphogenesis [34]. In the chapter 3, it was investigated that SL induces the photomorphogenesis of *Arabidopsis* in the STH7-dependent manner. The transcript level of *STH7* was up-regulated and more up-regulated when wild-type plants were treated with GR24 and the mixture of GR24 and Brz, respectively (Fig. 4-3). This result correlated to the shortest hypocotyls shown in wild-type and *STH7ox* with co-treatment of GR24 and Brz (Fig. 4-2). Moreover, BL reduced effect of GR24 in the increase of STH7-GFP signal

in nucleus of hypocotyl cells (Fig. 4-4). This result also correlated to the antagonist effect of GR24 and BL in the inhibition of hypocotyl elongation (Fig. 4-1). STH7 has been reported as a negative regulator of BR [25], therefore the previous published microarray data from Sun et al. [19] and Fan et al. [25] were used to investigate the relationship between *STH7*-regulated genes and BR-regulated genes. The result indicated that 50% of genes up-regulated by *STH7* overlapped with genes down-regulated by BR and they were the genes mediating light-adapted responses such as, *STH7*, the genes early light inducible genes, such as *ELIP2*, and the anthocyanin biosynthesis related genes, such as *CHI* (Fig. 4-5). Those connections of *STH7*-upregulated and BR-repressed genes including *ELIP2* and *CHI* as well as some of their homologs such as, *ELIP1*, *CHS* and *FLS1* may cause higher expression levels of these genes in *STH7ox* comparing to those in wild-type (Fig. 4-6). Furthermore, the transcript levels of those genes were clearly enhanced by the co-treatment of GR24 and Brz (Fig. 4-7). These results suggest that STH7 is the component integrating SL and BR signal in the light-adapted development.

Since BIL1 and BES1 are the specific positive regulators of BR signaling [29, 30], it was thought that the association between BR and SL could be caused by the interaction of these BR specific regulators and STH7. The double mutant analysis presented that *bil1-1D×STH7ox* displayed the small rosette leaves similar to those of single mutant of *STH7ox* whereas both *bes1-D×STH7ox* and *bes1-D×STH7-SRDX* displayed the curl and long petioles similarly to their single mutant, *bes1-D* (Fig. 4-8). After co-treatment with GR24 and Brz, hypocotyls of *bil1-1D×STH7ox* double mutants became shorter than those of *bil1-1D×STH7ox* double mutants to which either GR24 or Brz that are individually applied (Figs. 4-9) whereas both of *bes1-D*-related double mutants were insensitive to Brz (Figs. 4-10). Thus, characterization of phenotypes and responses to SL and Brz of these double mutants imply that STH7 is regulated by the different mechanism of BIL1 and BES1. Generally the BR positive regulators, BIL1 and BES1, act as the transcriptional repressor or activator of their downstream genes [30, 35]. In this study I found that SL and BR biosynthesis inhibitor Brz coordinately mediated the light-adapted growth depending on the function of STH7. The co-treatment of GR24 and Brz caused the significant up-regulation of *STH7* expression in *bes1-D* but not in *bil1-1D* (Fig. 4-13).

The result indicated that BIL1, but not BES1, should mainly repress *STH7* transcription (Fig. 4-22). To understand how BIL1 and BES1 proteins interact with *STH7* promoter, the electrophoretic mobility shift assay were performed. At 5 μM of proteins, only MBP-BIL1 could bind to *STH7* promoter in the upstream region between -313 bp to -113 bp (Figs. 4-17, 4-18 and 4-19A). BIL1 showed sequence identity of 88% to BES1 at the protein level [30, 35]. The dephosphorylation form of either BIL1 or BES1 promotes BR-induced growth. On the other hand, the nuclear-localized BIL1 regulates the BR signaling but the nuclear translocation of BES1 is not required for BR response [36, 37]. As indicated in Fig. 4-19 according to the increase in the Trx-His-BES1 concentration, the weak shifted bands became observed (Fig. 4-19B). These shifted bands might be caused by the weak interaction of BES1 protein and *STH7* promoter. Therefore, even though further experiments are required, it is assumed that the differences in binding properties between BIL1 and BES1 to the upstream of *STH7* might be caused by their different affinities to *STH7* promoter or the differences in physicochemical characters of BIL1 and BES1 proteins.

The upstream region of STH7 promoter between -313 bp to -113 bp contains two GATA boxes, one RAV1 box and one E-box (Fig. 4-20). The deletion of E-box (E-box-Δ) on *STH7* promoter destroyed the protein-DNA interaction (Fig. 4-21D). This result suggested that BIL1 binds to the E-box on the *STH7* promoter. To activate or suppress the transcript level of BR target genes, BIL1 and BES1 will bind to E-box and BRRE elements on the promoter of those genes [19, 38]. However, BES1 strongly binds to the BRRE site on the promoter than to the E-box since that BES1 was reported to interact with other transcription factors such as BIM1 and form the heterodimer to bind to E-box [39]. It is possible that BIL1 is more prone to interaction with E-box of *STH7* promoter and repress *STH7* expression than BES1 does. The repression of *STH7* transcription by BIL1 might be a key for the BR and SL crosstalk in the light-adapted development (Fig. 4-22). However, the *STH7* expression levels were highly up-regulated only in the plants co-treated with both SL and Brz. The single application of Brz showed weak increase of *STH7* transcription (Fig. 4-3) indicating that there might be other factors that work together with BIL1 and STH7 to control the photomorphogenesis.

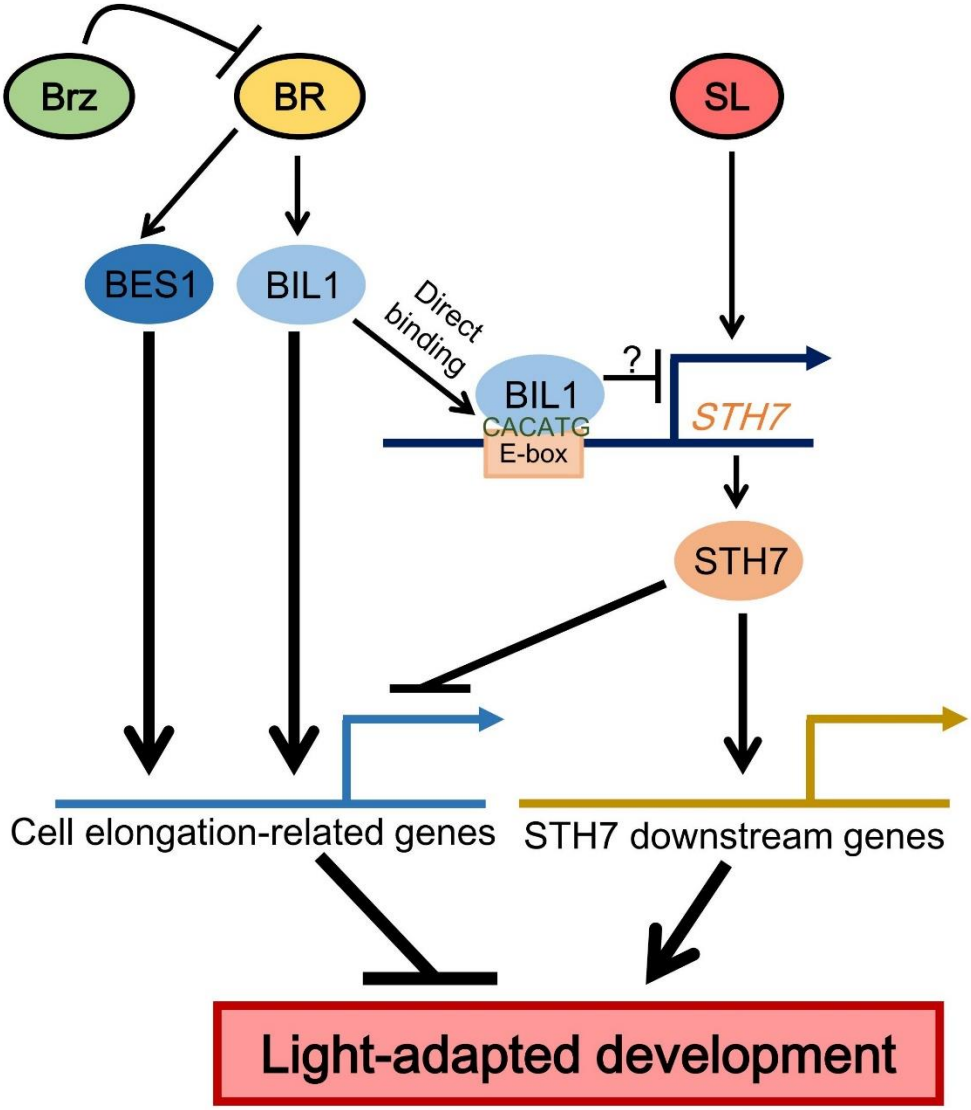

Fig. 4-22 The working model of strigolactones and brassinosteroids crosstalk on the light-adapted development

BIL1 and BES1 is the positive regulator of brassinosteroids (BR) which is inhibited by brassinazole (Brz). BIL1 directly bind to E-box cis-element of *STH7* promoter and suppress *STH7* transcript level. *STH7* is up-regulated by strigolactone (SL). STH7 induce the expression of its downstream genes and inhibit the cell elongation-related genes leading to influence the light-adapted development.

The analysis of light-responsive promoters suggested that GT-1 binding site (GGTTAA), G-box (CACGTG), and I-box that contains GATA motif is the light-response promoter elements [40]. The previous reports indicated that GATA1 and GATA2 could bind to GATA element [41, 42]. GATA2 is accumulated when plants receive light signal and is repressed by COP1 in the dark condition. Moreover, GATA2 directly controls genes that are regulated by both light signal and BR [42]. Since *STH7* promoter contain two GATA motifs (Fig. 4-20), it is possible that GATAs can bind to the GATA boxes on *STH7* promoter and coordinately induce the light-adapted response. Among the negative regulator of light-adapted response, the PIFs family have been reported that they could interact with BIL1 [43] and PIFs regulated the B-box gene expressions [44]. The previous published microarray data of PIF-regulated genes [43] were compared with STH7-regulated genes [25]. The data showed that 62% of *STH7*-regulated genes were also regulated by PIFs [Supplementary Fig. 1A]. The *STH7* expression was determined in the quadruple PIFs mutant (*pifq*). The *pifq* displayed the higher transcription of *STH7* than wild-type [Supplementary Fig. 1B]. It implied that PIFs might repress *STH7* expression. Previous published data suggested that BIL1 could interact with PIF4 and regulated cell elongation [43]. Moreover, the positive regulators of light-adapted development were suppressed by BIL1-PIFs interaction [43]. Together with all above data, PIFs and/or the interaction between BIL1 and PIFs might repress *STH7* transcription leading to inhibit the photomorphogenesis [Supplementary Fig. 1C]. However, this study demonstrated that BIL1 directly binds to *STH7* promoter and suppresses the expression of *STH7* and the subsequent photomorphogenesis (Fig. 4-22).

The chlorophyll and anthocyanin biosynthesis are the other factors indicating the light-adapted development [8, 9]. SL has been reported to regulate the anthocyanin accumulation depending on STH7 function (Fig. 3-11 and published in ref. [15]). Among *bil1-1D*-related and *bes1-D*-related double mutants, *bil1-1D×STH7ox* and *bes1-D×STH7ox* highly accumulated the anthocyanin. However, productions of anthocyanin in *bes1-D×STH7ox* double mutants were less than *bil1-1D×STH7ox* (Fig. 4-12). This implies that STH7 might work downstream of both BIL1 and BES1 to activate the anthocyanin biosynthesis but BES1 represses STH7 function less than BIL1. *bil1-*

1D×STH7ox and *bes1-D×STH7ox* accumulated higher level of total chlorophyll than their wild-type, while *bes1-D* and one line of *bes1-D×STH7-SRDX* accumulated lower level of total chlorophyll than wild-type (Fig. 4-11). Moreover, the total chlorophyll in a line of *bes1-D×STH7-SRDX* was lower than in *bes1-D* (Fig. 4-11B). The low chlorophyll content in *bes1-D* caused by the suppression of *GLK1* and *GLK2* expression [38] which are the key genes regulating the chloroplast development [38, 45]. The regulation of chlorophyll accumulation by STH7 and the repression of the chloroplast development in *bes1-D* might cause the less chlorophyll content in *bes1-D×STH7-SRDX* double mutant (Fig. 4-11B).

Since the inhibition of hypocotyl elongation is one of the responses of photomorphogenesis, the transcriptional regulation of genes that enhance the cell elongation were investigated in this research. *SAUR-AC1*, *TCH4*, and *PRE1* which are the cell elongation-related genes are known to be specifically repressed by BR [46–48]. Either GR24- or Brz-treatment down-regulated the expression of *SAUR-AC1*, *TCH4*, and *PRE1* in wild-type and *bil1-1D×STH7ox* (Fig. 4-14) supporting that SL suppresses the transcription of cell elongation-related genes as well as Brz. Moreover, in control treatment, both *bil1-1D×STH7-SRDX* and *bes1-D×STH7-SRDX* displayed higher expression of those cell elongation-related genes than in its pair double mutant, *bil1-1D×STH7ox* and *bes1-D×STH7ox*, respectively (Figs. 4-14 and 4-15). This result suggested that SL repressed the cell elongation-related genes through STH7. The activation of *STH7*-downstream target genes such as light-induced genes together with the repression of the cell elongation-related genes could be mediated by both SL and BR leading to induce the light-adapted development in *Arabidopsis* (Fig. 4-22).

4.4 Materials and Methods

4.4.1 Plant materials and growth conditions

Wild-type *Arabidopsis* ecotype Col, *STH7-overexpressing* (*STH7ox*), the functional defective *STH7* (*STH7-SRDX*), the BR gain-of-function *bil1-1D* and *bes1-D* were used in the experiment. The double mutants between the BR gain-of-function and *STH7* mutants were performed by the hybridization. The *bil1-1D* and *bes1-D* were utilized as the female plants whereas *STH7ox* and *STH7-SRDX* were used as the male plants. Seeds were collected after cross-pollination. Since, *STH7ox* and *STH7-SRDX* contained the hygromycin B resistant site, the successful hybridizations were screened by the selection of seedlings that can germinate under medium containing 30 μg/ml hygromycin B. These seedlings were planted and screened by hygromycin B until third generation (T_3) for selecting the *STH7* homogenous lines. Then, the double mutants which were the *STH7* homogeneity were checked the *bil1-1D* or *bes1-D* homogeneity by the genotyping PCR. The genomic DNA (gDNA) of the double mutants *Arabidopsis* were extracted. The gDNA of *bil1-1D*-related and *bes1-D*-related double mutants were amplified by their pair of following primers;

bil1-genotyping-forward: 5′-CATCGCCGACTTCTAAGAAC-3′
bil1-genotyping-reverse: 5′-TGCCATTTGGGTTTGCCTAGTTGT -3′
bes1-genotyping-forward: 5′-CTTCTTACTAATTTGAGAACCGAA -3′
bes1-genotyping-reverse: 5′-AAAACCATGAACTGAATGAAC -3′

The *bil1-1D* or *bes1-D* homogenous lines were investigated by the mutation at *Hpa*II restriction site from CCGG to CTGG in *bil1-1D* and *bes1-D*. The homogenous *bil1-1D×STH7ox*, *bil1-1D×STH7-SRDX*, *bes1-D×STH7ox* and *bes1-D×STH7-SRDX* were used throughout the experiment.

Seeds were surface-sterilized by ethanol and germinated on 1/2 MS medium containing 3% sucrose and 0.8% phyto agar (Duchefa, Haarlem, The Netherlands).

Arabidopsis were kept at 4 °C for 2 days and transferred to grow at 22 °C under 1.75 $\mu molm^{-2}s^{-1}$ as the weak light condition or 16/8 light/dark cycle depend on the experiments.

4.4.2 Measurement of *Arabidopsis* hypocotyls

Arabidopsis were grown under medium supplemented with 10 μM GR24, 10 nM BL, 0.3 μM Brz or the mixture among these 3 compounds depending on the experiment. The 0.1% (v/v) DMSO was used as control treatment. The 4-day-grown *Arabidopsis* were measured hypocotyl elongation by ImageJ software.

4.4.3 Quantitative real-time PCR

Plants were grown under weak light condition in medium containing with 10 μM GR24, 10 nM BL, 0.3 μM Brz or the mixture among these 3 compounds depending on the experiment for 4 days. The 0.1% (v/v) DMSO was used as control treatment. Plant samples were collected, frozen and homogenized in liquid nitrogen. The total RNA was extracted from the plant samples with a Total RNA Extraction Kit Mini for plants (RBC Bioscience, New Taipei City, Taiwan). The complementary DNA (cDNA) was synthesized using ReverTra Ace® qPCR RT Master Mix with gDNA remover (Toyobo, Osaka, Japan). The qRT-PCR was performed by using KAPA SYBR® FAST One-Step qRT-PCR Master Mix (Kapa Biosystems, Cape Town, South Africa). Transcript level of each gene was normalized to those of *ACT7* which is the constitutively expressed control gene. The primers that used for qRT-PCR were described as following;

STH7-forward: 5′-CCAATAAACTAGCCGGGAAA-3′
STH7-reverse: 5′-GCTCTGTCTTCTTGGCAAAAT-3′
ELIP1-forward: 5′-CGTTGCCGAAGTCACCATCTCC-3′
ELIP1-reverse: 5′-CCATCGCTAAACGTCCGTTAATCCT-3′
ELIP2-forward: 5′-TATTGACTACACGCAACATCAGAA-3′
ELIP2-reverse: 5′-GTTTTCTCCCTTTGATAACTCCAT-3′

CHS-forward: 5′-GGCTATTGGCACTGCTAACCCTGAG-3′

CHS-reverse: 5′-GTGACGTTTCCGAATTGTCGACTTG-3′

CHI-forward: 5′-CTCTCTTACGGTTGCGTTTTCG-3′

CHI-reverse: 5′-CACCGTTCTTCCCGATGATAGA-3′

FLS1-forward: 5′- GAATGGGGGCTATTCCAAGT-3′

FLS1-reverse: 5′- TCAACGCATCACGCTTTAAC-3′

SAUR-AC1-forward: 5′-GAGATATGTGGTGCCGGTTT-3′

SAUR-AC1-reverse: 5′-GTATTGTTAAGCCGCCCATT-3′

TCH4-forward: 5′-CGAGTCTTGGAACGCTGAT-3′

TCH4-reverse: 5′-CTTCTTGTTGAAAGCCACGG-3′

EXP1-forward: 5′-AACGCACACGCCACATTCTAC-3′

EXP1-reverse: 5′-TTTCCGTATCCACCAGCACCTC-3′

PRE1-forward: 5′-GAGGGATAATGAGGGATTTCG-3′

PRE1-reverse: 5′- CTATGTCACGTGTCACCACCATGTC-3′

ACT7-forward: 5′-GATATTCAGCCACTTGTCTGTGAC-3′

ACT7-reverse: 5′-CATGTTCGATTGGATACTTCAGAG-3′.

4.4.4 Preformation of 35S:STH7-GFP and fluorescence microscopy

Full length cDNA of *STH7* was amplified and then was recombinant cloned into pDONR201 by using GATEWAY BP kit (Invitrogen, California, USA). After that full length *STH7* was transferred into the destination vector pGWB5 by using GATEWAY LR kit (Invitrogen, California, USA) to generate transcriptional fusion and driven by CaMV 35S promoter. 35S:STH7-GFP vector was transformed into *Arabidopsis* ecotype Col by *Agrobacterium* using the floral dip transformation method. The seeds from transformed plants were collected and screened by 50 µg/ml kanamycin and 30 µg/ml hygromycin B until third generation (T_3) for selecting the homogenous lines. GFP signal in 35S:STH7-GFP transgenic plants were observed by laser scanning microscope LSM700 (Carl Zeiss, Jena, Germany).

4.4.5 Microarray data

The microarray data between BR-regulated genes and *STH7*-regulated genes were performed by two sources of the previous published microarray. The BR-repressed genes were obtained from genes that response to BL treatment [19]. The *STH7*-regulated genes were obtained from genes affected in *STH7ox/BZS1ox* [25]. Then, those microarray data were pooled by the function "Vlookup" in Microsoft Excel. The light response-related genes and the pigment biosynthesis-related genes were obtained from TAIR database (www.arabidopsis.org).

4.4.6 Chlorophyll and anthocyanin measurement

Wild-type *Arabidopsis*, *bil1-1D*, *bes1-D*, *bil1-1D×STH7ox*, *bil1-1D×STH7-SRDX*, *bes1-D×STH7ox* and *bes1-D×STH7-SRDX* were planted in 1/2 MS medium under weak light conditions for 7 days. The cotyledons were cut and were collected around 10–20 mg for chlorophyll and anthocyanin extractions. The chlorophyll content was measured according to Porra et al. [49]. The anthocyanin content was measured according to Ito et al. [50]. The chlorophyll and anthocyanin were extracted and measured at the same manner as described in the materials and methods of chapter 3.

4.4.7 Recombinant proteins production

The recombinant BIL1 protein fused with maltose binding protein (MBP-BIL1) was the gift from Mr. Shohei Nosaki, Department of Applied Biological Chemistry, The University of Tokyo and CSRS, Riken. BILl-MBP protein was dissolved in the buffer containing 20 mM Tris-HCl (pH 7.5), 250 mM NaCl, 1 mM DTT and 5% glycerol. The recombinant BES1 protein was fused to thioredoxin-histidine (Trx-His-BES1). Full-length cDNA of BES1 was amplified by primers of BES1-*Kpn*I-forward 5′-**GTTA**GGTACCATGACGTCTGACGGAGCA-3′ and BES1-*Eco*RI-reverse 5′-**GCGC**GAATTCTCAACTATGAGCTTTACCATT-3′. Underlines indicate the addition of *Kpn*I and *Eco*RI site in forward and reverse primer, respectively. The bold letters

indicate the adapter site for efficient cut by those restriction enzymes. BES1 full-length cDNA was cloned into pET-32a(+) (Novagen, Wisconcin, USA). Trx-His-BES1 was expressed in *Escherichia coli* strain BL21 (Rosetta) at 22°C for 5 h. Then, protein was purified by TALON® Metal Affinity Resins (Clontech, California, USA) according to its instruction and eluted by the buffer containing 20 mM HEPES (pH 7.0), 150 mM NaCl and 1 mM DTT.

4.4.8 Electrophoretic mobility shift assay (EMSA)

Various DNA probes of *STH7* promoter were amplified by PrimeSTAR GXL DNA Polymerase (Takara, Kyoto, Japan) by lists of followed specific primers;

STH7*(I)*, -468 bp -forward: 5′-TCTGCCTCCTTCTATGAAACC-3′
STH7*(II)*, -313 bp -forward: 5′-GGCATTGAAAGCAAAGGAGA-3′
STH7*(III)*, -113 bp -forward: 5′-GGTCCAAAGGTACAAGTTGAGG-3′
GATA-Δ, -217 bp -forward: 5′-GCCAACACATTATTCTTACCC-3′
RAV1-Δ, -203 bp -forward: 5′-CTTACCCTTTTGCCCACACT-3′
E-box, -158 bp -forward: 5′-CTCACCCACATGAGTGTCTCT-3′
E-box-Δ, -146 bp -forward: 5′-GGCCAGTGTCTCTACATAAACA-3′
(underline indicate adapter sequence)
STH7, +27 bp -reverse: 5′-TCACAAACAGCACACCAAATC-3′

The reverse primer of *STH7* was fused with 6-carboxyfluorescein (FAM) which is the fluorescent dye at the 5′ terminal. The untagged reverse primer was used to produce the specific inhibitors. The *CPD* probe receiving from Mr. Shohei Nosaki was used as the positive control for MBP-BIL1 and Trx-His-BES1. Its sequence is shown below (underlined indicate the BR-responsive element, BRRE);

FAM-5′-GCAGAAACCCCCCGTGTGCCCACTCTCCCC-3′
-3′-CGTCTTTGGGGGGCACACGGGTGAGAGGGG-5′

Each of 35 nM DNA probe was mixed with 5 µM or 10 µM of recombinant proteins in the binding buffer containing 5 mM $MgCl_2$, 2.5% glycerol, 5 mM EDTA, and 0.5 µg sonicated salmon sperm DNA (ssDNA) utilized as the nonspecific competitor. The specific competitor produced from untagged reverse primer was used at 5-folds (175 nM) or 10-folds (350 nM) of each DNA probe. The described concentrations are the final concentration of total 20 µl reaction. The DNA probes and the recombinant proteins were incubated at room temperature for 20 min, then run on 7.5% polyacrylamide gel (Native PAGE) in 0.5X TBE buffer at 10 mA, 150 V, 4 °C for 2 h. After that, polyacrylamide gel was detected by Typhoon 9400 imager (Amersham Biosciences, Buckinghamshire, England). The 526 nm emission filter and green laser was used for detection of FAM-tagged DNA.

4.5 Supplementary data

The integrations among BIL1, STH7 and PIFs were hypothesized as the alternative pathway to control the light-adapted development (see discussion).

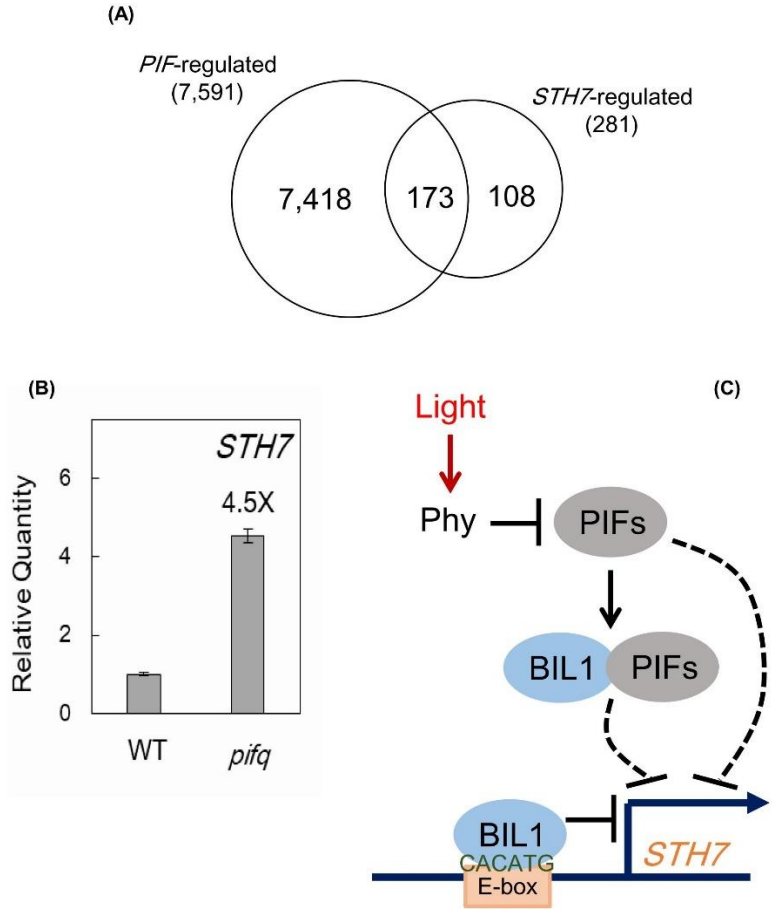

Supplementary Fig. 1 Integration among BIL1, STH7, and PIFs

Overlapping of *PIF*-regulated gene obtained from Oh et al. [43] and *STH7*-regulated genes obtained from Fan et al. [25] (A). Relative transcript levels of *STH7* in wild-type *Arabidopsis* and *pifq* mutant were compared (B). Hypothesis pathway of the integration among BIL1, STH7 and PIFs (C). BIL1 direct bind to E-box cis-element of *STH7* promoter leading to suppress *STH7* transcript level is investigated from EMSA result in this thesis. PIFs and/or BIL1-PIFs interaction might repress *STH7* transcription leading to inhibit light-adapted development.

4.6 References

[1] Depuydt S, Hardtke CS. Hormone signalling crosstalk in plant growth regulation. Curr Biol. 2011;21:R365–R373.

[2] Gazzarrini S, McCourt P. Cross-talk in plant hormone signalling: what Arabidopsis mutants are telling us. Ann Bot. 2003;91:605–612.

[3] Kuppusamy KT, Walcher CL, Nemhauser JL. Cross-regulatory mechanisms in hormone signaling. Plant Mol Biol. 2009;69:375–81.

[4] Jaillais Y, Chory J. Unraveling the paradoxes of plant hormone signaling integration. Nat Struct Mol Biol. 2010;17:642–645.

[5] Li QF, He JX. Mechanisms of signaling crosstalk between brassinosteroids and gibberellins. Plant Signal Behav. 2013;8:e24686-1–9.

[6] Li QF, Wang C, Jiang L, Li S, Sun SS, He JX. An interaction between BZR1 and DELLAs mediates direct signaling crosstalk between brassinosteroids and gibberellins in *Arabidopsis*. Sci Signal. 2012;5: 1–11.

[7] Lau OS, Deng XW, Plant hormone signaling lightens up: integrators of light and hormones. Curr Opin Plant Biol. 2010;13:571–577.

[8] Eckardt NA. From darkness into light: factors controlling photomorphogenesis. The Plant Cell. 2001;13:219–221.

[9] Wu SH. Gene expression regulation in photomorphogenesis from the perspective of the central dogma. Annu Rev Plant Biol. 2014;65:311–333.

[10] Osterlund MT, Hardtke CS, Wei N, Deng XW. Targeted destabilization of HY5 during light-regulated development of *Arabidopsis*. Nature. 2000;405:462–466.

[11] Vandenbussche F, Habricot Y, Condiff AS, Maldiney R, Van der Straeten D, Ahmad M. HY5 is a point of convergence between cryptochrome and cytokinin signalling pathways in *Arabidopsis thaliana*. Plant J. 2007;49:428–441.

[12] Al-Babili S, Bouwmeester HJ, Strigolactones, a novel carotenoid-derived plant hormone. Annu Rev Plant Biol. 2015;66:161–186.

[13] Xie X, Yoneyama K. The strigolactone story. Annu Rev Phytopathol. 2010;48:93–117.

[14] Tsuchiya Y, Vidaurre D, Toh S, Hanada A, Nambara E, Kamiya Y, et al. A small-

molecule screen identifies new functions for the plant hormone strigolactone. Nat Chem Biol. 2010;6:741–749.
[15] Thussagunpanit J, Nagai Y, Nagae M, Mashiguchi K, Mitsuda N, Ohme-Takagi M, et al. Involvement of STH7 in light-adapted development in *Arabidopsis thaliana* promoted by both strigolactone and karrikin. Biosci Biotechnol Biochem. 2017;81:292–301.
[16] Gangappa SN, Botto JF. The BBX family of plant transcription factors. Trends Plant Sci. 2014;19:460–470.
[17] Mashiguchi K, Sasaki E, Shimada Y, Nagae M, Ueno K, Nakano T, et al. Feedback-regulation of strigolactone biosynthetic genes and strigolactone-regulated genes in *Arabidopsis*. Biosci Biotechnol Biochem. 2009;73:2460–2465.
[18] Wei C, Chien C, Ai L, Zhao J, Zhang Z, Li KH, Burlingame AL, Sun Y, Wang Z. The *Arabidopsis* B-BOX protein BZS1/BBX20 interacts with HY5 and mediates strigolactone regulation of photomorphogenesis. J Genet Genomics. 2016;43:555–563.
[19] Sun Y, Fan XY, Cao DM, Tang W, He K, Zhu JY, et al. Integration of brassinosteroid signal transduction with the transcription network for plant growth regulation in Arabidopsis. Dev Cell. 2010;19:765–777.
[20] Clouse SD. Brassinosteroids. Arabidopsis Book. American Society of Plant Biologists. 2011.
[21] Fujioka S, Yokota T. Biosynthesis and metabolism of brassinosteroids. Annu Rev Plant Biol. 2003;54:137–164.
[22] Thussagunpanit J, Jutamanee K, Homvisasevongsa S, Suksamrarn A, Yamagami A, Nakano T, Asami T. Characterization of synthetic ecdysteroid analogues as functional mimics of brassinosteroids in plant growth. J Steroid Biochem Mol Biol. 2017;172:1–8.
[23] Asami T, Min YK, Nagata N, Yamagishi K, Takatsuto S, Fujioka S, et al. Characterization of brassinazole, a triazole-type brassinosteroid biosynthesis inhibitor, Plant Physiol. 2000;123:93–99.
[24] Asami T, Mizutani M, Fujioka S, Godai H, Min YK, Shimadai Y, et al. Selective interaction of triazole derivatives with DWF4, a cytochrome P450 monooxygenase of the brassinosteroid biosynthetic pathway, correlates with brassinosteroid deficiency. J Biol Chem. 2001;276:25687–25691.

[25] Fan XY, Sun Y, Cao DM, Bai MY, Luo XM, Yang HJ, et al. BZS1, a B-box protein, promotes photomorphogenesis downstream of both brassinosteroid and light signaling pathways. Mol Plant. 2012;5:591–600.

[26] Harari-Steinberg O, Ohad I, Chamovitz DA. Dissection of the light signal transduction pathways regulating the two *early light-induced protein* genes in Arabidopsis. Plant Physiol. 2001;127:986–997.

[27] Hutin C, Nussaume L, Moise N, Moya I, Kloppstech K, Havaux M. Early light-induced proteins protect *Arabidopsis* from photooxidative stress. Proc Natl Acad Sci USA. 2003;100:4921–4926.

[28] Albert NW, Lewis DH, Zhang H, Irving LJ, Jameson PE, Davies KM. Light-induced vegetative anthocyanin pigmentation in Petunia. J Exp Bot. 2009;60:2191–2202.

[29] Belkhadir Y, Jaillais Y. The molecular circuitry of brassinosteroid signaling. New Phytol. 2015;206:522–540.

[30] He JX, Gendron JM, Sun Y, Gampala SS, Gendron N, Sun CQ, et al. BZR1 is a transcriptional repressor with dual roles in brassinosteroid homeostasis and growth responses. Science. 2005;307:1634–1638.

[31] Lee S, Lee S, Yang KY, Kim YM, Park SY, Kim SY, Soh MS. Overexpression of PRE1 and its homologous genes activates Gibberellin-dependent responses in *Arabidopsis thaliana*. Plant Cell Physiol. 2006;47:591–600.

[32] Jia KP, Luo Q, He SB, Lu XD, Yang HQ. Strigolactone-regulated hypocotyl elongation is dependent on cryptochrome and phytochrome signaling pathways in *Arabidopsis*. Mol Plant. 2014;7:528–540.

[33] Gangappa SN, Botto JF. The Multifaceted Roles of HY5 in Plant Growth and Development. Mol Plant. 2016;9:1353–1365.

[34] Sarmiento F. The BBX subfamily IV: additional cogs and sprockets to fine-tune light-dependent development. Plant Signal Behav. 2013;8:e23831-1–7.

[35] Yin Y, Wang ZY, Mora-Garcia S, Li J, Yoshida S, Asami T, et al. BES1 accumulates in the nucleus in response to brassinosteroids to regulate gene expression and promote stem elongation. Cell. 2002;109:181–191.

[36] Gendron JM, Wang ZY. Multiple mechanisms modulate brassinosteroid signaling. Curr Opin Plant Biol. 2007;10:436–441.

[37] Vert G, Chory J. Downstream nuclear events in brassinosteroid signalling. Nature. 2006;441:96–100.
[38] Yu X, Li L, Zola J, Aluru M, Ye H, Foudree A, et al. A brassinosteroid transcriptional network revealed by genome-wide identification of BESI target genes in *Arabidopsis thaliana*. Plant J. 2011;65:634–646.
[39] Yin Y, Vafeados D, Tao Y, Yoshida S, Asami T, Chory J. A new class of transcription factors mediates brassinosteroid-regulated gene expression in *Arabidopsis*. Cell. 2005;120:249–259.
[40] Terzaghi W, Cashmore A. Light-regulated transcription. Annu Rev Plant Physiol Plant Mol BioI. 1995;46:445–474.
[41] Jeong MJ, Shih MC. Interaction of a GATA factor with cis-acting elements involved in light regulation of nuclear genes encoding chloroplast glyceraldehyde-3-phosphate dehydrogenase in *Arabidopsis*. Biochem Biophys Res Commun. 2003;300:555–562.
[42] Luo XM, Lin WH, Zhu S, Zhu JY, Sun Y, Fan XY, et al. Integration of light- and brassinosteroid-signaling pathways by a GATA transcription factor in *Arabidopsis*. Dev Cell. 2010;19:872–883.
[43] Oh E, Zhu JY, Wang ZY. Interaction between BZR1 and PIF4 integrates brassinosteroid and environmental responses. Nat Cell Biol. 2012;14:802–809.
[44] Zhang X, Huai J, Shang F, Xu G, Tang W, Jing Y, et al. A PIF1/PIF3-HY5-BBX23 transcription factor cascade affects photomorphogenesis. Plant Physiol. 2017;174:2487–2500.
[45] Waters MT, Wang P, Korkaric M, Capper RG, Saunders NJ, Langdale JA. GLK transcription factors coordinate expression of the photosynthetic apparatus in *Arabidopsis*. Plant Cell. 2009;21:1109–1128.
[46] Nakamura A, Shimada Y, Goda H, Fujiwara MT, Asami T, Yoshida S. AXR1 is involved in BR-mediated elongation and *SAUR-AC1* gene expression in Arabidopsis, FEBS Lett. 2003;553:28–32.
[47] Iliev EA, Xu W, Polisensky DH, Oh M, Torisky RS, Clouse SD, et al. Transcriptional and posttranscriptional regulation of Arabidopsis *TCH4* expression by diverse stimuli. Roles of cis regions and brassinosteroids. Plant Physiol. 2002;130:770–783.
[48] Zhang LY, Bai MY, Wu J, Zhu JY, Wang H, Zhang Z, et al. Antagonistic HLH/bHLH

transcription factors mediate brassinosteroid regulation of cell elongation and plant development in rice and *Arabidopsis*. Plant Cell. 2009;21:3767–3780.
[49] Porra RJ, Thompson WA, Kriedemann PE. Determination of accurate extinction coefficients and simultaneous equations for assaying chlorophylls a and b extracted with four different solvents: verification of the concentration of chlorophyll standards by atomic absorption spectroscopy. Biochim Biophys Acta Bioenergetics. 1989;975:384–394.
[50] Ito S, Nozoye T, Sasaki E, Imai M, Shiwa Y, Shibata-Hatta M, et al. Strigolactone regulates anthocyanin accumulation, acid phosphatases production and plant growth under low phosphate condition in *Arabidopsis*. PLoS One. 2015;10:1–17.

Chapter 5 Conclusions and Future plans

5.1 Conclusions

The photomorphogenesis is the important process in plant development to light. This process is regulated by various plant hormones including SL and BR. Treatment of SL and BR on *Arabidopsis* is the tool to investigate functions of these plant hormones in the light-adapted development. Since the concentrations of natural BRs in plant is very low and the synthetic BRs are expensive, the seeking of BR mimic compounds is important solution to solve this problem. Among three hydroxysteroid compounds, DHECD and α-DHECD have the BR-like function but ECD which are their synthetic precursor does not mimic BR activity. DHECD and α-DHECD rescue the shortened hypocotyls of the *Arabidopsis* BR-deficient mutant but they were less active than BL. DHECD and α-DHECD activate BR signal transduction pathway by the enhancement of the accumulation of dephosphorylated BIL1/BZR1, a master transcription factor in BR signaling. Therefore, DHECD and α-DHECD could be used as BR mimic compounds.

In contrast with BR, SL and KAR regulate the light-adapted development by the inhibition of hypocotyl elongation. GR24, a synthetic SL and KAR_1, a KAR could up-regulate the expression of *STH7* which is the transcription factor belonging to the double B-box zinc finger subfamily. The functional defective *STH7* (*STH7-SRDX*) was insensitive to both GR24 and KAR_1 on the decrease of hypocotyl length. Moreover, treatment of GR24 or KAR_1 up-regulated the photosynthesis-related genes in *STH7ox* indicating that STH7 is essential for the light-adapted process. SL and KAR induce the photomorphogenesis of *Arabidopsis* in the STH7-dependent manner.

The application of BR inhibitor, Brz, increased the effect of SL on the inhibition of hypocotyl elongation and on the up-regulation of *STH7*. The *bil1-1D×STH7ox* double mutant displayed the shortened hypocotyl similar to *STH7ox* and *bil1-1D×STH7-SRDX* was insensitive to both SL and Brz indicating that STH7 works downstream of BIL1. Moreover, the binding of BIL1 protein to E-box element on the *STH7* promoter was

confirmed. SL and BR play an antagonistic role in light-adapted development of *Arabidopsis* likely in the STH7-dependent manner.

5.2 Future plans

In this study, DHECD and α-DHECD were found to have BR mimic activity. However, their activities were less than BL. To produce more potent BR mimic compounds, the reducing the polarity of the side chains of DHECD and α-DHECD could be the good try to increase their BR-like activity. Moreover, DHECD and α-DHECD will be applied in agriculture. I presume that DHECD and α-DHECD can increase crop yield and alleviate effects of the inappropriate environments such as heat stress and drought stress as well as the commercial BRs.

Furthermore, this study investigated that BR and SL play antagonistic functions to regulate the light-adapted development in the STH7-dependent manner. Although BIL1 can directly bind to E-box of *STH7* promoter and suppresses *STH7* transcription, it is still unclear that there are other pathways mediate BIL1 and STH7 or not. I hypothesize that PIFs may relate BIL1 and STH7 and work together to influence in the light-adapted development. The expression analyses of *PIFs* consisting of *PIF1*, *PIF3*, *PIF4* and *PIF5* in wild-type *Arabidopsis*, *bil1-1D* and *bes1-1D* will be investigated. The binding activity of the recombinant PIF proteins, that is down-regulated in *bil1-1D* and/or *bes1-1D*, to *STH7* promoter will also be checked. Moreover, *pif1*, *pif3*, *pif4* and *pif5* mutants as well as *pifq* quadruple mutant will be used to investigate their response to SL and BR by the measurement of their hypocotyl elongation and *STH7* expression level.

Lastly, other indicators of the light-adapted responses such as, the opened cotyledons, the chloroplast development and the photosynthetic rate should be observed in detail to more clarify the crosstalk between SL and BR. Those indicators also can be used to confirm the regulation of SL and BR in the photomorphogenesis.

Abstract

論文の内容の要旨

応用生命化学　　専攻
平成 27 年度博士課程　　入学
氏名　ジュティポーン　タッサグンパニト
指導教員名　　浅見　忠男

論文題目 Study on Signal Molecules Regulating Strigolactones and Brassinosteroids Function
（ストリゴラクトン・ブラシノステロイドの機能を制御するシグナル分子に関する研究）

Chapter 1. Introduction

Plant hormones are the small molecules which influence physiological processes consisting mainly of growth, differentiation and development in plants. Plant growth regulators are chemicals which mimic natural plant hormones and widely used for increasing crop yield and for studying how plants response to plant hormones. In this study, I focused on two kinds of plant hormone, brassinosteroids (BRs) and strigolactones (SLs).

BRs are a group of steroidal plant hormone. BRs have various effects on a wide spectrum of cellular responses including cell division, cell elongation and so on. SLs were first identified as seed germination stimulants of root-parasitic weeds. SLs are also known as plant hormones involved in the regulation of various phenomena such as the suppression of shoot branching. Identification and characterization of *Arabidopsis*

biosynthetic and signaling mutants of BRs and SLs are the basic way for studying BRs and SLs functions. The phenotypes of these mutants as well as the phenotypes induced by their agonists or biosynthesis inhibitors are both important for elucidating signal factors regulating functions of BRs and SLs.

Not only each plant hormone functions but also the crosstalk among hormones is essential for understanding plant responses to plant hormones. Previous data suggested that there are some crosstalks between SLs and BRs in the photomorphogenesis or light-adapted development. As reported in the previous study, STH7, a member of B-box zinc-finger proteins, exists downstream of BR signal and could be one of the candidates that mediate the crosstalk. It was also reported that *STH7* gene expression is up-regulated by SL. Here, to elucidate the crosstalk between BR and SL, I investigated the two possibilities. Firstly, BR mimics that exert BR like activity. Secondly, STH7 that could be a factor mediating the SL-BR crosstalk.

Chapter 2. Characterization of Synthetic Ecdysteroid Analogues as Functional Mimics of Brassinosteroids

The concentrations of BRs are very low in many plants, and consequently, the yield of naturally occurring BRs from plants is typically poor. Several plant species produce ecdysteroids, which are known as insect molting steroid hormones. In this study, I evaluated the biological activities of three hydroxysteroidal compounds, 20-hydroxyecdysone (ECD), 7,8-dihydro-8α-20-hydroxyecdysone (DHECD), and 7,8-dihydro-5α,8α-20-hydroxyecdysone (α-DHECD), and compared their activities with that of brassinolide (BL), the most potent BR. ECD was obtained at amount of quantity from stem bark of *Vitex glabrata*, a common plant in Thailand. ECD was readily converted to DHECD and α-DHECD, by the catalytic hydrogenation and the subsequent base-catalyzed epimerization.

The potency of these three hydroxysteroidal compounds as functional mimics of BRs in rice and *Arabidopsis* was investigated. In rice, DHECD and α-DHECD enhanced

the degree of lamina inclination, as do BRs. In *Arabidopsis*, DHECD and α-DHECD increased hypocotyl length in the wild-type, and also partially overcame the hypocotyl shortening caused by brassinazole (Brz), a specific BR biosynthesis inhibitor. DHECD and α-DHECD partially reduced dwarfism in the BR-biosynthesis-deficient mutant, *det2*. Treatment with DHECD or α-DHECD decreased the expression of the BR down-regulated genes, and increased the expression of BR up-regulated genes, such as *TCH4* and *SAUR-AC1*. Moreover, DHECD and α-DHECD induced the accumulations of dephosphorylated BIL1/BZR1 that enhance BR signaling as a master transcription factor. In contrast, ECD did not show BR mimic activity.

Chapter 3. Strigolactone and Karrikin Promote Light-adapted Development of *Arabidopsis thaliana* in a STH7 Function Dependent Manner

SLs and karrikins (KARs), which are a class of seed germination stimulant containing a methyl-butenolide moiety, were used in this study. Both SLs and KARs have been reported to inhibit hypocotyl elongation which can be thought as one of the light-adapted developments. The previous data of my group showed that SL and KAR can enhance *STH7* expression level. STH7 was reported as a positive regulator of photomorphogenesis. From this reason, STH7 could be a candidate protein that functions in linking SL and KAR to induce light-adapted development.

GR24, a synthetic SL analogue and KAR_1, a KAR, inhibited the hypocotyl elongation under weak light condition. To investigate roles of SLs and KARs in photomorphogenesis of *Arabidopsis* seedlings, *STH7*-overexpressing (*STH7ox*) and functionally defective *STH7* (*STH7-SRDX*) mutants were prepared. *STH7-SRDX* mutants were less sensitive to hypocotyl inhibition induced by both GR24 and KAR_1 treatment under weak light condition. Moreover, *Arabidopsis* SL signal mutant (*max2-1),* biosynthesis mutant (*max3-1*), receptor mutant (*d14-1*) and KAR receptor mutant (*kai2-1*) were used to investigate the effect of SL and KAR on light-adapted development. The hypocotyl of *max2-1* was insensitive to both GR24 and KAR_1 implying that MAX2 is important for both SL and KAR signal transduction. The effect of racemic mixture of

GR24 (*rac*-GR24), pure enantiomer of GR24 that has the same configuration as 5DS ($GR24^{5DS}$), and pure enantiomer of GR24 that has the same configuration as *ent*-5DS ($GR24^{ent\text{-}5DS}$) was compared on those mutants. $GR24^{5DS}$ significantly inhibited *kai2-1* hypocotyl elongation but not *d14-1*. While, $GR24^{ent\text{-}5DS}$ showed a significant reduction of *d14-1* hypocotyls but not of *kai2-1*. These results support that $GR24^{5DS}$ and $GR24^{ent\text{-}5DS}$ is received separately by D14 and KAI2, respectively. Moreover, KAR_1 reduced *d14-1* hypocotyls but could not decrease *kai2-1* hypocotyls indicating that KAR is perceived by KAI2.

The anthocyanin content was increased in *STH7ox* when de-etiolated under light conditions and GR24-treated plants enhanced the anthocyanin production. GR24 and KAR_1 treatment significantly increased the expression level of photosynthesis-related genes, suggesting that SL and KAR induce light-adapted development in the STH7-dependent manner.

Chapter 4. Coordination of STH7 and the Brassinosteroid Regulated Molecules Mediates the Crosstalk between Strigolactone and Brassinosteroid in Light-adapted Development

SLs promote the light-adapted development in *Arabidopsis* hypocotyls elongation, but BRs function oppositely to stimulate hypocotyl elongation. To investigate the possibility of crosstalk between these two hormones, effects of SL and BR on the hypocotyl elongation under weak light condition were investigated. The result showed that BL repressed the effect of GR24 on the inhibition of hypocotyl elongation in wild-type *Arabidopsis*. The quantitative real-time PCR (qRT-PCR) analysis showed that the expression level of *STH7* was synergistically up-regulated by the co-application of GR24 and Brz. To understand functions of STH7, *STH7ox* and *STH7-SRDX* mutants were used. *STH7-SRDX* mutant was insensitive to GR24 and weakly but significantly responded to Brz in the inhibition of hypocotyls. Moreover, Brz enhanced the effect of GR24 on the inhibition of hypocotyl elongation in both wild-type and *STH7ox*. To investigate roles of STH7 in SL and BR crosstalk suggested above, genes both STH7-regulated and BR-

regulated were analyzed by using the previously published microarray data. In overlapping genes in the *STH7*-upregulated and the BR-repressed genes, half of them, including *STH7*, *ELIP2* and *CHI*, were the genes related to the light-adapted development. The qRT-PCR showed that the co-application of GR24 and Brz highly up-regulated the transcript level of *ELIP2*, *CHI* and their homologs.

Next, the double mutant analysis between *STH7ox* or *STH7-SRDX* and the BR gain-of-function *bil1-1D* or *bes1-D*, were performed to investigate the SL and BR crosstalk. The *bil1-1D*×*STH7ox* double mutant exhibited a small rosette, a high contents of chlorophyll and anthocyanin like *STH7ox*. Co-treatment of GR24 and Brz in *bil1-1D*×*STH7ox* double mutants induced shorter hypocotyls than individual application of either GR24 or Brz did. In contrast both *bes1-D*×*STH7ox* and *bes1-D*×*STH7-SRDX* double mutants were insensitive to Brz. Either GR24 or Brz treatments down-regulated the expression of *SAUR-AC1* and *TCH4* in wild-type and *bil1-1D*×*STH7ox*. This result supports that SL suppresses the transcription of cell elongation-related genes as same as Brz. Moreover, the increase of *STH7* expression by co-treatment of GR24 and Brz was clearly shown in *bil1-1D* but not in *bes1-D* mutant. The results implied that BIL1 might mainly repress *STH7* transcription. Furthermore, the electrophoretic mobility shift assay showed that BIL1 interacted with E-box (CACATG) in *STH7* promoter.

Conclusion

The photomorphogenesis is mediated by various plant hormones including SL and BR. Among three hydroxysteroid compounds, DHECD and α-DHECD had BR-like function. DHECD and α-DHECD activated BR signal transduction pathway by accumulating dephosphorylated form of BIL1/BZR1, which activates BR signaling. Therefore, DHECD and α-DHECD could be used as BR mimic compound to suppress the light-adapted growth.

In contrast with BR, SL and KAR stimulate the light-adapted development. GR24 and KAR_1 up-regulated the expression of *STH7*. The hypocotyl growth in *STH7-SRDX*

mutant was insensitive to GR24 and KAR_1. Moreover, treatment of both GR24 and KAR_1 up-regulated the photosynthesis-related genes in the STH7-dependent manner indicating that STH7 is essential for the light-adapted process.

The application of Brz enhanced effects of SL on the inhibition of hypocotyl elongation and on the up-regulation of *STH7*. The *bil1-1D×STH7ox* double mutant displayed the shortened hypocotyl similar to *STH7ox*, whereas *bil1-1D×STH7-SRDX* was insensitive to both SL and Brz. Lastly, the binding of BIL1/BZR1 protein to E-box element on the *STH7* promoter was confirmed. Above results suggested that STH7 works downstream of BIL1/BZR1. I think SL and BR play an antagonistic role in light-adapted development of *Arabidopsis* likely in the STH7-dependence.

Publications

Thussagunpanit J, Nagai Y, Nagae M, Mashiguchi K, Mitsuda N, Ohme-Takagi M, Nakano T, Nakamura H, Asami T. Involvement of STH7 in light-adapted development in *Arabidopsis thaliana* promoted by both strigolactone and karrikin. Biosci Biotechnol Biochem. 2017;81:292–301.

Thussagunpanit J, Jutamanee K, Homvisasevongsa S, Suksamrarn A, Yamagami A, Nakano T, Asami T. Characterization of synthetic ecdysteroid analogues as functional mimics of brassinosteroids in plant growth. J Steroid Biochem Mol Biol. 2017;172:1–8.

Acknowledgements

Firstly, I would like to express my sincere gratitude to my supervisor, Prof. Dr. Tadao Asami who gave me the inspiration for studying PhD in Japan and allowed me to do the interesting and challenging research topic. In addition, I would like to gratefully thank you Assist. Prof. Dr. Hidemitsu Nakamura, The University of Tokyo and Dr. Takeshi Nakano, CSRS, Riken for the merciful discussion in every experiment. My dissertation cannot be success without the revision and consulting from above professors.

My studying in Japan fully support by the Japanese government (Monbukagakusho, MEXT) scholarship. Since some part of this dissertation initiated from my Master's degree thesis that I did in Thailand, I would like to sincere thank you to my pervious supervisor, Assoc. Prof. Dr. Kanapol Jutamanee, Kasetsart University, Thailand and the DPST project for financial support. Some chemicals, materials and data in this work were provided from many people. The hydroxysteriodal compounds that used in this dissertation were synthesized by Prof. Dr. Apichart Suksamrarn and his team at Ramkhamhaeng University, Thailand. Furthermore, I would like to thank Assist. Prof. Dr. Jun Takeuchi, Shizuoka University for advice concerning the 3D chemical structures of hydroxysteriodal compounds and the brassinosteroid-binding receptor. The *STH7ox* mutant was performed by previous Master's degree students in my laboratory, Ms. Miyu Nagae and Ms. Yuko Nagai. The seeds of *STH7-SRDX* were provided from Prof. Dr. Masaru Ohme-Takagi, Saitama University. MBP-BIL1 is the gift from Mr. Shohei Nosaki, Department of Applied Biological Chemistry, The University of Tokyo and CSRS, Riken. Moreover, I would like to thank you the worthy data from Assist. Prof. Dr. Kiyoshi Mashiguchi, Tohoku University. He found that *STH7* was up-regulated by strigolactone. From above materials, useful data, and helpful discussion made me could do the experiment in this dissertation.

During my PhD life, I has received the great help from many people in my laboratory. Assoc. Prof. Dr. Masatoshi Nakajima advised me about the presentation in every attended conferences and daily life in Japan. Many thanks Dr. Kai Jiang, Dr. Ikuo

Takahashi, and Ms. Naiyanate Charoensanti-Tanaka for every help and discussion about my experiment. I offer my appreciation to Ms. Kyoko Shimazu who helped me handle various documents and gave useful information since before coming to Japan. Moreover, I would like to thank you the Japanese Language Center, the University of Tokyo for the providing of the Japanese language courses from the elementary to the intermediate skills. Understanding in Japanese language made my life in Japan being happier. In Japan, I also have Thai friends who have gave me the great time. Thanks all of members in the Somtum group and in Thai students' association in Japan who support me both academic and recreational activities. Furthermore, many thanks my friend in Thailand, Mr. Weerasin Soonjaroon, Kasetsart University for discussion.

Finally, I gratefully appreciate my family, especially my beloved grandmother and sisters for an encouragement. Without the valuable guidance and supports from all of person described above, the dissertation cannot be finished as this book. If this dissertation is worthy, I would like to give all of goodness to my teachers and professors who have taught me in both academic subjects and life learning.

December 15, 2017

Jutiporn Thussagunpanit